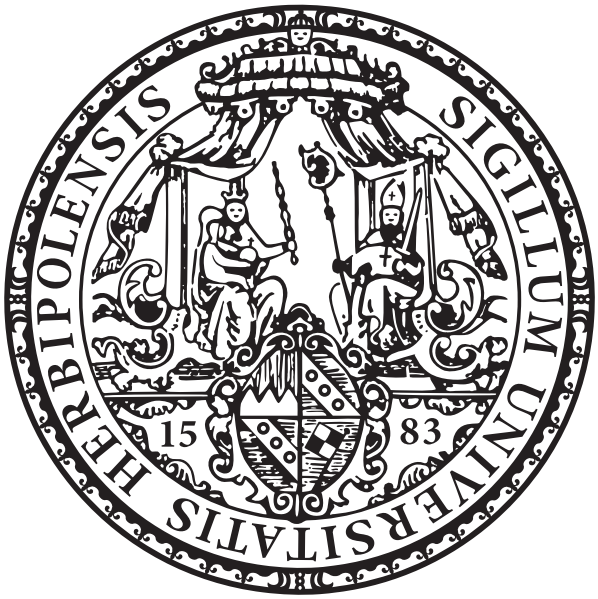

Studies on platelet interactions with the coagulation system and on modulators of platelet (hem)ITAM signaling in genetically modified mice

• • •

Studien zur Thrombozyteninteraktion mit der Gerinnungskaskade und Modulation des hem(ITAM) Signalwegs in genetisch veränderten Mäusen

Doctoral thesis for a doctoral degree
at the Graduate School of Life Sciences,
Julius-Maximilians-Universität Würzburg,
Section Biomedicine

submitted by

Ayesha Anjum Baig

from Aligarh, India

Würzburg, 2018

Submitted on: _____

Office stamp

Members of the *Promotionskomitee*:

Chairperson:	**Prof. Dr. Manfred Gessler**
Primary Supervisor:	**Prof. Dr. Bernhard Nieswandt**
Supervisor (Second):	**Prof. Dr. Johan W. M. Heemskerk**
Supervisor (Third):	**Prof. Dr. Guido Stoll**
Date of Public Defense:	**_____**
Date of Receipt of Certificates:	**_____**

To

My parents, sisters and husband
whose wishes and encouragement
enabled me to reach this stage

Table of Contents

Summary

Activated platelets and coagulation jointly contribute to physiological hemostasis. However, pathological conditions can also trigger unwanted platelet activation and initiation of coagulation resulting in thrombosis and precipitation of ischemic damage of vital organs such as the heart or brain. The specific contribution of procoagulant platelets, positioned at the interface of the processes of platelet activation and coagulation, in ischemic stroke had remained uninvestigated. The first section of the thesis addresses this aspect through experiments conducted in novel megakaryocyte- and platelet-specific TMEM16F conditional KO mice (cKO). cKO platelets phenocopied defects in platelets from Scott Syndrome patients and had severely impaired procoagulant characteristics. This led to decelerated platelet-driven thrombin generation and delayed fibrin formation. cKO mice displayed prolonged bleeding times and impaired arterial thrombosis. However, infarct volumes in cKO mice were comparable to wildtype (WT) mice in an experimental model of ischemic stroke. Therefore, while TMEM16F-regulated platelet procoagulant activity is critical for hemostasis and thrombosis, it is dispensable for cerebral thrombo-inflammation in mice.

The second section describes the generation and initial characterization of a novel knockin mouse strain that expresses human coagulation factor XII (FXII) instead of endogenous murine FXII. These knockin mice had normal occlusion times in an experimental model of arterial thrombosis demonstrating that human FXII is functional in mice. Therefore, these mice constitute a valuable tool for testing novel pharmacological agents against human FXII – an attractive potential target for antithrombotic therapy.

Glycoprotein (GP)VI and *C-type lectin-like receptor 2* (CLEC-2)-mediated (hem)*immunoreceptor tyrosine-based activation motif* (ITAM) signaling represent a major pathway for platelet activation. The last section of the thesis provides experimental evidence for redundant functions between the two members of the Grb2 family of adapter proteins - Grb2 and Gads that lie downstream of GPVI and CLEC-2 stimulation. *In vitro* and *in vivo* studies in mice deficient in both Grb2 and Gads (DKO) revealed that DKO platelets had defects in (hem)ITAM-stimulation-specific activation, aggregation and signal transduction that were more severe than the defects observed in single Grb2 KO or Gads KO mice. Furthermore, the specific role of these adapters downstream of (hem)ITAM signaling was essential for maintenance of hemostasis but dispensable for the known CLEC-2 dependent regulation of blood-lymphatic vessel separation.

Zusammenfassung

Aktivierte Thrombozyten und die Gerinnungskaskade bilden gemeinsam die Grundlage der physiologischen Hämostase. Daneben können jedoch auch pathologische Bedingungen Thrombozytenaktivierung herbeiführen und die Gerinnungskaskade auslösen und somit zum Gefäßverschluss führen, was häufig ischämische Schäden lebenswichtiger Organe wie beispielsweise des Herzens oder des Gehirns verursachen kann. Prokoagulante Thrombozyten befinden sich an der Schnittstelle zwischen Thrombozytenaktivierung und der Gerinnungskaskade, ihre Funktion bei der Pathogenese des ischämischen Schlaganfalls wurde jedoch bisher nicht im Detail untersucht. Der erste Teil dieser Doktorarbeit widmet sich dieser Fragestellung durch die Analyse von neu generierten konditionalen, Megakaryozyten- und Thrombozyten-spezifischen *Tmem16f Knockout* Mäusen. TMEM16F-defiziente Thrombozyten wiesen ähnliche Defekte wie die Thrombozyten von Scott-Syndrom-Patienten sowie stark beeinträchtigte prokoagulante Eigenschaften auf. Diese Defekte gingen mit signifikant verlangsamter thrombozytenabhängiger Thrombingenerierung und verzögerter Fibrinbildung einher. TMEM16F-Defizienz führte zu verlängerter Blutungszeit und beeinträchtigte in einem experimentellen Modell die Bildung arterieller Thromben. TMEM16F-defiziente Mäuse wiesen jedoch im Vergleich zu wildtypischen Mäusen keinerlei Unterschiede im experimentellen ischämischen Schlaganfall auf. TMEM16F-gesteuerte prokoagulante Thrombozytenfunktion ist demnach kritisch für Hämostase und Thrombose, während sie eine untergeordnete Rolle in zerebraler Thrombo-Inflammation spielt.

Der zweite Teil dieser Arbeit befasst sich mit der Generierung und Erstbeschreibung einer neuen Mauslinie, welche den humanen Hageman-Faktor (FXII) anstelle des endogenen murinen FXII exprimiert. In den resultierenden Knock-in Mäusen war die Bildung okklusiver arterieller Thromben nach chemisch induzierter Gefäßverletzung nicht beeinträchtigt, was zeigt, dass der humane FXII im Maussystem voll funktionstüchtig ist. Somit können diese Mäuse in der Zukunft als ein wertvolles Werkzeug zum Testen neuer pharmakologischer Ansätze zur Herabsetzung der FXII-Aktivität eingesetzt werden, welche einen vielversprechenden Targets neuartiger antithrombotischer Behandlungsansätze darstellt.

Die thrombozytären Rezeptoren Glykoprotein (GP)VI und *C-type lectin-like receptor 2* (CLEC-2) lösen (hem)*immunoreceptor tyrosine-based activation motif* (ITAM)-gekoppelte Signalwege aus, welche eine eine Schlüsselrolle in der Thrombozytenaktivierung spielen. Der dritte Teil dieser Doktorarbeit liefert experimentelle Hinweise für überlappende Funktionen der Adapterproteine Grb2 und Gads in der (hem)ITAM-anhängigen Signalkaskade. *In*

vitro und *in vivo* Studien zeigten, dass Grb2/Gads-doppeldefiziente Thrombozyten (hem)ITAM-spezifische Defekte in der Aktivierung, Aggregation und Signaltransduktion aufweisen, die im Vergleich zu einzeldefizienten Thrombozyten deutlich ausgeprägter sind und somit eine redundante Rolle der Adapterproteine offenbaren. Während Grb2 und Gads gemeinsam an der Aufrechterhaltung physiologischer Hämostase beteiligt sind, tragen sie nicht entscheidend zur bekannten CLEC-2-abhängigen Regulation der Trennung von Blut- und Lymphgefäßen bei.

1. Introduction

1.1. Platelets and their role in primary and secondary hemostasis

Platelets are anucleate cells of the hematopoietic system produced from precursor cells called megakaryocytes in the bone marrow. The primary role of these cells is to undertake meticulous surveillance of the integrity of the vessel wall. Upon any injury to blood vessels leading to denudation of the endothelial layer, circulating platelets are exposed to thrombogenic components of the subendothelial extracellular matrix (ECM) which leads to their rapid activation and initiation of primary hemostasis resulting in the formation of a hemostatic platelet plug to terminate active bleeding.[1, 2]

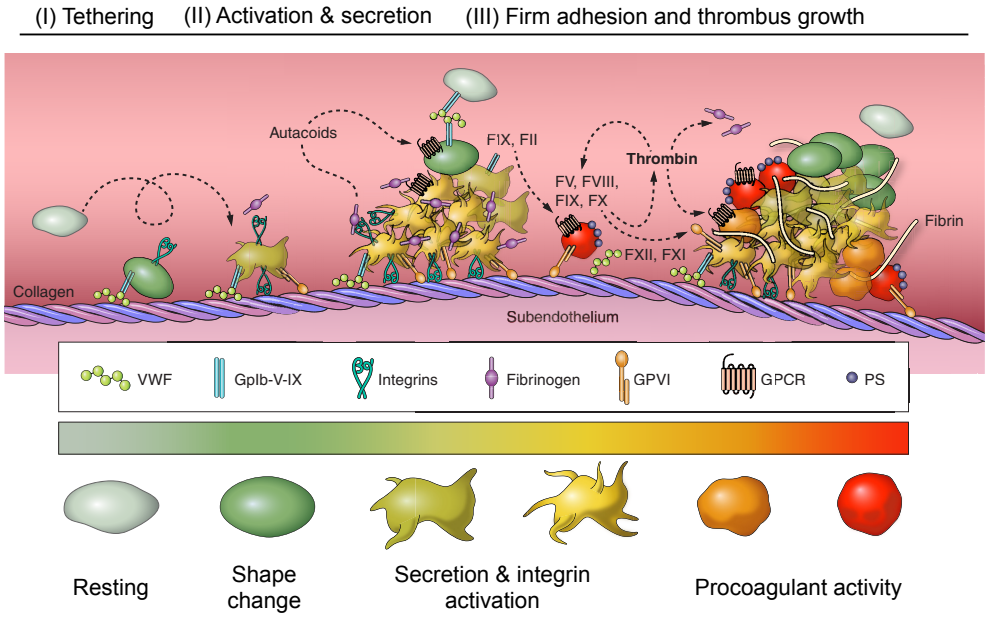

Figure 1. Platelet activation. The process of platelet activation can be divided into three main stages (I) Tethering – the deceleration of platelets at the site of injury through interaction between platelet glycoprotein (GP)Ib-V-IX complex and von Willebrand factor (vWF). (II) Activation and secretion – Binding of GPVI to collagen initiates cellular activation that causes platelet shape change, granule release and change in conformation of integrins to an active state. The secondary mediators released from platelets as well as thrombin generated through the extrinsic and intrinsic pathways of coagulation stimulate GPCR receptors that further strengthens the activation response (III) Firm adhesion and thrombus growth – activated integrins mediate firm platelet adhesion to the vessel wall and platelet-platelet interaction through binding of integrin αIIbß3 to fibrinogen leads to thrombus growth. Increase in intracellular Ca^{2+} concentrations due to platelet activation results in phosphatidylserine exposure on the surface of platelets providing a catalytic surface for the assembly of the coagulation complexes and acceleration of thrombin production. Thrombin converts soluble fibrinogen to fibrin for the formation of a stable clot. Bottom - Platelet shape change from resting to procoagulant with heat map indicative of intracellular Ca^{2+} concentration (green corresponds to low and red to high intracellular Ca^{2+} concentration). (Modified from Versteeg H. *et al. Physiol Rev* 2011).[3]

In humans, approximately 150,000 – 400,000 platelets are present in one µL of blood with a life span of about 10 days, whereas in mice approximately 1,000,000 platelets/µL circulate with an approximate life span of 4.5 - 5.5 days. Both mouse and human platelets are discoid in shape but mouse platelets with an average diameter of 1-2 µm are smaller than human platelets that have an average diameter of 3-4 µm. Most platelets are never activated during their life span and old and activated platelets are cleared from the circulatory system by macrophages in the liver and spleen.[4, 5]

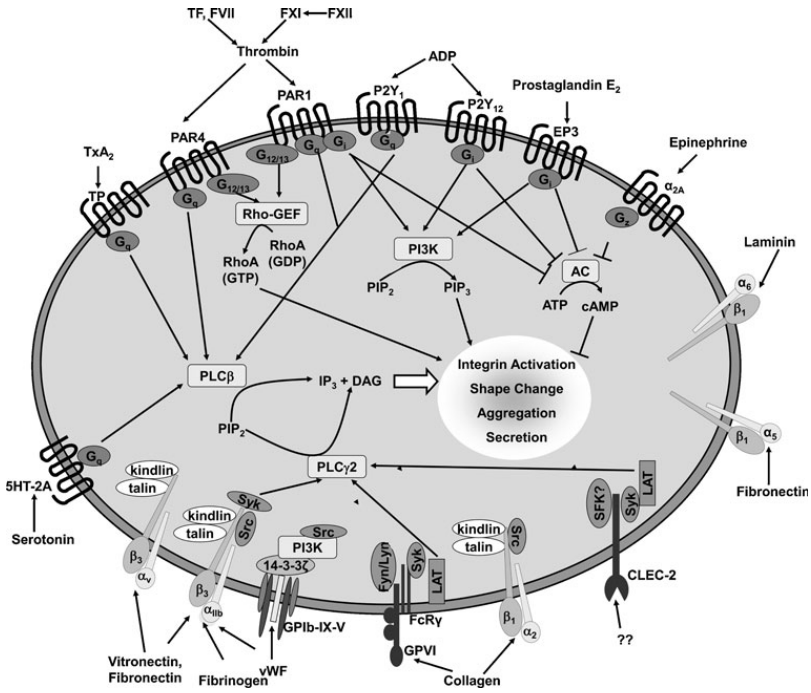

Figure 2. There are three major families of glycoproteins on the platelet surface that mediate platelet activation, aggregation and thrombus growth – GPCRs, (hem)ITAM receptors and integrins. Downstream of both GPCRs and (hem)ITAM receptors - tyrosine phosphorylation and activation of an effector phospholipase (PL)Cγ isoform (PLCγ2 or PLCβ) is achieved, leading to a sustained increase in intracellular Ca^{2+} concentrations. This results in a myriad of platelet responses including shape change, granule release, integrin activation and procoagulant activity, ultimately leading to the formation of a primary platelet plug that halts active bleeding. (Taken from Stegner D. *et al. J Mol Med* 2011).[1]

However, when these cells encounter an injury to the vessel wall, their prompt activation is achieved through three distinct steps – tethering, activation and secretion, followed by firm adhesion and thrombus growth (Figure 1). These stages of activation are accomplished with the involvement of several adhesion and signaling receptors present on the platelet surface. This includes integrins, G protein-coupled receptors (GPCRs) and (hem)ITAM receptors (Figure 2).

Circulating platelets are first decelerated through interactions between von Willebrand factor (vWF) immobilized on collagen in the ECM and the glycoprotein (GP)Ib-V-IX complex on platelets. This is termed tethering and allows further interaction between receptor GPVI and its physiological ligand collagen. GPVI binding to collagen initiates the ITAM signaling cascade leading to change in the conformation of integrins from a low affinity to a high affinity state, platelet shape change and granule release. In parallel, the secondary hemostatic response is initiated through the extrinsic pathway of coagulation with the interaction of coagulation factor VIIa and tissue factor (TF), and through the intrinsic pathway of coagulation with activation of coagulation factor XII, e.g. by polyphosphates released from activated platelets, leading to generation of thrombin. Outside-in signaling through activated integrins, and stimulation of GPCRs by thrombin and soluble mediators released from activated platelets, further strengthens the platelet activation response. Platelet-platelet interactions through binding of integrin αIIbß3 to fibrinogen results in aggregate formation and thrombus growth. The process of activation is also accompanied by rapid remodeling of the cytoskeleton leading to platelet shape change from discoid to spherical, to spreading on the reactive surface (through formation of filopodia and lamellipodia) to acquiring a ballooned morphology characteristic of procoagulant transformation marked by high intracellular Ca^{2+} concentration and surface exposure of phosphatidylserine (PS) (Figure 1). Procoagulant platelets further support the secondary hemostatic response by providing a catalytic scaffold for the assembly of coagulation complexes accelerating the process of thrombin generation and conversion of soluble fibrinogen to insoluble fibrin for the formation of a stable clot (Figure 1).[1, 2]

1.2. Procoagulant platelets – role of phospholipid scramblases

Like all resting cells, platelets maintain plasma membrane phospholipid asymmetry, which means that the neutral cholinephospholipids - phosphatidylcholine (PC) and sphingomyelins (SM) are predominantly located in the outer leaflet of the plasma membrane, whereas nearly all of the negatively charged aminophospholipids - phosphatidylserine (PS) and phosphatidylethanolamine (PE) - are present in the inner leaflet. This lack of symmetry in phospholipid distribution is maintained by the concerted activity of two transporters known as flippase and floppase. Flippases (aminophospholipid translocases) specifically transport PS and PE from the outer leaflet to the inner leaflet with relatively fast kinetics (within seconds to minutes). The less specific floppases transport all phospholipids, especially PC from the inner to the outer leaflet, but with about ten times slower kinetics. Thereby a dynamic steady state

of differential distribution of phospholipids between the cytosolic and extracellular leaflets of the plasma membrane is achieved.[6-8]

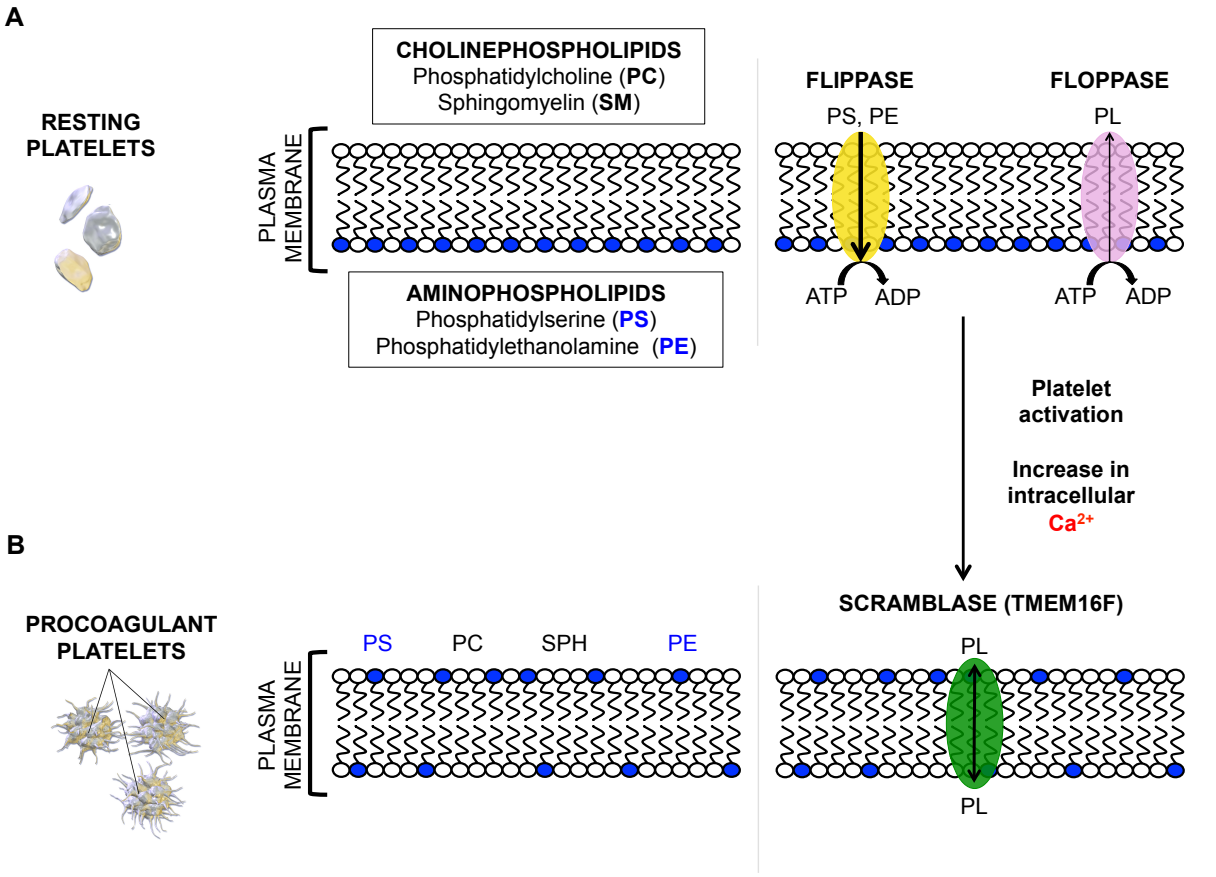

Figure 3. Role of flippase, floppase and scramblases in maintaining phospholipid distribution between the two leaflets of the plasma membrane. (A) Resting platelets: Neutral cholinephospholipids (phospholipid head illustrated in white) are predominantly located in the extracellular leaflet of the plasma membrane. Negatively charged aminophospholipids (phospholipid head illustrated in blue) are principally maintained on the cytoplasmic leaflet of the plasma membrane. This differential distribution of phospholipids is maintained by the ATP-dependent activity of flippases and floppases. (B) Activated, procoagulant platelets: Platelet activation results in increase in intracellular calcium concentrations that attenuates the activity of the flippases and floppases and activates the scramblases. The non-specific bidirectional transport of phospholipids by the activity of scramblases abolishes phospholipid asymmetry between the two leaflets of platelet plasma membrane. Such platelets are procoagulant as the negatively charged aminophospholipids serve as catalytic scaffolds for binding of the tenase and prothrombinase complexes of the coagulation cascade. TMEM16F is the only identified scramblase in platelets. PL- Phospholipids. (Modified from Lhermusier *et al*., *J Thromb Haemost* 2011).[9]

The activities of flippases and floppases bear three similarities – 1) transport of phospholipids is unidirectional, 2) against the concentration gradient and 3) ATP-dependent. The molecular identity of flippases and floppases in platelets remains uncertain, but some of the candidate

proteins identified in other cell types include members of the P4-ATPase family recognized to function as flippases (ATP11A, ATP11C), and some of the members of the family of multidrug resistance proteins are thought to function as floppases.[7, 9, 10]

When platelets are strongly activated, resulting in significant and sustained increase in intracellular calcium concentrations, the activity of flippases and floppases is attenuated, and a third transporter known as scramblase is activated. The phospholipid transport through a scramblase is non-specific, bidirectional, towards equilibrium and ATP-independent. As a result of phospholipid scramblase activity, plasma membrane phospholipid asymmetry is abolished and negatively charged PS and PE also get oriented towards the outer leaflet in activated platelets (Figure 3).[9]

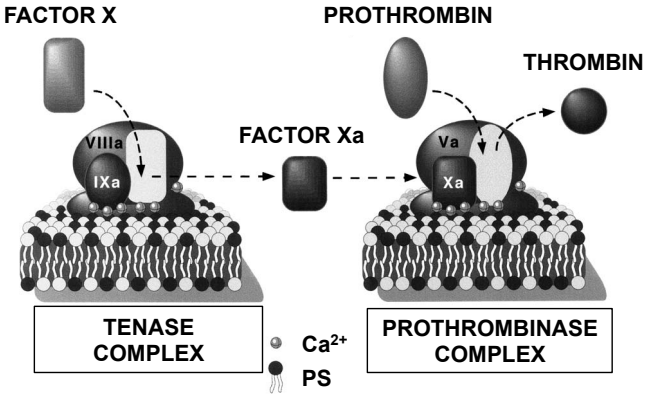

Figure 4. Assembly of the tenase and prothrombinase complexes on procoagulant platelets. Tenase and prothrombinase are multimolecular enzymatic complexes that form on negatively charged phospholipids (phosphtidylserine - PS) present on the procoagulant platelet surface. The tenase complex includes the activated enzyme FIX (FIXa) which along with the non-enzymatic co-factor activated FVIII (VIIIa) activates the zymogen FX. The activated enzyme FX (FXa) along with co-factor activated FV (FVa) forms the prothrombinase complex over the procoagulant platelet surface that converts prothrombin to thrombin. When assembled in the form of complexes over procoagulant platelets, the catalytic efficiencies of the enzymes are dramatically increased compared to the intrinsic efficiencies of the enzymes. (Taken from Zwaal *et al., Biochimica et biophysics acta* 2004).[6]

Such platelets with surface-exposed PS are referred to as 'procoagulant' as it has been shown that the exposed PS serves as a catalytic anchoring site for the assembly of the tenase (FIXa & FVIIIa) and the prothrombinase (FXa & FVa) complexes of the coagulation cascade on the platelet surface (Figure 4). This amplifies the coagulation response, and the generation of thrombin is enhanced by five to ten orders of magnitude leading to stable clot formation.[9] This amplification occurs in part as a consequence of concentration of the coagulation factors at a localized area of injury due to the scaffold provided by procoagulant

platelets, resulting in much higher local concentrations of the proteases at the site of injury, as compared to their usual concentration in plasma.[6]

The molecular identity of a scramblase had remained a mystery for several decades with a number of proteins being proposed as candidates, but eventually identified not to possess scramblase function. This includes the protein phospholipid scramblase 1 (PLSCR1) which was purified from the membrane of erythrocytes and identified to be a scramblase. Yet no defects in PS exposure in activated platelets from PLSCR1-deficient mice were observed, ruling out the hypothesis that scramblase activity is associated with PLSCR-1.[11, 12]

Suzuki *et al.* adopted an elegant approach that eventually led to the identification of the first scramblase, TMEM16F (Transmembrane protein 16F). They performed several cycles of cell sorting on a mouse B cell line, Ba/F3 after stimulation with the calcium ionophore A23187 that caused reversible PS exposure. Fluorescently labeled annexin A5 was used for cell sorting, based on its specific binding to PS. Eventually, the authors attained a subline that strongly exposed PS, with an annexin A5 staining a 100-fold higher than the native cell line. Following generation of a cDNA library and sequencing, a clone with constitutive PS exposure expressing a mutated form of TMEM16F was identified and TMEM16F was recognized to support scramblase activity.[13]

1.2.1. TMEM16F (Calcium-dependent phospholipid scramblase)

TMEM16F belongs to the transmembrane protein 16 (TMEM16) or Anoctamine (Ano) family of proteins which consists of 10 members – TMEM16 A to H, J & K (or Ano 1-10). The family of proteins was termed ‘Anoctamines’ as the first two characterized members TMEM16A & 16B were reported to be channels for anions (calcium-activated chloride channels) and to possess 8 transmembrane domains (Anoctamin – Anion+Octa=8).[14] However, more recent studies have predicted that members of the protein family are in fact organized into 10 transmembrane domains and that all members are not anion channels.[15-17]. Therefore, the nomenclature ‘TMEM16 family’ as well as ‘Anoctamin family’ of proteins is used in parallel – although the name ‘Anoctamin’ or *Ano* is now the official HUGO nomenclature and has replaced *TMEM16* in GenBank.

The *Ano6* gene is located on chromosome 12 in humans and chromosome 15 in mice, coding for the 106 kDa TMEM16F protein.

Although TMEM16F was identified to play an important role in the scramblase process, after its identification there was lack of consensus and evidence on whether it itself possesses scramblase function, or is an ion channel that regulates an as-yet unidentified scramblase.[13, 18]

Over the years a significant body of data has accumulated to indicate that TMEM16F possesses both functions - that of a phospholipid scramblase as well as an ion channel. Malvezzi *et al.* identified afTMEM, a homologue of mammalian TMEM16 isolated from the fungus *Aspergillus fumigatus* that displays this dual function. The authors reported both functions to be orchestrated by a single calcium-binding site.[19] A breakthrough in ascertaining the possibility that a TMEM16 family member could itself function as a scramblase came in 2014, when Brunner *et al.* elucidated the structure of nhTMEM16 from the fungus *Nectria haematococca*.[15] The authors found nhTMEM16 to be a homodimeric protein with 10 transmembrane helices and a conserved calcium-binding site to function as a calcium-activated lipid scramblase (Figure 5B). Furthermore, Scudieri *et al*. performed studies using heterologous expression of splice variants of TMEM16F in HEK-293 cells, reporting both scramblase and channel activity, enhanced by an activating mutation and diminished upon silencing of endogenous TMEM16F expression.[20]

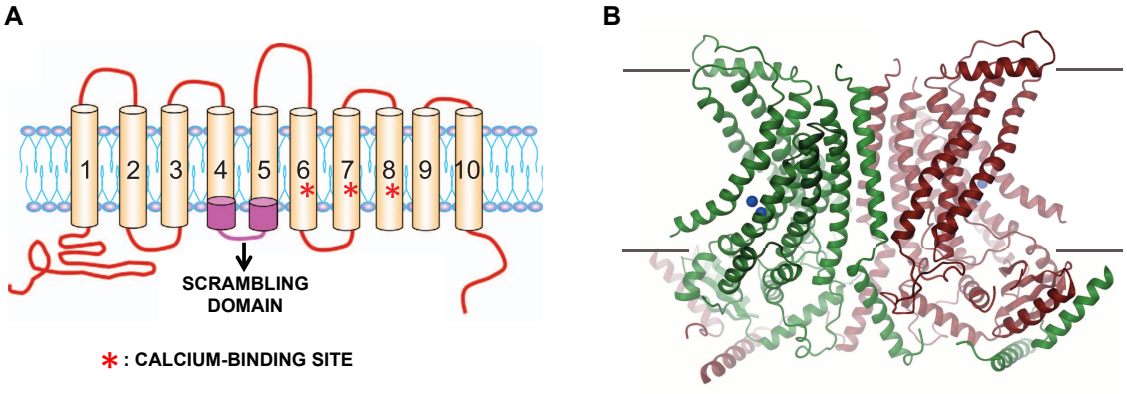

Figure 5. The platelet calcium-dependent scramblase – TMEM16F. (A) Schematic illustration of TMEM16F – a 35 amino acid domain located between transmembranes domains IV and V of TMEM16F is sufficient to confer lipid scrambling activity to TMEM16A, which is a Ca^{2+} activated Cl^- channel without endogenous scramblase activity. This domain in TMEM16F is named the scrambling domain, or SCRD.[21] Six glutamate and aspartate residues located in transmembrane segments of VI – VIII are involved in direct binding of Ca^{2+}. (B) Ribbon representation of structure of nhTMEM16, a TMEM family member from the fungus *Nectria haematococca.* (Modified from Nagata *et al., Cell Death and Differ.* 2016 and Brunner *et al., Nature* 2014).[8, 15]

The nature of the channel function is still a matter of discussion.[18, 22] The majority of investigations have identified TMEM16F to be an anion channel. However these reports differ in their description of the characteristics of the anion channel - it has been reported to be an outwardly rectifying chloride channel (ORCC),[23, 24] but also to be a calcium activated chloride channel (CaCC, like 2 other well-known members of the family TMEM16A and TMEM16B).[25, 26] On the other hand, another report identified it to be associated with cation conductance and to form a small conductance calcium-activated cation channel (SCAN).[27]

A lot of the current understanding of the functions of the platelet scramblase TMEM16F comes from studies performed in Scott Syndrome, a congenital bleeding disorder caused by loss of function mutations in *Ano6*. This aspect is described in detail in section 1.2.1.1.

Besides TMEM16F, other members of the TMEM16 family including TMEM16C, 16D, 16G and 16J have also been found to possess phospholipid scramblase activity.[16, 17] However, no other TMEM16 family member apart from TMEM16F is expressed in human platelets. The expression of TMEM16B, 16H and 16K is reported in mouse platelets, but with extremely lower expression levels compared to TMEM16F.[28]

1.2.1.1. Scott Syndrome

Scott Syndrome is a rare congenital bleeding disorder characterized by decreased ability of blood cells to exteriorize PS to the outer leaflet of their plasma membrane. Weiss *et al.* identified the first patient, Mrs. Scott, in 1979 with this moderate to severe bleeding disorder. They reported a 34-year-old woman who had suffered several provoked bleeding episodes over the years, such as uncontrolled bleeding post surgery, which could be controlled by adequate platelet coverage. However, she presented with normal coagulation parameters, and unaltered platelet activation and aggregation. Further studies revealed that her platelets displayed impaired procoagulant activity as shown by reduced prothrombin consumption. Further, Majerus *et al.* pinpointed that the defect in prothrombin consumption arises from diminished number of Factor V binding sites on the patient's platelets.[29]

Toti *et al.* described a second patient with a striking similarity to Mrs. Scott's clinical presentations in the year 1996.[30] In both patients, the defect in PS exposure was not only seen in platelets, but also in stimulated erythrocytes and immortalized lymphocytes.

When two independent studies investigated the procoagulant activity of platelets in close, asymptomatic relatives of the two Scott Syndrome patients, both found indications for

autosomal recessive inheritance pattern, as the father, mother and son of the first patient, and the son and daughter of the second patient presented with a somewhat reduced prothrombinase activity intermediate between that of the control and that of the Scott Syndrome patient.[30, 31]

Several years later, in 2010, Suzuki *et al.* identified the first scramblase TMEM16F, and showed a loss of function mutation in the *Ano6* gene in one of the Scott Syndrome patients (G-to-T homozygous mutation at the splice acceptor site in intron 12 that caused skipping of exon 13, frame shift and premature termination of protein translation).[13] Mapping of the genetic defects in another Scott Syndrome patient also revealed loss of function mutations in the *Ano6* gene (compound heterozygous mutation in TMEM16F – a transition at the first nucleotide of intron 6 disrupting the donor splice site consensus sequence, and a nucleotide insertion in exon 11 predicting a frame shift and premature termination of translation).[32] These studies established firmly that TMEM16F is involved in conferring procoagulant potential to blood cells.

For several years, only three Scott Syndrome patients were known.[33] Recently, another patient was identified.[34] The hallmarks of a Scott Syndrome phenotype include moderate bleeding, reduced prothrombin consumption, impaired calcium-induced phospholipid scrambling and microparticle shedding in platelets, RBCs and WBCs and defective calcium-induced bleb formation in platelets (further described in section 1.2.1.3).[33]

In addition to humans, a Scott Syndrome-like phenotype is also observed in a family of inbred German shepherd dogs and is known as Canine Scott Syndrome (CSS). The symptoms observed in these dogs are similar to those observed in humans – reduced PS exposure and microparticle formation in platelets, and a mild to moderate bleeding tendency.[35] A point mutation in the *Ano6* gene has been identified to result in the loss of TMEM16F protein expression in CSS platelets.[36]

1.2.1.2. Procoagulant platelets in arterial thrombosis and ischemic stroke

Transformation of platelets to a procoagulant state is an integral step of the hemostatic response initiated upon vessel wall injury that leads to effective termination of active bleeding. Therefore not surprisingly, uncontrolled provoked bleeding is the major clinical manifestation of Scott Syndrome patients.[6] Constitutive TMEM16F knockout (KO) mice are reported to have prolonged bleeding times compared to wild-type (WT) mice in the saline

model for bleeding time measurement.[27] In contrast Fujii *et al.* reported comparable bleeding times in megakaryocyte- and platelet- specific TMEM16F conditional KO and WT mice.[28]

Notably, in an experimental model of $FeCl_3$-induced thrombus formation in the carotid artery, TMEM16F constitutive KO mice were profoundly protected from arterial thrombosis.[27] In addition, megakaryocyte- and platelet-specific TMEM16F mice challenged in a model of photochemical injury-induced thrombosis in testicular veins showed development of fragile thrombi that frequently embolized under the forces of blood flow, while stable thrombi developed in veins of WT mice under these conditions.[28]

Overall, these findings in Scott Syndrome patients as well as TMEM16F constitutive and conditional KO mice indicated an important role for TMEM16F-mediated platelet procoagulant activity in hemostasis, and both arterial and venous thrombosis.

It is known that both platelets and the coagulation system strongly influence infarct progression after ischemic stroke.[37] Genetic ablation or pharmacological inhibition of coagulation factor XII (FXII) that initiates the intrinsic pathway of coagulation confers protection from development of reperfusion injury in experimental models of ischemic stroke as tested in both mice and rats.[38-40] Thrombin, the final product of the coagulation cascade, and its receptors - protease activated receptors (PARs) - are also implicated in the progression of damage following focal cerebral ischemia.[41] Thrombin concentrations are significantly increased in the ischemic caudate 4 h and 24 h following 90 min of transient middle cerebral artery occlusion (tMCAO) in rats and administration of hirudin, a specific inhibitor of thrombin, into the ischemic caudate significantly reduced infarct volumes following tMCAO in addition to ameliorating neurologic deficits.[42] Antithrombin (AT) is an endogenous serpin that inactivates several enzymes of the coagulation cascade. Intraperitoneal administration of AT 3 h after tMCAO in mice and 3 h after tMCAO or permanent MCAO (pMCAO) in rats resulted in reduced infarct volumes and improved neurologic outcomes.[43]

Taking these results into account, there is ample evidence for a prominent role of both platelets and components of the coagulation cascade in the pathology of ischemic stroke. However, the consequences of specifically targeting the crosstalk between platelet activation and coagulation for infarct progression after ischemic stroke are unknown.

1.2.1.3. The multifarious roles of TMEM16F

It has been shown that both PS exposure and membrane ballooning or swelling support platelet procoagulant activity. Platelet ballooning is a tightly regulated process leading to increased surface area of the platelet membrane for augmented binding of vitamin K-dependent coagulation factors.[44, 45] Membrane ballooning is abolished in Scott Syndrome platelets, as well as in platelets from mice deficient in TMEM16F, revealing a role for the scramblase in this process.[44, 46] Whether this activity is linked to the scramblase or channel function of TMEM16F remains to be established.

An unexpected role for TMEM16F in bone mineralization has also been demonstrated. TMEM16F constitutive KO mice generated by targeted deletion of exon 1 show reduced skeleton size and other skeletal deformities associated with impaired bone mineralization. Such defects have not been reported for Scott Syndrome patients. Notably, 60% of these TMEM16F constitutive KO mice were reported to die at birth.[47]

Mattheij *et al*. also documented reduced viability of TMEM16F deficient mice demonstrating a role for the protein in embryogenesis and survival. The authors reported embryos to present with major abdominal and intra-cranial bleeding and exencephaly.[46]

Besides the well-established role for TMEM16F in PS exposure and microparticle formation, membrane swelling, survival and channel activity, in recent years its involvement in a wide repertoire of disease states has also become apparent. Mice deficient in TMEM16F have greater cartilage erosion and damage in an experimental model of rheumatoid arthritis due to impaired production of anti-inflammatory protein bearing microvesicles from neutrophils that are able to penetrate the cartilage. This revealed a protective role for TMEM16F activity in arthritis.[48] TMEM16F also supports immune defense by macrophages.[49] Intestinal epithelial cells express TMEM16F that contributes to precipitating diarrhea during cholera infection.[50] Using myeloid lineage specific TMEM16F conditional KO mice Batti *et al.* demonstrated a role for TMEM16F expressed on microglial cells in the pathogenesis of neuropathic pain.[51] TMEM16F was also identified as a lipid scramblase in T cells where it functions to limit excessive T cell responses in chronic viral infections.[52] A genome-wide association mapping narrowed down upon *Ano6* as one of the top three candidate genes to play a role in acute lung injury. Significant inverse association between mRNA levels of *Ano6* and lung inflammation was reported.[53] In a very recent study, binding of human immunodeficiency

virus (HIV) to its receptors in target cells has been shown to trigger TMEM16F-induced PS exposure that serves to facilitate HIV-1 entry into the cell.[54]

In summary, since the identification of TMEM16F in 2010 and the recent confirmation of its scramblase activity, its role in several (patho)physiological processes has been increasingly recognized generating even further interest in identifying processes where calcium-induced phospholipid scrambling plays a role.

1.2.2. Xkr-8 (Caspase-dependent phospholipid scramblase)

The process of PS exposure through the activity of a scramblase does not only have a functional role for platelet activation and procoagulant activity, but in most cells it marks the process of apoptosis – where exposed PS serves as a signal on apoptotic cells such that they can be engulfed by phagocytes. Using platelets from a Scott Syndrome patient, it has been shown that TMEM16F independent pathways also lead to PS-exposure in platelets when stimulated with proapoptotic agents ABT737 or ABT263, that activate caspase-dependent apoptosis.[55] This indicated the involvement of alternative mechanisms for PS exposure in apoptotic cells.

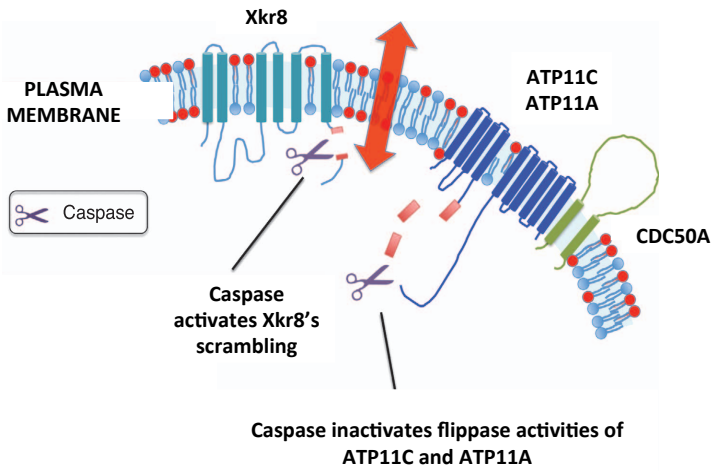

Figure 6. The caspase-dependent scramblase Xkr-8. For PS exposure in apoptotic cells, caspase 3 or caspase 7-mediated cleavage inactivates flippases (ATP11C and ATP11A associated with CDC50A), whereas caspase cleavage of scramblase Xkr8 leads to its activation. Caspase-dependent phospholipid scrambling abolishes phospholipid asymmetry and causes irreversible exposure of PS on the extracellular leaflet. Macrophages recognize the exteriorized PS on apoptotic cells and engulf them. (Taken from Nagata *et al., Cell Death Differ*. 2016).[8]

The identity of a scramblase that elicits apoptotic PS exposure has only recently been determined. The Nagata lab, which also uncovered the scramblase activity of TMEM16F, identified the mammalian protein Xkr-8 and its *C.elegans* homologue CED-8 to promote apoptotic PS exposure. Mouse Xkr-8 knockout cells were unable to expose PS during apoptosis and were not efficiently engulfed by phagocytes.[56]

Xkr-8 belongs to the family of Xk-related protein family that consists of 9 members in humans and 8 members in mice. In addition to Xkr-8, a report by Suzuki *et al.* also identified Xkr-4 and Xkr-9 as proteins that support apoptotic PS exposure. All three proteins, Xkr 4, 8 and 9 were found to contain caspase recognition sites in their C-terminal region, which needs to be cleaved during apoptosis in order to activate scramblase activity (Figure 6). However, it remains to be seen whether Xkr proteins are scramblases themselves, or whether they are proteins that promote PS exposure.

There are key differences in apoptotic PS exposure versus activation-induced PS exposure. While the activity of TMEM16F requires increased intracellular calcium concentrations, the activity of Xkr-8 requires cleavage by caspases. Also, while activation-induced PS exposure is reversible in nature, apoptosis-driven PS exposure is not.[8, 57, 58]

Xkr-4 is specifically expressed in the brain, and Xkr-9 is specifically expressed in eyes and intestine. On the other hand, Xkr-8 has broad tissue expression.[57] However, platelet proteomics data indicates that Xkr-4, 8 or 9 are not expressed in human or mouse platelets.[59] Therefore a platelet scramblase that supports apoptotic PS-exposure remains to be identified.

1.3. The intrinsic pathway of coagulation

The coagulation cascade, the ultimate goal of which is to convert fibrinogen to fibrin, can be initiated either through interaction of coagulation FVII with exposed tissue factor on damaged subendothelium – this pathway is known as the extrinsic pathway of coagulation. Alternatively, it can be initiated through activation of FXII (Hageman factor) when it comes in contact with negatively charged surfaces – the branch of the coagulation cascade known as the intrinsic pathway or the contact pathway (Figure 7). For several decades, only the extrinsic pathway of coagulation was considered to be of physiological relevance, as humans with a deficiency of FXII do not suffer from hemostatic defects, and no physiological triggers were known that would activate zymogen FXII to the active serine protease FXIIa. On the other hand, deficiency of FVII in humans results in a severe bleeding diathesis. [37]

In 2005, FXII knockout (FXII KO) mice were tested in *in vivo* models of hemostasis and arterial thrombosis for the first time. These studies revealed that similar to the situation in humans, deficiency of FXII has no effect on bleeding times in mice. However, surprisingly, FXII deficient mice were profoundly protected from thrombotic vessel occlusion, revealing a novel role for the coagulation factor in this pathological process.[60] A year later, FXII KO mice were also reported to be protected in the tMCAO model of ischemic stroke with strikingly lower infarct volumes and improved functional outcomes 24 h after induction of 60 min focal cerebral ischemia followed by reperfusion.[38] Interestingly, 'rescue experiments' were performed in both these studies where purified human FXII was infused *i.v*. into FXII KO mice followed by testing in models of arterial thrombosis and stroke. The presence of human FXII in the mouse system deficient in endogenous murine FXII reverted the phenotype observed in the KO mice i.e. supplementation with human FXII resulted in vessel occlusion times and infarct volumes comparable to WT mice in the two models respectively.[38, 60] These studies provided important indications that human FXII is functional within murine physiology.

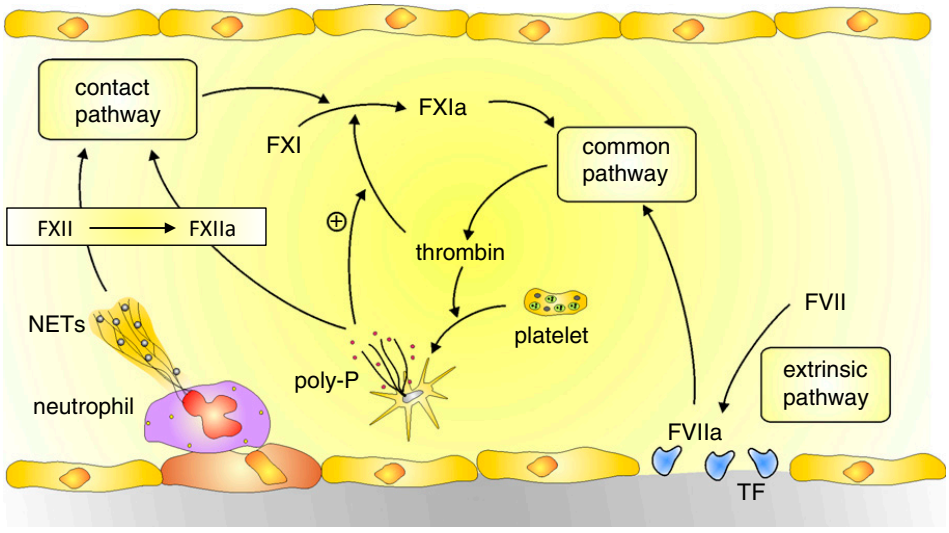

Figure 7. Tissue factor (TF) exposed on the endothelial cells at the site of vessel wall injury triggers the extrinsic pathway of coagulation on interaction with activated factor VIIa. Polyphosphates released from dense granules of activated platelets initiate the contact (intrinsic) pathway of coagulation by activating FXII. Neutrophil extracellular traps (NETs) formed when activated neutrophils release protein-decorated modified chromatin, can also activate FXII. Both the intrinsic and the extrinsic pathways converge into the common pathway of coagulation and thrombin generation that converts fibrinogen to fibrin. (Taken from Fredenburgh *et al. Blood* 2017).[61]

The *F12 gene* encoding FXII is located on chromosome 5 in humans and consists of 13 exons, whereas it is located on chromosome 13 in mice and is composed of 14 exons. Both

code for an 80 kDa FXII zymogen, with a 71% amino acid sequence identity between the human and mouse protein.[62]

In addition to its role in the intrinsic pathway of coagulation, activation of FXII also initiates the pro-inflammatory kallikrein-kinin system, which leads to the conversion of high-molecular-weight kininogen to bradykinin that plays a role in various inflammatory processes.

Non-physiological activators of FXII have long been known and include glass and the silicate kaolin. The latter is frequently employed to carry out the clinical diagnostic test aPTT (activated partial thromboplastin time) to determine blood-clotting times. Physiological activators of FXII have been identified more recently and are still the subject of ongoing research. These *in vivo* activators include negatively charged polyP released from platelet dense granules, neutrophil extracellular traps (NETs), as well as heparin and misfolded proteins.[63]

1.3.1. Targeting FXII – protection from arterial thrombosis and ischemic stroke

Currently employed antithrombotic therapies are characterized by the common adverse effect of inducing bleeding complications. Therefore, targeting FXII has emerged as a promising alternative to provide protection from thrombosis without altering hemostasis, There are numerous reports in literature on the use of different classes of FXII/FXIIa inhibitors including antibodies, small-molecule inhibitors and oligonucleotides, with favorable results in a variety of experimental models including extracorporeal circulatory systems, thrombosis and the tMCAO model of ischemic stroke.[64]

The biological FXIIa inhibitor infestin-4 obtained from the midgut of *Triatoma infestans* fused to recombinant human albumin (rHA-Infestin-4) has been tested in models of arterial thrombosis in mice and rats and has been found to completely abolish occlusive thrombus formation without altering hemostasis.[39, 65] Inhibition of FXIIa with rHA-Infestin-4 also provided protection from progression of ischemic damage in experimental models of stroke in both mice and rats.[40, 66] A number of blocking antibodies against FXII/FXIIa have also been developed. The humanized antibody 3F7 that blocks FXIIa has been tested in experimental models of arterial and venous thrombosis where it provided protection from pathological thrombosis without altering bleeding times. 3F7 has also been tested as an anticoagulant in an extracorporeal membrane oxygenation (ECMO) cardiopulmonary bypass system in rabbits

where its anticoagulant activity was comparable to that of the routinely used anticoagulant heparin. While the gas-exchanging capillaries of the oxygenators of the ECMO system were blocked within minutes due to blood clotting and deposition of fibrin in the experimental setup where rabbits were pre-treated with saline, pre-treatment with either heparin or 3F7 prevented fibrin deposition in the ECMO system, with 3F7 having the added advantage that it does not adversely affect the hemostatic response.[67] Another blocking antibody, 15H8 that inhibits activation of FXII has been tested in a primate thrombosis model where collagen-coated vascular grafts were inserted into arteriovenous shuts in baboons. Pre-treatment of the animals with 15H8 reduced fibrin and platelet accumulation within the thrombogenic grafts.[68]

These encouraging results have highlighted the potential for the use of FXII inhibitory agents as treatment options for thrombo-inflammatory disease states, as well as their use as safe antithrombotics.

1.4. (Hem)ITAM signaling in mouse platelets – GPVI and CLEC-2

One of the major pathways for platelet activation involves immunoreceptor tyrosine-based activation motif (ITAM)-regulated signaling. Human platelets express two receptors bearing the classical ITAM-motif Yxx(I/L)x(6-12)Yxx(I/L), i.e. tyrosine separated from a leucine or isoleucine by two other amino acids, and two such sequences typically separated by 6-12 amino acids. The first of these receptors is glycoprotein (GP)VI-FcRγ-chain complex. GPVI is an immunoglobulin (Ig) surface receptor that is non-covalently associated with a FcRγ-chain homodimer. Each chain of this homodimer contains one copy of the ITAM motif in its cytoplasmic tail and thus FcRγ-chain serves as the signaling subunit of the receptor complex.[69, 70] The second ITAM receptor is the IgG constant fragment (Fc) receptor, FcγRIIA. In addition, human platelets also express C-type lectin-like receptor 2 (CLEC-2) that bears the so-called hemITAM motif i.e. a single YxxL motif in the intracellular domain. On the other hand, mouse platelets only express the GPVI-FcRγ-chain complex and CLEC-2 (Figure 8).[71]

ITAM and hemITAM signaling in platelets bear several similarities. In both pathways the YxxL motifs are docking sites for a similar set of signaling molecules containing Src Homology 2 (SH2) domains, and the activation of both initiates a tyrosine phosphorylation signaling cascade which finally results in the activation of the effector enzyme PLCγ2.[72] Ligand binding of GPVI results in receptor crosslinking and activation through phosphorylation of tyrosine residues on the ITAM motifs of the FcRγ-chain by the Src family kinases (SFK) Fyn and Lyn.

This further leads to recruitment of the tandem SH2 domain bearing tyrosine kinase Syk, the phosphorylation and activation of which results in the recruitment and activation of the adapter linker for activation of T cells (LAT) and the assembly of the LAT signalosome which encompasses several other adapters proteins and enzymes (Figure 8). However, ITAM and hemITAM signaling differ from each other in the sequence of the first steps of the tyrosine phosphorylation cascade. Upon ligand engagement of CLEC-2, dimerization of the receptor takes place followed by phosphorylation of the YXXL motifs of the dimer primarily by the kinase Syk, whereas phosphorylation of the FcRγ-chain ITAM is SFK dependent.[73, 74]

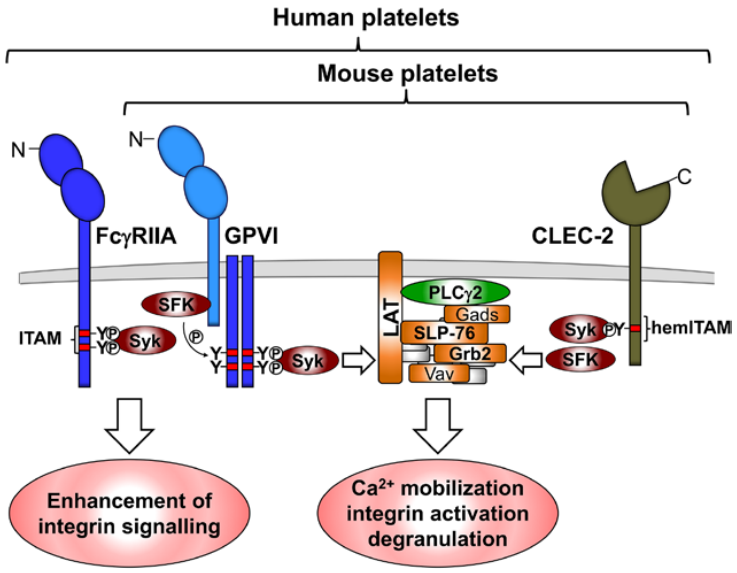

Figure 8. Platelet (hem)ITAM receptors. The Fc receptor FcγRIIA is expressed in human but not mouse platelets. It signals through an ITAM motif in its cytoplasmic tail and plays an important role in integrin outside-in signaling. The receptor GPVI is associated with a homodimer of FcRγ-chain that bears the ITAM motif in its cytoplasmic tail. Ligand binding of GPVI leads to phosphorylation of FcRγ-chain ITAM motifs by Src family kinases (SFK). This recruits and activates the spleen tyrosine kinase Syk which in turn results in recruitment and activation of the adapter LAT and the assembly of the LAT signalosome incorporating several other adapter proteins (depicted in orange) as well as effector proteins (depicted in green). The hemITAM receptor CLEC-2 bears a single YxxL motif that is phosphorylated by the kinase Syk on dimerization of the receptor following ligand engagement. This is followed by assembly of the LAT signalosome similar to signaling events downstream of GPVI. (Taken from Stegner *et al., ATVB* 2014).[71]

A notable observation in studies involving a number of important players of (hem)ITAM signaling is the frequent existence of functional redundancy between closely related proteins. There are instances of absolute functional redundancy, for example Vav1 and Vav3 that play critical but redundant roles in the activation of PLCγ2 through GPVI.[75] The Src like adapter

proteins SLAP and SLAP2 that negatively regulate (hem)ITAM signaling are also functionally redundant.[76] Besides these, there are cases where the nature of functional compensation is such that one isoform plays a more important role than the other, as is the case for PLCγ isoforms. Between PLCγ1 and PLCγ2, it is the latter that plays a predominant role in murine platelets.[77] Also between the Tec kinase Btk and Tec, it is the former that plays a more prominent role in platelet activation through GPVI.[78] On the other hand, there are no known compensatory functional homologues for proteins Syk and SLP-76.[79]

GPVI has been known to bind to, and to be activated by sub-endothelial matrix proteins collagen and laminin.[70] Recently, two independent studies also reported the binding of GPVI to fibrin, the end product of the coagulation cascade.[80, 81] GPVI binding to fibrin also leads to receptor activation. While collagen, the major physiological ligand for GPVI, is also a ligand for the integrin α2β1 and glycoprotein (GP)V,[70, 82] collagen related peptide (CRP) and the snake venom toxin convulxin are known GPVI specific ligands.[70] CRP contains repeat glycine-proline-hydroxyproline (GPO) motifs in a helical conformation, the well-defined structure that GPVI recognizes in collagen. Convulxin, the toxin obtained from the venom of rattlesnake *Crotalus durissus terrificus,* is capable of crosslinking four GPVI receptors and thus is a very powerful stimulus for GPVI activation.[79, 83]

The only known physiological ligand of CLEC-2 is podoplanin, expressed in several tissues including kidney podocytes (hence the name), lung alveolar cells, lymphatic endothelial cells and some tumors.[70] However, an intravascular ligand that is expressed in platelets and vascular endothelium remains to be determined. *In vitro*, binding of the snake venom toxin rhodocytin to CLEC-2 also initiates the hemITAM-signaling pathway.[84]

1.4.1. (Hem)ITAM signaling in hemostasis, thrombosis and vascular integrity

It is now well recognized that the signaling processes involved in hemostasis and thrombosis can be partially uncoupled.[85, 86] While GPCR-regulated platelet signaling pathways have been predominantly implicated to be important for the physiological process of hemostasis, many key players in the (hem)ITAM signaling pathway have been identified to play a less prominent role in hemostasis with a greater contribution in other processes, including pathological thrombosis formation.[86, 87]

In mice, genetic ablation, specific antibody-induced down-regulation on circulating platelets or blockade of the ITAM receptor GPVI all yield protection from pathological thrombus formation

with minimal impact on the physiological hemostatic response.[86] Antibody-mediated specific down-regulation of the hemITAM receptor CLEC-2 from circulating platelets in mice also results in profound protection from arterial thrombosis accompanied with only a moderate hemostatic defect.[88] The kinase Syk, downstream of (hem)ITAM signaling exhibits a similarly skewed disposition exhibiting a greater role for thrombosis than hemostasis. Megakaryocyte- and platelet-specific Syk KO mice are protected from thrombosis with only moderately prolonged bleeding times. On the other hand, pharmacological inhibition of Syk in mice also resulted in protection from occlusive thrombus formation with unaltered bleeding times in experimental models.[89, 90] In addition, demonstrating their contribution to thrombo-inflammatory disease states, depletion of GPVI, or Syk deficiency in mice provided protection from ischemia/reperfusion injury without precipitating intracerebral bleeding in the experimental tMCAO model of ischemic stroke.[89, 91] These promising results have led to the exploration of several of these molecules as novel targets for designing antithrombotic agents.

Interestingly, studies in mice with a megakaryocyte- and platelet-specific deficiency in the adapter protein Grb2, a component of the LAT signalosome downstream of (hem)ITAM signaling revealed a greater impact of the loss of the protein on hemostasis compared to thrombosis.[92]

Besides their classical role in hemostasis, the involvement of platelets in several other processes such as separation of lymphatics and blood vasculature during embryogenesis and vascular integrity in inflammation has been increasingly recognized. Knockout mice deficient in either CLEC-2, Syk, SLP-76 or PLCγ2 exhibit blood-lymphatic mixing and embryonic/perinatal lethality due to hemorrhages indicating an important role for hemITAM signaling in the proper development of lymphatic and blood vasculature.[87] A specific role for (hem)ITAM signaling in the maintenance of vascular integrity and prevention of development of hemorrhages during inflammation has also been recognized. Defective GPVI and CLEC-2 signaling, or deficiency of adapter protein SLP-76 lead to loss of platelet-mediated vascular integrity in experimental models of immune complex-mediated inflammation of the skin, or LPS-induced inflammation in the lung.[93]

1.4.2. Role of adapters in (hem)ITAM signaling

Adapter proteins lack intrinsic enzymatic activity, yet they are important for protein-protein and protein-lipid interactions that facilitate the formation of three-dimensional signaling complexes. These proteins contain conserved interaction domains through which communication with other proteins is mediated (e.g. SH2 domain for binding to tyrosine-based signaling motifs and SH3 domains for binding to proline-rich sequences). Therefore, adapter proteins help to recruit signal-transducing proteins to large signaling complexes and form an association between surface receptors and cytosolic signaling pathways such that appropriate cellular responses can be achieved to externally applied stimuli.[94]

A number of adapter proteins are involved in the assembly of signaling complexes downstream of GPVI and CLEC-2 activation (Figure 8).[71] One such protein is linker for activation of T cells (LAT). LAT is a transmembrane adapter protein with a short extracellular domain, and a large cytoplasmic domain through which it serves to recruit intracellular SH2 domain-containing signaling molecules to the plasma membrane owing to the presence of numerous tyrosine residues.[94] Following GPVI or CLEC-2 stimulation, tyrosine phosphorylation of the kinase Syk leads to recruitment and tyrosine phosphorylation of LAT that then associates with other adapter proteins and enzymes. The importance of LAT for platelet function is underscored by defective tyrosine phosphorylation of effector enzyme PLCγ2 in LAT-deficient platelets as well as defective hemostasis and thrombosis in LAT KO mice in comparison to WT mice.[95, 96] The adapter proteins that are known to form a part of the LAT signalosome include SLP-76, Grb2, Gads and Vav proteins that are all cytosolic proteins.[71, 94] SLP-76 is important for signaling downstream of GPVI and integrin αIIbß3.[97] Mice deficient in SLP-76 display fetal hemorrhages and perinatal lethality as well as blood and lymphatic vessel mixing as described in the previous section.[98, 99] In addition, knock-in mice with tyrosine to phenylalanine mutations in SLP-76 are protected in an experimental model of thrombosis.[100] Therefore the adapter plays an important role in platelet function downstream of (hem)ITAM signaling. The role of adapter proteins Grb2 and Gads for platelet function is described in detail in section 1.5.

The proteins Vav1 and Vav3 are associated with adapter function in addition to being guanine nucleotide exchange factors (GEFs) for the Rho/Rac family of small GTP-binding proteins. They have been shown to play key roles in mediating platelet activation downstream of ITAM signaling. However, it is not known whether this activity arises due to their adapter function or due to their GDP/GTP exchange factor activity.[75]

1.5. Grb2 family of adapter proteins

The Grb2 family of adaptor proteins consists of three members – growth factor receptor-bound protein 2 (Grb2); Grb2 related adaptor protein (Grap) and Grb2 related adaptor protein downstream of Shc (Gads, also known as Grap2). All three members have a similar structure, with a central Src Homology 2 (SH2) domain through which binding to tyrosine phosphorylated sequences takes place, flanked by two Src Homology 3 (SH3) domains that allow direct complex formation with proline-rich regions of other proteins (Figure 9). [101]

Grb2 has a broad expression in tissues, while the expression of Grap and Gads is limited to the hematopoietic cells. However, only two members of this adaptor protein family are expressed in platelets – Grb2 and Gads.[59, 102]

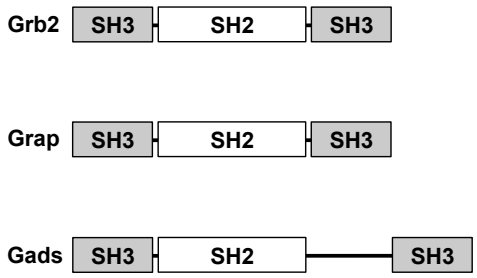

Figure 9. Schematic representation of the Grb2 family of adapter proteins. All three members, Grb2, Grap and Gads contain a central SH2 domain for binding to phospho-tyrosines. Two SH3 domains that mediate binding to proline-rich regions of other proteins flank the central SH2 domain. Gads differs from the other two family members as it contains a unique 'linker region' between the SH2 domain and the carboxy-terminal SH3 domain. (Modified from Liu *et al., Oncogene* 2001).

Both Grb2 and Gads can bind to the adaptor LAT and are integral components of the LAT signalosome downstream of (hem)ITAM signaling. There are three sites for association of Grb2 with LAT, at phospho-tyrosines Y171, Y191 and Y226. Gads can associate with LAT at Y191, and to a lesser extent at Y171.[95]

1.5.1. Role of Gads in platelet function

Studies on effects of the loss of Gads on some aspects of platelet function were reported in 2008 when Hughes *et al.* conducted experiments in mice with a constitutive deletion of Gads. The deficiency of Gads resulted in only minor defects in platelet function when stimulated

with the GPVI specific agonist CRP, or the CLEC-2 specific agonist rhodocytin. Impaired platelet aggregation and secretion were observed, but only on stimulation with low concentration of (hem)ITAM agonists. These responses were comparable to WT platelet responses on stimulation with the GPCR agonist thrombin or on stimulation with higher concentration of CRP and rhodocytin. In addition, a small decrease in tyrosine phosphorylation of SLP-76 and PLCγ2 was observed on stimulation with either CRP or rhodocytin. Surprisingly, the authors also reported a very small but consistent decrease in tyrosine phosphorylation of Syk, a kinase that lies upstream of the assembly of LAT signalosome in the (hem)ITAM signaling cascade. No defects were seen in platelet spreading on fibrinogen or vWF/botrocetin, as well as platelet adhesion and aggregation on collagen under flow conditions. Importantly, these mice were not challenged in *in vivo* experimental models of hemostasis or thrombosis.

Based on these results, the authors reported Gads to play a relatively minor role in mediating platelet activation via GPVI and CLEC-2 and hypothesized that either there exist Gads-independent pathways of platelet activation downstream of LAT and SLP-76, or the role of Gads is masked by the presence of the second protein family member Grb2.[95]

1.5.2. Role of Grb2 in platelet function

Grb2 constitutive KO mice are embryonic lethal, indicating important functions of the adapter protein for embryo development.[103] In 2014, comprehensive studies on the effects of loss of Grb2 on platelet function conducted in megakaryocyte- and platelet-specific conditional KO mice (Grb2 KO) were reported from our laboratory. Dütting *et al.* observed a much more severe (hem)ITAM specific signaling defect in platelets obtained from Grb2 KO mice than was reported for platelets from Gads KO mice.

Platelets lacking Grb2 displayed severely impaired activation and aggregation responses on stimulation with low and intermediate concentrations of the GPVI specific agonists CRP and convulxin, as well as the CLEC-2 specific agonist rhodocytin, whereas the activation and aggregation responses were comparable to WT platelets on stimulation with GPCR agonists thrombin, ADP and the TxA_2 analog U46619. The defects in platelet aggregation could be overcome on stimulation with higher agonist concentrations. Grb2 KO platelets also showed significantly reduced PS exposure on stimulation with CRP and rhodocytin, and impaired calcium mobilization on stimulation with CRP indicating a prominent role of Grb2 in promoting

(hem)ITAM-regulated procoagulant activity in platelets. Grb2 KO platelets also display dramatically reduced adhesion and aggregation on collagen under flow compared to WT mice as tested in an *ex vivo* flow chamber assay.

These defects in activation and aggregation studies corroborated by signaling defects in tyrosine phosphorylation studies – while the proteins upstream of the LAT signalosome (CLEC-2, FcRγ-chain, Syk) had normal levels of tyrosine phosphorylation, on stimulation with convulxin or rhodocytin, tyrosine phosphorylation of LAT at Y191 and tyrosine phosphorylation of proteins downstream of LAT (PLCγ2, SLP-76, Vav3) was significantly reduced, but not abolished.

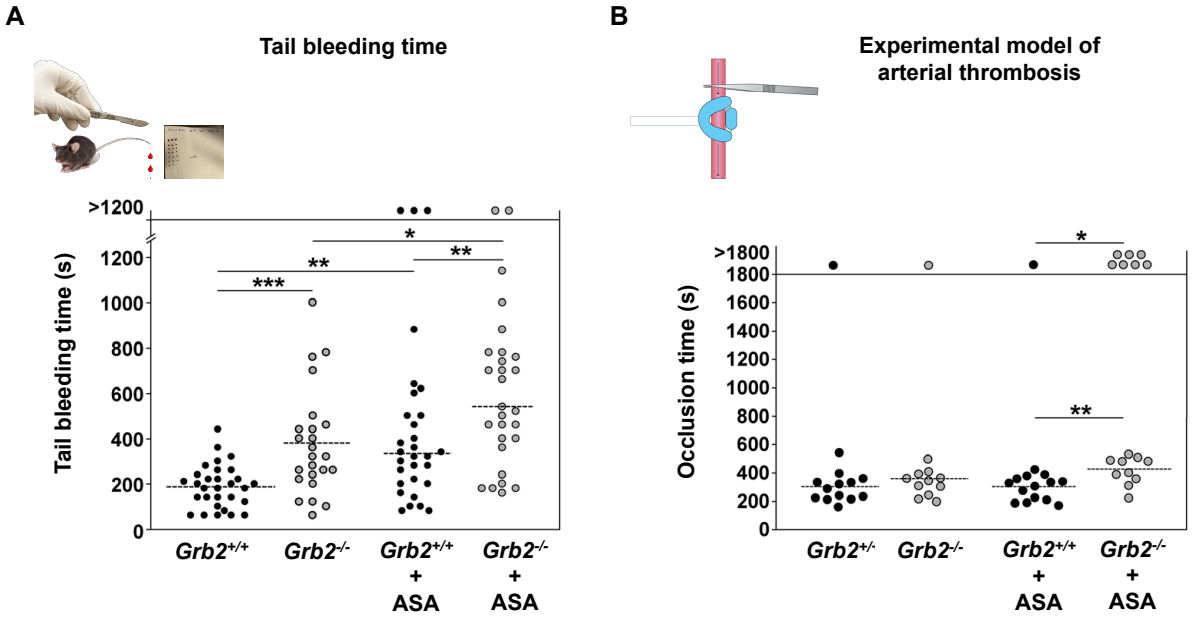

Figure 10. *In vivo* consequences of megakaryocyte- and platelet-specific Grb2 deficiency with or without acetylsalicylic acid (ASA) treatment. (A) Experimental model of hemostasis – measurement of bleeding time by filter paper method. 1 mm of the tail tip of anaesthetized mice was removed with a scalpel and blood was blotted on a filter paper until cessation of bleeding. The impairment in hemostasis in Grb2 KO mice (*Grb2*$^{-/-}$) was further exacerbated on interfering with TxA_2 synthesis through *i.v.* administration of 1 mg/kg ASA 15 min before the start of the experiment. (B) Experimental model of arterial thrombosis. Thrombosis was induced by mechanical injury of the abdominal aorta through a single firm compression with forceps. While the time to stable vessel occlusion was comparable between WT and Grb2 KO animals without ASA treatment, Grb2 KO animals showed defective thrombosis following treatment with ASA. Each dot represents one animal. *P<0.05, **P<0.01,***P<0.001. (Taken from Dütting *et al., Circ. Res*. 2014)[92]

Surprisingly, when Grb2 KO mice were challenged in *in vivo* models of hemostasis and thrombosis, a very different degree of impairment of platelet function was seen compared to the *in vitro* experiments. In the hemostasis assay, analyzed by measuring tail bleeding times by filter paper method, these mice displayed only minor defects in hemostatic function and a

large variation was recorded in bleeding times recorded for individual animals. Even more surprisingly, in the experimental models of arterial thrombosis, no differences were observed between WT and Grb2 KO mice. However, when WT and Grb2 KO animals were challenged in experimental hemostasis and thrombosis models after the administration of acetylsalicylic acid to interfere with thromboxane (TxA_2) synthesis, the bleeding times in Grb2 KO animals was even further increased than without asprin treatment, and two populations were observed in the case of the thrombosis model – occlusion times were significantly prolonged than those observed in WT animals for some KO animals, while in others, stable vessel occlusion was not observed in the 30 min observation period (Figure 10). Thus, the authors could show experimentally that the inconsistency between the *in vitro* and *in vivo* observations arises partially due to compensation of the defective (hem)ITAM signaling through TxA_2-induced GPCR signaling pathways.

However, taking into account the residual phosphorylation of LAT and PLCγ2 in the absence of Grb2, and the less pronounced (hem)ITAM signaling defects in Grb2 KO mice compared to LAT KO mice, the authors speculated that the presence of Gads could be compensating for the loss of Grb2 in Grb2 KO animals.[92]

1.6. Aims of this thesis

The first aim of this thesis was to investigate the relevance of TMEM16F-mediated platelet procoagulant activity in the pathology of arterial thrombosis and ischemic stroke. It is now known that cerebral-ischemic stroke is a thrombo-inflammatory disease condition and its progression involves a myriad of contributing factors including platelets, immune cells and components of the coagulation cascade. However, the role of procoagulant platelets in these settings had remained uninvestigated. Therefore, platelet function and procoagulant activity was characterized in a novel TMEM16F conditional knockout mouse line in which the KO mice lack the scramblase specifically in megakaryocytes and platelets. This mouse line served as a model to study the impact of impaired platelet procoagulant response for arterial thrombosis and ischemic stroke using *in vivo* experimental models.

The second section of this thesis dealt with the generation and characterization of novel humanized coagulation FXII knockin mice that express human factor XII instead of endogenous murine FXII. These mice will serve as a unique tool to test experimental anti-thrombotic agents directed against human FXII in an *in vivo* system that closely mimics the hemodynamic and spatiotemporal interactions encountered in humans.

The third part of this thesis focused on examining the possibility of redundant roles between the closely related adapter proteins Grb2 and Gads for platelet activation and function downstream of (hem)ITAM signaling. Functional compensation between closely related key proteins downstream of (hem)ITAM signaling has been frequently observed and previous investigations on the role of either Grb2 or Gads in platelet function have hypothesized redundancy between the two proteins, although this had not been tested experimentally. Therefore, Grb2/Gads double knockout mice lacking both adapters in megakaryocytes and platelets were generated and platelet function assessed in *in vitro* and *in vivo* studies.

2. Materials and Methods

2.1. Materials

2.1.1. Kits and Reagents

Reagent	Company
2,3,5-triphenyltetrazolium chloride	Sigma-Aldrich (Schnelldorf, Germany)
A23187	Merck Millipore (Darmstadt, Germany)
Adenosine diphosphate (ADP)	Sigma-Aldrich (Schnelldorf, Germany)
Agarose	Roth (Karlsruhe, Germany)
Alexa Fluor 647-Fibrinogen	Life Technologies (New York, USA)
Amersham® Hyperfilm®, ECL	GE Healthcare (Little Chalfont, UK)
Ammonium persulphate (APS)	Roth (Karlsruhe, Germany)
Apyrase (Grade III)	Sigma-Aldrich (Schnelldorf, Germany)
Bovine serum albumin (BSA)	AppliChem (Darmstadt, Germany)
Bovine serum albumin (BSA), low endotoxin	PAA (Cölbe, Germany)
Brij® O10	Sigma-Aldrich (Schnelldorf, Germany)
Collagen Horm® suspension + SKF sol.	Takeda (Linz, Austria)
cOmplete, Mini protease inhibitor cocktail (# 11836153001)	Roche Diagnostics (Mannheim, Germany)
Convulxin	Enzo Life Sciences (Lörrach, Germany)
Cryo-Gel	Leica Biosystems (Wetzlar, Germany)
Dade® Innovin (tissue factor)	Siemens Healthcare Diagnostics (Deerfield, IL, USA)
$DiOC_6$	AnaSpec (Reeuwijk, The Netherlands)
dNTP Mix (10 mM)	Life Technologies (Darmstadt, Germany)

Reagent	Company
DreamTaq hot start DNA polymerase	ThermoFischer Scientific (Darmstadt, Germany)
EDTA	AppliChem (Darmstadt, Germany)
Factor XII Human ELISA Kit (ab108835)	Abcam (Cambridge, UK)
Fat-free dry milk	AppliChem (Darmstadt, Germany)
$FeCl_3 \cdot 6\ H_2O$	Roth (Karlsruhe, Germany)
Fentanyl	Janssen-Cilag (Neuss, Germany)
Fibrinogen from human plasma (# F3879)	Sigma-Aldrich (Schnelldorf, Germany)
Fibrinogen from human plasma (# F4883)	Sigma-Aldrich (Schnelldorf, Germany)
Flumazenil	AlleMan Pharma (Pfullingen, Germany)
GeneRuler DNA Ladder Mix	Life Technologies (Darmstadt, Germany)
Glutaraldehyde solution (25%)	Science Services (Munich, Germany)
Heparin sodium	Ratiopharm (Ulm, Germany)
HEPES (4-(2-hydroxyethyl)-1-piperazine-ethanesulfonic acid)	Life Technologies (Darmstadt, Germany)
IGEPAL® CA-630	Sigma-Aldrich (Schnelldorf, Germany)
Immobilon-P transfer membrane, PVDF, 0.45 µm	Merck Millipore (Darmstadt, Germany)
Indomethacin	Sigma-Aldrich (Schnelldorf, Germany)
Ionomycin, free acid	Merck Millipore (city?)
Isoflurane CP®	cp-pharma (Burgdorf, Germany)
Medetomidine	Pfizer (Karlsruhe, Germany)
Midazolam	Roche (Grenzach-Wyhlen, Germany)
Midori Green Advanced DNA stain	Nippon Genetics Europe (Düren, Germany)
Naloxon	AlleMan Pharma (Pfullingen, Germany)
NuPAGE® LDS Sample Buffer (4x)	ThermoFischer Scientific (Darmstadt, Germany)

Reagent	Company
NuPAGE® MOPS SDS running buffer	ThermoFischer Scientific (Darmstadt, Germany)
NuPAGE® Novex® 4-12% Bis-Tris Gels, 1mm, 10 well, 15 well	ThermoFischer Scientific (Darmstadt, Germany)
PageRuler Prestained Protein Ladder (# 26616, 26619)	Life Technologies (Darmstadt, Germany)
Paraformaldehyde (PFA)	Sigma-Aldrich (Schnelldorf, Germany)
Phenol/chloroform/isoamyl alcohol	Roth (Karlsruhe, Germany)
Prostacyclin (PGI_2)	Calbiochem (Bad Soden, Germany)
Protease inhibitor cocktail (# P8340)	Sigma-Aldrich (Schnelldorf, Germany)
Proteinase K, recombinant, PCR grade (20 mg/ml)	Life Technologies (Darmstadt, Germany)
Purified Human FXII (#HCXII-0155)	Haematologic Technologies (Vermont, USA)
RiboLock RNase inhibitor (40U/µL)	ThermoFischer Scientific (Darmstadt, Germany)
RNase A (# R4875)	Sigma-Aldrich (Schnelldorf, Germany)
Rotiphorese® Gel 30 (37,5:1) acrylamide	Roth (Karlsruhe, Germany)
SeeBlue® Plus2 pre-stained standard	Life Technologies (Darmstadt, Germany)
SERVA BlueBlock PF	SERVA Electrophoresis GmbH, Heidelberg
Sodium orthovanadate	Sigma-Aldrich (Schnelldorf, Germany)
Sphero™ AccuCount fluorescent particles	Spherotech (Fulda, Germany)
Streptavidin-HRP (# 016-030-084)	Jackson ImmunoResearch (West Grove, PA, USA)
SuperScript™ III Reverse transcriptase	ThermoFischer Scientific (Darmstadt, Germany)
Taq DNA polymerase (5 U/µl without BSA) (# EP0282)	Life Technologies (Darmstadt, Germany)
TEMED (N,N,N',N'-Tetramethylethylen-ediamine)	Roth (Karlsruhe, Germany)

Reagent	Company
Thrombin from human plasma (# 10602400001)	Roche Diagnostics (Mannheim, Germany)
TMB substrate reagent set	BD Biosciences (Heidelberg, Germany)
TRIzol® reagent	ThermoFischer Scientific (Darmstadt, Germany)
Tween® 20	Roth (Karlsruhe, Germany)
U-46619	Enzo Life Sciences (Lörrach, Germany)
Western Lightning® Plus-ECL	PerkinElmer (Baesweiler, Germany)

Collagen-related peptide (CRP) was generated as previously described.[104] Annexin A5 was generously provided by Jonathan F. Tait, University of Washington Medical Center and conjugated to DyLight 488 by standard methods. Rhodocytin was isolated as described.[105]

2.1.2. Antibodies

Purchased primary and secondary antibodies

Antibody	Company
Goat anti-rabbit IgG-HRP (#7074)	Cell Signaling (Danvers, MA; USA)
Mouse Anti-GRB2 (clone 3F2) (#05-372)	Merck Millipore (Darmstadt, Germany)
Mouse anti-phosphotyrosine (clone 4G10)	Merck Millipore (Darmstadt, Germany)
Rabbit anti-actin (#A2066)	Sigma-Aldrich (Schnelldorf, Germany)
Rabbit anti-GADS (#06-983)	Merck Millipore (Darmstadt, Germany)
Rabbit anti-GAPDH (#9545)	Sigma-Aldrich (Schnelldorf, Germany)
Rabbit anti-human FXII (#PA5-26672)	ThermoFischer Scientific (Darmstadt, Germany)
Rabbit anti-mouse IgG-HRP (#P0260)	DAKO (Hamburg, Germany)

Rabbit anti-phospho-LAT (Y191) (#3584)	Cell Signaling (Danvers, MA; USA)
Rabbit anti-total-LAT (#9166)	Cell Signaling (Danvers, MA; USA)
Rabbit anti-phospho-PLCγ2 (Y759) (#3874)	Cell Signaling (Danvers, MA; USA)
Rabbit anti-phospho-Syk (Y525/526) (clone C87C1) (#2710)	Cell Signaling (Danvers, MA; USA)
Rabbit anti-total- PLCγ2 (B-10) (#sc-5283)	Santa Cruz (Heidelberg, Germany)
Rabbit anti-total-Syk (clone D1I5Q) (#12358)	Cell Signaling (Danvers, MA; USA)

Prof. Karl Kunzelmann from the Department of Physiology, University of Regensburg, kindly provided the rabbit anti-Ano6 antibody.[24]

Monoclonal rat antibodies generated or modified in our laboratory

Antibody	Clone	Isotype	Antigen	References
p0p4	15E2	IgG2b	GPIbα	[106]
p0p3	7A9	IgG2a	GPIbα	[106]
DOM2	89H11	IgG2a	GPV	[107]
p0p6	56F8	IgG2b	GPIX	[107]
JAQ1	98A3	IgG2a	GPVI	[69]
INU1	11E9	IgG1	CLEC-2	[88]
ULF1	97H1	IgG2a	CD9	unpublished
LEN1	12C6	IgG2b	α2	[69]
EDL1	57B10	IgG2a	β3	[106]
JON2	14A3	IgG2a	αIIbβ3	[107]
JON/A	4H5	IgG2b	αIIbβ3	[108]
MWReg30	5D7	IgG1	αIIbβ3	[109]
WUG 1.9	5C8	IgG1	P-selectin	[110]
LEN/B	23C11	IgG2b	α2β1	[111]

2.1.3. Mice

The generation of TMEM16F constitutive, and megakaryocyte- and platelet-specific conditional KO mice is described in detail in section 3.1.1 and Figure 12. Mouse *Anoctamin6* (*Ano6*) gene has 20 exons spanning 184 kb on chromosome 15. A targeting strategy was designed to conditionally delete exon 3 of the *Ano6* gene by *Cre-loxP* system. This was designed to result in the generation of a frame-shift mutation and the introduction of a premature stop codon leading to the formation of a truncated, non-functional protein.

For generation of humanized factor XII-knockin mice (hFXII-KI – mice that express human FXII instead of endogenous mouse FXII), the entire sequence of mouse *F12* gene was replaced by the human *F12* gene sequence. The targeting strategy employed is depicted in Figure 11.

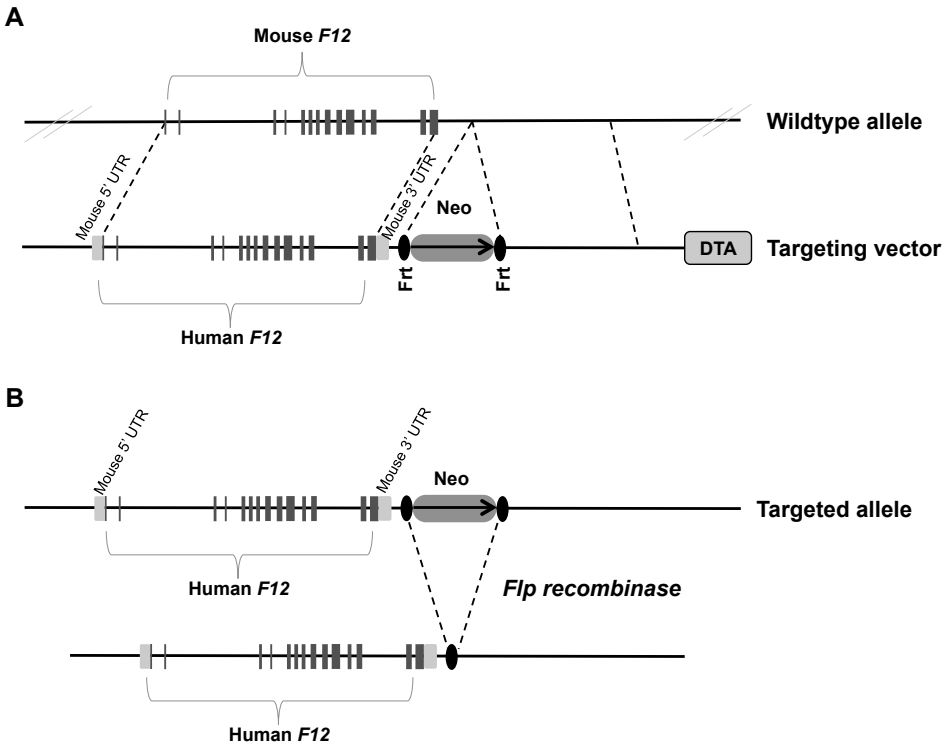

Figure 11. Generation of hFXII-KI mice. The *F12* gene is located on chromosome 13 in mice and is composed of 14 exons. Human *F12* gene is located on chromosome 5 and is composed of 13 exons. Both encode for an 80 kDa FXII with a 71% protein identity between humans and mice (A) For generation of hFXII-KI mice, the entire *F12* mouse gene was replaced by *F12* human gene. A neomycin resistance (neo) cassette flanked by Frt sites was used for selection of targeted alleles. (B) Mice bearing the targeted allele were intercrossed with mice expressing the *Flp* recombinase to eliminate the Neo selection cassette to obtain humanized FXII-knockin mice (hFXII-KI)

The generation of megakaryocyte- and platelet-specific *Grb2* conditional knockout (Grb2 KO – *Grb2* $^{fl/fl\ Pf4\text{-}Cre+/-}$) mice has been previously described.[92] The generation of *Gads* knockout mice (Gads KO – *Gads* $^{-/-}$) has also been previously described.[95] The Gads KO mice on a C57BL/6 background were received from the group of Prof. Steve Watson (Institute of Cardiovascular Sciences, University of Birmingham). The Grb2 KO mice were inter-crossed with the Gads KO mice for the generation of animals with a double deficiency of both adapter proteins Grb2 and Gads (Grb2/Gads double knockout mice, DKO - *Gads* $^{-/-}$/ *Grb2* $^{fl/fl\ Pf4\text{-}Cre-/-}$).

Animals on a C57BL/6 background, between 8-12 weeks of age were used for experiments, unless stated otherwise. Littermates were used as controls. Animal studies were approved by the district government of Lower Frankonia (Bezirksregierung Unterfranken).

2.1.4. Buffers

If not stated otherwise, all buffers were prepared in deionized water obtained from MilliQ Water Purification System (Millipore, Schwalbach, Germany). pH was adjusted with HCl or NaOH.

Cacodylate buffer, pH 7.2

Sodium cacodylate	0.1 M

Coagulation medium (HEPES buffer pH 7.45)

NaCl	136 mM
HEPES	10 mM
KCl	2.7 mM
Glucose	0.1%
$CaCl_2$	6.3 mM
$MgCl_2$	3.2 mM

Fluorescent thrombin substrate (Thrombin generation assay)

Z-GGR-AMC	2.5 mM
HEPES	20 mM
NaCl	140 mM
$CaCl_2$	200 mM
BSA	6%

Laemmli sodium dodecyl sulfate (SDS) sample buffer (4x)

Tris-HCl, pH 6.8	200 mM
Glycerol	40%
Bromophenol blue (3',3",5',5"-tetra-bromophenol-sulphonphthalein)	0.04%
SDS	8%
ß-mercaptoethanol (reducing conditions)	20%

Laemmli running buffer for SDS-PAGE

Tris	0.25 M
Glycine	1.92 M
SDS	35 mM

Loading dye solution (6x) for analysis of PCR products

Tris buffer (150 mM)	33%
Glycerin	60%
Bromophenol blue (3',3",5',5"-tetra-bromophenol-sulphonphthalein)	0.04%

Lysis buffer for DNA isolation

Tris base	100 mM
EDTA	5 mM
NaCl	200 mM
SDS	0.2%
Proteinase K (20 mg/mL) – added just before addition to samples	100 µg/mL

Lysis buffer for immunoprecipitation (2x)

NaCl	150 mM
Tris, pH 7.5	20 mM
Brij O10	1%
NaF	10 mM
Na_3VO_4	1 mM
Protease inhibitor cocktail	1%

Lysis buffer for platelet lysates, pH 8

Tris, pH 7.4	15 mM
NaCl	155 mM
EDTA	1 mM
NaN_3	0.005%
IGEPAL CA-630	1%
Protease inhibitor cocktail	1%

Lysis buffer (2x) for tyrosine phosphorylation studies, pH 7.5

NaCl	300 mM
Tris	20 mM
EGTA	2 mM
EDTA	2 mM
NaF	10 mM
Na_3VO_4	4 mM
IGEPAL CA-630	1%
Protease inhibitor cocktail	1%

Phosphate-buffered saline (PBS), pH 7.14

NaCl	137 mM
KCl	2.7 mM
KH_2PO_4	1.5 mM
$Na_2HPO_4 \times 2H_2O$	8 mM

PRP reagent (Thrombin generation assay)

HEPES	20 mM
NaCl	140 mM
BSA	0.5%
Tissue factor	3 pM

RIPA buffer

NaCl	150 mM
Triton X-100	1%
Sodium deoxycholate	0.5%
SDS	0.1%
Tris, pH 8.0	50 mM
Protease inhibitor cocktail	1%

Semi-dry transfer buffer

Tris-Ultra	75 mM
Glycine	80 mM
Methanol	40%

Separating gel buffer (SDS-PAGE), pH 8.8

Tris-HCl	1.5 M

Sodium citrate, pH 7.0

Sodium citrate	0.129 M

Sorensen's buffer, pH 7.4

KH_2PO_4	100 mM
Na_2HPO_4	100 mM

Stacking gel buffer (SDS-PAGE), pH 6.8

Tris HCl	0.5 M

Stripping buffer (“mild”), pH 2.0

SDS	1%
Glycine	25 mM
in PBS	

TAE buffer (50x)

Tris base	0.2 M
Acetic acid	5.7%
EDTA (0.5 M)	10%

TE buffer

Tris base	10 mM
EDTA	1 mM

Tris-buffered saline (TBS), pH 7.3

Tris-HCl	20 mM
NaCl	137 mM

TBS-T (Wash buffer for Western blotting)

TBS (1x)	
Tween® 20	0.1%

Tyrode-HEPES buffer, pH 7.4

NaCl	134 mM
Na_2HPO_4	0.34 mM
KCl	2.9 mM
$NaHCO_3$	12 mM
HEPES	5 mM
$MgCl_2$	1 mM
Glucose	5 mM
BSA	0.35%

2.2. Methods

2.2.1. Molecular biology and biochemistry

2.2.1.1. Genotyping of mice by PCR

2.2.1.1.1. Isolation of DNA from mouse ear samples

For extraction and purification of DNA for mouse genotyping, ear tissue obtained by punching for mouse identification was used. The ear tissue was lysed by shaking overnight with 500 µL lysis buffer supplemented with 2.5 µL Proteinase K at 56 °C. The Phenol-Chloroform method of extraction was used for DNA isolation and purification. For this, a mixture of phenol/chloroform/isoamyl alcohol (500 µL) was added to the lysed tissue samples, followed by thorough mixing and then centrifugation at 10,000 rpm at room temperature (RT). The upper phase was carefully collected and added to 500 µL isopropanol in fresh Eppendorf tubes. Thorough mixing and centrifugation at 14,000 rpm at 4°C followed to pellet the DNA. Post centrifugation, the supernatant was decanted and the DNA pellet was washed with 70% ethanol. After a final centrifugation at 14,000 rpm and decantation of supernatant, the DNA pellet was allowed to dry at 37 °C for 30 min. The purified DNA was dissolved in 50 µL TE buffer by shaking at 37 °C for 30 min. This was used further for genotyping by PCR.

2.2.1.1.2. Polymerase chain reactions

Reaction mixture for *Ano6* and *Pf4*-Cre PCRs (25 µL final volume)

Genomic DNA	1 µL
Forward primer (1:10 in H_2O, stock: 100 pmol/µL)	1 µL
Reverse primer (1:10 in H_2O, stock: 100 pmol/µL)	1 µL
dNTPs (stock: 10 mM)	1 µL
10x Taq buffer	2.5 µL
$MgCl_2$ (stock: 25 mM)	2.5 µL
Taq polymerase (5 U/ µL)	0.25 µL
H_2O	15.75 µL

Primers for *Ano6* WT or floxed allele PCR

Forward (Ano6-F): 5´ ATG TCT GTC AGA TAC TGC TCT TCA 3´
Reverse (Ano6-R): 5´ CAG CAA CTA GTT CAT GCA TGT GG 3´

Thermocycling conditions for PCR

96 °C	3 min	
94 °C	30 s	35 cycles
63.3 °C	30 s	
72 °C	60 s	
72 °C	10 min	

Results

WT:	211 bp
Floxed allele:	267 bp

Primers for *Pf4*-Cre PCR

Forward: 5´ CCC ATA CAG CAC ACC TTT TG 3´
Reverse: 5´ TGC ACA GTC AGC AGG TT 3´

Thermocycling conditions for PCR

96 °C	5 min	
94 °C	30 s	35 cycles
54.1 °C	30 s	
72 °C	45 s	
72 °C	3 min	

Results

WT:	No band
Pf4 Cre positive:	450 bp

Reaction mixture for Grb2 WT or floxed allele PCR (50 µL final volume)

Genomic DNA	1 µL
Forward primer	0.2 µL
Reverse primer	0.2 µL
dNTPs (stock: 10 mM)	1 µL
10x DreamTaq Buffer	5 µL
DreamTaq Hot Start DNA polymerase (5 U/µL)	0.5 µL
DMSO	0.5 µL
H_2O	41.6 µL

Primers for Grb2 WT or floxed allele PCR

Forward (Grb2_2S): 5' CCA GCA CAC ATG TCC TGC CTT C 3'
Reverse (Grb2_2AS): 5' GGT GGC TCA CAA CCA CCT ATA AC 3'

Thermocycling conditions for PCR

94 °C	4 min	
94 °C	20 s	35 cycles
63 °C	20 s	
72 °C	30 s	
72 °C	10 min	

Results

WT:	241 bp
KO:	209 bp
Heterozygous:	Both bands and an additional band higher than these two

Reaction mixture for GADS WT or KO PCR 25 µL final volume)

Genomic DNA	1 µL
Forward primer (1:10 in H_2O, stock: 100 pmol/µL)	1 µL
Reverse primer (1:10 in H_2O, stock: 100 pmol/µL)	1 µL
dNTPs (stock: 10 mM)	0.5 µL
10x DreamTaq Buffer	2.5 µL
DreamTaq Hot Start DNA polymerase (5 U/µL)	0.25 µL
H_2O	18.75 µL

Primers for GADS WT PCR

Forward (GADS 1): 5´ AGA TCA GGG TCA CCG GG 3´
Reverse (GADS 2): 5´ ACA GCG TCT CTT CAC CAC 3´

Thermocycling conditions for PCR

94 °C	10 min	
94 °C	60 s	32 cycles
56 °C	60 s	
72 °C	60 s	
72 °C	5 min	

Results

WT:	350 bp
KO:	No band

Primers for GADS KO PCR

Forward (Neo 1): 5´ GCA CGC AGG TTC TCC GGC 3´
Reverse (Neo 2): 5´ GTC CTG ATA GCG GTC CGC C 3´

Thermocycling conditions for PCR

94 °C	10 min	
94 °C	60 s	29 cycles
56 °C	60 s	
72 °C	60 s	
72 °C	5 min	

Results

WT:	No band
KO:	639 bp

Reaction mixture for hFXII WT and hFXII-knockin PCRs (25 µL final volume)

Genomic DNA	1 µL
Forward primer (1:10 in H_2O, stock: 100 pmol/µL)	1 µL
Reverse primer (1:10 in H_2O, stock: 100 pmol/µL)	1 µL
dNTPs (stock: 10 mM)	0.5 µL
10x DreamTaq Buffer	2.5 µL
DreamTaq Hot Start DNA polymerase (5 U/µL	0.25 µL
H_2O	18.75 µL

Thermocycling conditions for PCR

95 °C	5 min	
95 °C	30 s	40 cycles
67.5 °C	30 s	
72 °C	30 s	
72 °C	10 min	

Primers for hFXII WT PCR

Forward (hFXII-WT-F): 5´ GGA GCA AGC TTG ACC AAT CTC TAC 3´
Reverse (hFXII-WT-R): 5´ TCT CTC AGT CAC CTG AAC TAG CAG 3

Results

hFXII WT mice (expressing mouse FXII):	261 bp
hFXII Neo-KI mice or KI mice (mice bearing the targeted allele):	No band

Primers for hFXII knockin PCR

Forward (hFXII-WT-F): 5´ GGA GCA AGC TTG ACC AAT CTC TAC 3´
Reverse (hFXII-Mut-R): 5´ CTT GTA TCC ACC CAG TCT GGT TG 3´

Results

hFXII WT mice (expressing mouse FXII):	No band
hFXII Neo-KI mice or KI mice (mice bearing the targeted allele with or without neomycin resistance cassette):	342 bp

Reaction mixture for hFXII-Geno PCR (25 µL final volume)

Genomic DNA	1 µL
Forward primer (1:10 in H_2O, stock: 100 pmol/µL)	1 µL
Reverse primer (1:10 in H_2O, stock: 100 pmol/µL)	1 µL
dNTPs (stock: 10 mM)	0.5 µL
10x DreamTaq Buffer	2.5 µL
DreamTaq Hot Start DNA polymerase (5 U/µL)	0.25 µL
H_2O	18.75 µL

Primers for hFXII-Geno PCR

Forward (hFXII-FRTGeno-For): 5´ GGA ATC GTG GTG CGG ATA GT 3´
Reverse (hFXII-FRTGeno-Rev): 5´ ACC ACC ATG CCA GGC TTA AA 3´

Thermocycling conditions for PCR

96 °C	3 min	
94 °C	30 s	40 cycles
65 °C	30 s	
72 °C	40 s	
72 °C	10 min	

Results

hFXII WT mice (expressing mouse FXII):	148 bp
hFXII Neo-KI mice (mice bearing the targeted allele with the neomycin resistance cassette):	No band
hFXII KI mice (mice bearing the targeted allele without the neomycin resistance cassette):	245 bp

2.2.1.2. Reverse transcription polymerase chain reaction (RT-PCR)

Washed platelets were isolated from whole blood as described in section 2.2.2.5. Platelets from three mice per genotype were pooled and lysed using a determined volume of RIPA buffer in order to adjust platelet count between samples to equal levels. The mRNA was isolated by the acid guanidinium thiocynate-phenol-chloroform extraction method using TRIzol reagent (Invitrogen). 1 mL TRIzol was added to each pooled sample and thoroughly mixed by vortexing, then further allowed to stand at RT for 10 min. This was followed by addition of 250 µL chloroform and thorough mixing. After being allowed to stand at room temperature for 10 min, the samples were centrifuged at 10,000 rpm for 10 min at 4 °C. The upper phase was carefully transferred to 1 mL ice-cold isopropanol, mixed well and stored at -20 °C overnight. The samples were then centrifuged at 14,000 rpm for 10 min at 4 °C to obtain RNA as a pellet. The pellet was washed with 70% ethanol. After decanting the ethanol the RNA pellet was allowed to dry at RT for 30 min. The pellet was solubilized in RNAase free water supplemented with Ribolock. The RNA quality and concentration was determined with a Nanodrop device.

cDNA was generated from the mRNA template using SuperScript III reverse transcriptase (ThermoFischer Scientific) according to the manufacturer's instructions.

Mastermix 1	
mRNA	1 µg
Oligo(dT)18 primer	2 µL
DEPC treated water	to 20 µL

Mastermix 2	
5x first-strand buffer	4 µL
DTT (100 mM)	2 µL
dNTPs	1 µL
RiboLock RNase inhibitor (40 U/µL)	0.1 µL
SuperScript III Reverse Transcriptase (200 U/ µL)	0.5 µL

Mastermix 1 was prepared and denatured at 70 °C for 5 min followed by cooling on ice for 2 min. This was combined with mastermix 2 and the enzymatic reaction was carried out at 42 °C for 60 min followed by enzymatic inactivation at 70 °C for 10 min. The cDNA obtained was used for RT-PCR

Reaction mixture:

cDNA as template	1 µL
Forward primer (1:10 in H_2O, stock: 100 pmol/µL)	0.5 µL
Reverse primer (1:10 in H_2O, stock: 100 pmol/µL)	0.5 µL
dNTPs (stock: 10 mM)	0.5 µL
10x Taq Buffer	2.5 µL
$MgCl_2$ (stock: 25 mM)	2.5 µL
Taq polymerase (5 U/ µL)	0.3 µL
H_2O	17.2 µL

The following primers were used to detect the *Ano6* transcript through exon 3 to exon 4: 5'-TGACCAGACAATTGTCTGCC-3' and 5'-CACGAGGATGAAGTCGATTC-3' (expected product size 142 bp). The primers used for the detection of actin as a control were: 5'-GTGGGCCGCTCTAGGCACCAA-3' and 5'-CTCTTTGATGTCACGCACGATTTC-3' (expected product size 500 bp).

Thermocycling conditions:

96 °C	3 min	
94 °C	30 s	40 cycles
56 °C	30 s	
72 °C	40 s	
72 °C	5 min	

2.2.1.3. Preparation of platelet lysates and Western blotting

Platelet-rich plasma (PRP) was obtained from whole blood as described in section 2.2.2.5 and then 5 % EDTA in PBS was used to wash platelets twice instead of Tyrode's buffer. Platelets were adjusted to a count of 2 × 10^6 platelets/µL and lysed with RIPA buffer containing protease inhibitors, for 20 min on ice. The lysate was centrifuged at 14,000 rpm for 10 min at 4 °C to remove cell debris. The protein concentration of the supernatant was determined by Bradford method and it was mixed with 4x Laemmli buffer (reducing or non-reducing). Samples were boiled at 95 °C for 5 min. Proteins were separated on an 8 % or 10% SDS-PAGE gel and transferred onto a PVDF membrane by wet or semi-dry transfer. The membrane was blocked with 5 % non-fat milk for 1 h at RT and subsequently incubated with the primary antibody overnight at 4 °C. Proteins were visualized following incubation with HRP-conjugated secondary antibody for 1 h at room temperature and using the ECL detection kit.

Western blot experiments to detect Grb2 or Gads protein expression in Grb2 KO, Gads KO and Grb2/Gads DKO platelets were performed by Dr. Elizabeth Haining from our laboratory.

For the Ano6 Western blot, platelet lysates were mixed with reducing Laemmli buffer and not boiled. 50 µg protein was loaded per lane. 1:500 anti-mouse Ano6 antibody (1 mg/mL) was used as primary antibody.

2.2.2. *In vitro* or *ex vivo* analysis of platelet function

2.2.2.1. Determination of platelet count and surface glycoprotein expression

For the determination of surface expression levels of the major glycoproteins on the platelet surface, 50 µL of blood was obtained from the retro-orbital plexus of mice in 300 µL of 20 U/mL heparin using heparinized capillaries. This heparinized whole blood was diluted in PBS and 50 µL aliquots were stained with saturating amounts of FITC-labeled antibodies against major platelet glycoproteins as indicated in Figure 15C and listed in section 2.1.2. The incubation of whole blood with fluorophore-labeled antibodies was performed for 15 min at RT and the staining was terminated by addition of 500 µL 1x PBS. The samples were analyzed on a FACSCalibur (BD Biosciences) and the data obtained was analyzed on FlowJo version 7.6.

Platelet count was determined as described previously.[112] Heparinized blood (50 µL) was diluted 1:20 in PBS. 50 µL of this diluted sample was stained for 15 min at RT with phycoerythrin (PE)-conjugated anti-integrin αIIbβ3 antibody (clone JON2) and anti-GPV fluorescein isothiocynate (FITC)-conjugated antibody (clone DOM1) to identify the platelet population in whole blood. After 15 min, 500 µL of PBS was added, followed by addition of fluorescent beads of a known count (AccuCount fluorescent particles, 5.2 µm; Spherotec). The samples were analyzed on a FACSCalibur (BD Biosciences) for 90 s each. The platelet count was calculated using the following formula:

$$\frac{A}{B} \times \frac{C}{D} = number\ of\ cells\ per\ \mu l$$

A = number of events for the test sample

B = number of events for the fluorescent particles

C = number of fluorescent particles per 50 µL (as mentioned on the data sheet of the particular batch of particles used)

D = volume of test sample initially used in µL

2.2.2.2. Determination of whole blood parameters

Heparinized whole blood (50 µL) was obtained as described in the previous section and diluted 1:20 in PBS. This diluted whole blood was used to measure blood parameters in an automated hematology analyzer (Sysmex KX-21TM), which gave values for parameters such as MPV (mean platelet volume), WBC count, RBC count, hemoglobin levels and hematocrit.

2.2.2.3. Isolation of plasma and measurement of coagulation parameters (aPTT & PT)

Mice were bled using sodium citrate as anticoagulant. Whole blood was centrifuged at 3000 g for 8 min at RT to fractionate the plasma from the blood cells. Post centrifugation, the upper phase (plasma) was carefully collected into a fresh Eppendorf tube and stored at -80 °C until measurement of coagulation parameters - activated partial thromboplastin time (aPTT) and prothrombin time (PT) at the Central Laboratory, University Hospital of Würzburg, in collaboration with Dr. Sabine Herterich.

2.2.2.4. Flow cytometric analysis of platelet activation

Two parameters were used as a measure of platelet activation in a FACS assay. First, the activation of the most abundant integrin on the platelet surface αIIbß3, on agonist stimulation was measured by utilizing PE-coupled JON/A antibody. Second, the surface exposure of P-selectin, which is stored in the alpha-granules of platelets, was used as a measure of degranulation response of platelets on agonist stimulation using a FITC-labeled anti-P-selectin antibody. For the assay, heparinized whole blood obtained as described in section 2.2.2.1 was washed twice in Tyrode-HEPES buffer to eliminate heparin and then diluted in Tyrode-HEPES buffer containing 2 mM $CaCl_2$. Aliquots of 50 µL of this diluted blood was activated with the indicated concentration of agonists, and stained with antibodies JON/A-PE and anti P-selectin-FITC, for 8 min at 37 °C and further 8 min at RT. The reaction was stopped by addition of 500 µL 1x PBS. Unstimulated samples were used as resting controls. The samples were analyzed on a FACSCalibur (BD Biosciences) and the data obtained was analyzed on FlowJo version 7.6.

2.2.2.5. Preparation of washed platelets

Mice were bled from the retro-orbital plexus under isoflurane anesthesia. Blood was collected in an Eppendorf tube containing 300 µL (6 U) heparin or 10% of 0.129 M sodium citrate as anticoagulant. The platelet-rich plasma (PRP) was fractionated from whole blood by 2 cycles of centrifugation at 300 *g* for 6 min at room temperature (RT). The upper white phase (PRP) was carefully collected without any contamination by the lower red phase. For the preparation of washed platelets, PRP was centrifuged at 800 *g* for 5 min at RT leading to obtain a platelet pellet. After re-suspension in modified Tyrodes-HEPES buffer supplemented with prostacyclin (0.1 µg/mL) and apyrase (0.02 U/mL) to prevent platelet activation, the platelets were washed twice by centrifugation at 800 *g* for 5 min at RT. Platelet count was measured by hematology analyzer (Sysmex KX-21TM) and adjusted to 5×10^5 platelets/µL by re-suspending in modified Tyrodes-HEPES buffer containing 0.02 U/mL apyrase.

2.2.2.6. Platelet aggregation studies

The aggregation response of platelets on agonist stimulation was measured on a Fibrintimer 4 channel aggregometer (APACT Laborgeräte und Analysensysteme). An aliquot of 50 µL of washed platelets were diluted with 110 µL Tyrodes-HEPES buffer supplemented with 2 mM $CaCl_2$ and 100 µg/mL human fibrinogen (except in the case of thrombin stimulation where fibrinogen was not used). The platelet suspension was continuously stirred at 1,000 rpm. 30 s after starting the measurement, the indicated agonists were added and the aggregation curve recorded for 10 min. In case of ADP stimulation, 50 µL PRP with a platelet concentration of 1.5×10^5 platelets/µL was used instead of washed platelets.

2.2.2.7. Measurement of Phophatidylserine (PS)-exposure in platelets

Washed platelets were rested for 30 min at 37 °C and then diluted 1:10 in modified Tyrodes-HEPES buffer containing 2 mM $CaCl_2$, but no BSA, to attain a final concentration of 5×10^4 platelets/µL. Aliquots of 50 µL of the diluted samples were co-stained with annexin A5-DyLight-488 to label PS and JON/A-PE to label the platelet population, and stimulated with 10 µM ionomycin, 10 µM A23187 or co-stimulated with 10 µg/mL CRP and 0.1 U/mL thrombin for 5 min at RT. The reaction was terminated by addition of 500 µL modified Tyrodes-HEPES buffer containing 2 mM $CaCl_2$ (without BSA). Unstimulated platelet samples were used as resting controls. Samples were analyzed on a FACSCalibur (BD Biosciences)

and the data obtained was analyzed on FlowJo version 7.6. The FL-1 histogram was gated into three regions:

- Annexin A5 Negative (99 % of events in WT resting condition)
- Annexin A5 High (90 % of the events in the WT ionomycin stimulated condition)
- Annexin A5 Low (intermediate population between Annexin A5 Negative and Annexin A5 High)

Simultaneously, 50 µL of the diluted sample was also stimulated with the same agonists under similar conditions, but stained with anti P-selectin FITC antibody as a measurement of α-granule release and thus platelet activation.

2.2.2.8. Measurement of platelet membrane ballooning through changes in light transmission

Increase in light transmission through a suspension of platelets (i.e. clearance of turbidity) served as a measure of transformation of platelets to a more rounded and translucent morphology (membrane ballooning) when subjected to stimulation with the calcium ionophore ionomycin. It has been previously reported that ionomycin treatment does not lead to platelets aggregation, but instead causes membrane ballooning.[113] Changes in light transmission were recorded for 10 min on a Fibrintimer 4 channel aggregometer (APACT Laborgeräte und Analysensysteme). Aliquots of 50 µL of washed platelets were diluted with 110 µL Tyrodes-HEPES buffer supplemented with 2 mM $CaCl_2$ and 100 µg/mL human fibrinogen. The platelet suspension was continuously stirred at 1,000 rpm. 5 µg/mL CRP was used to stimulate the platelet suspension after 150 s as a control to ascertain reactivity of platelet samples. For further measurements, 30 s after starting the measurement JON/A F(ab)'$_2$ fragments were added at a concentration of 20 µg/mL to block αIIbβ3 integrins and thus prevent aggregation.[108] 120 s after addition of JON/A F(ab)'2 fragments, the platelet suspension was stimulated with either 5 µg/mL CRP (as a control for effective inhibition of platelet aggregation) or 20 µM ionomycin, to study the process of platelet ballooning.

2.2.2.9. Protein phosphorylation studies

Washed platelets were prepared as described in section 2.2.2.5, except that the second wash step was performed using Tyrodes buffer without BSA supplementation, and the platelet count was adjusted to 700,000/µL. The platelet suspension was allowed to rest for 10

min at 37 °C and then treated with 10 µM indomethacin, 2 U/mL apyrase and 5 mM EDTA to prevent platelet activation by second wave mediators and platelet aggregation. Following 5 min incubation at 37 °C, the platelet suspension was taken into a cuvette and continuously stirred at 1,000 rpm, the temperature being maintained at 37 °C. A quarter of the sample volume was withdrawn as 0 s time point and immediately added to an equal volume of ice-cold 2x lysis buffer. The remaining platelet suspension was stimulated with the indicated agonists (convulxin or rhodocytin), and samples were taken at 30 s, 90 s and 300 s post stimulation, and immediately added to equal volumes of ice-cold 2x lysis buffer. The platelet lysates were centrifuged at 14,000 rpm for 10 min at 4 °C and the supernatants were collected.

For platelet signaling studies using phospo-specific antibodies, the platelet lysates were mixed with 4x SDS reducing sample buffer, incubated at 70 °C for 10 min and then subjected to Western blot analysis as described in section 2.2.1.3.

For pan-tyrosine phosphorylation studies using the 4G10 antibody, the platelet lysates were mixed with 4x NuPAGE LDS sample buffer containing ß-mercaptoethanol and incubated at 70 °C for 10 min. Proteins were separated on NuPAGE Novex 4-12 % gradient Bis-Tris gels using 1x NuPAGE MOPS SDS Running buffer. The gels were run at 4 °C in the cold room. Further steps were performed as described above, using the anti-phosphotyrosine antibody 4G10 as primary antibody.

For both kinds of experiments, SERVA BlueBlock PF protein free blocking reagent was used for blocking and for diluting the primary and secondary antibodies.

2.2.2.10. Thrombin generation assay

PRP was fractionated from citrate-anti-coagulated whole blood by two cycles of centrifugation at 300 *g* for 6 min. Platelets were pelleted from PRP by another centrifugation step at 800 *g* for 5 min and the supernatant (PPP, platelet poor plasma) was pooled from the samples originating from mice of the same genotype. Platelets were adjusted to a concentration of 1.5 × 10^5 platelets/µL in the respective pooled PPP to form the PRP. PRP was left unstimulated or stimulated with the indicated agonists (10 µM A23187 or co-stimulated with 20 µg/mL CRP & 5 mM PAR-4 peptide) and immediately pipetted into a 96-well plate. All samples were pipetted in duplicate. Each well contained recombinant tissue factor (3 pmol/L). Tissue factor initiated thrombin generation was quantified using the calibrated automated thrombogram (CAT) method adapted for mouse plasma as described previously.[114, 115] The machine was

preheated to 37 °C and thrombin generation was monitored by addition of a fluorescent thrombin substrate (Z-Gly-Gly-Arg aminomethyl coumarin, 2.5 mmol/L) to each well. First-derivative curves of the accumulation of fluorescence intensity over time were converted into curves of nanomolar thrombin, using a thrombin calibrator. The Ca^{2+} ionophore A23187 was used in this assay and not ionomycin, as plasma proteins quench the latter. Experiments were performed with Sarah Beck from our laboratory.

2.2.2.11. Platelet adhesion and fibrin formation on collagen/tissue factor under flow conditions

Ex vivo assay for detection of fibrin clot formation under flow was performed as described previously.[116] Rectangular coverslips (24 × 60 mm) were coated with microspots of 100 ng Horm type I collagen with/ without 10 pg recombinant human tissue factor, and were subsequently blocked with 1 % BSA. Citrate anti-coagulated blood (1 part Na-citrate, 9 parts blood) was obtained and pre-labeled with $DiOC_6$ to mark platelets, Alexa fluor (AF)647-fibrinogen to detect fibrin(ogen) and AF 568-annexin A5 to visualize PS exposure and platelet membrane ballooning. Blood was taken in a 1 mL syringe and mixed with coagulation medium taken in another 1 mL syringe and, with the aid of a Y-shaped flattened mixing tube and two pulse-free micro-pumps, perfused as a mixture (ratio 10:1) over the coated coverslip placed in a custom-made parallel plate flow chamber. Images were recorded using an EVOS AMF 4300 digital inverted microscope at 60x magnification every 1.5 min until fibrin formation was observed, or for an observation period of 8 min. Experiments were performed with Dr. Frauke Swieringa from the Department of Biochemistry, Cardiovascular Research Institute Maastricht (CARIM), University of Maastricht.

2.2.2.12. Scanning electron microscopy (SEM)

Following the *ex vivo* flow chamber assay for detection of fibrin clot formation, for the WT or cKO samples where fibrin formation was observed to take place, the coverslip was carefully removed from the parallel plate flow chamber 1 min after fibrin formation. The coverslip was rinsed with HEPES buffer (including glucose and BSA, both 0.1% w/v) followed by addition of 300 µL of 2.5% glutaraldehyde in cacodylate buffer to fix the samples (30 min at RT, followed by 4 °C overnight). The coverslips were then washed with Sorenson's buffer. The area bearing the fibrin clot was carefully cut out using a diamond cutter. The samples were placed in 6-well plates and subjected to sequential dehydration by submerging them in increasing

concentrations of acetone – 30% acetone for 15 min; 50% acetone for 20 min; 70% acetone for 30 min; 90% acetone for 45 min; 100% acetone for 30 min; fresh 100% acetone for 30 min. The dehydrated samples were dried in a critical point dryer and mounted onto SEM stubs. The prepared samples were imaged on a JEOL JSM-7500F microscope.

2.2.3. *In vivo* analysis of platelet function

2.2.3.1. Anesthesia

Mice were anesthetized by intraperitoneal injection of a combination of midazolam/medetomidine/fentanyl (5/0.5/0.05 mg/kg body weight).

2.2.3.2. Tail bleeding assay (Hemostasis model)

The bleeding time assay was performed using the filter paper method. Mice were anesthetized and 2 mm of the tail tip was cut off with a scalpel. Tail bleeding time was monitored by gently absorbing blood drops onto a filter paper every 20 s without making direct contact to the wound site. Bleeding was considered to have ceased when no blood was observed to blot onto the filter paper. The experiment was performed until cessation of bleeding, or until the end of a 20 min observation period.

Dr. Elizabeth Haining from our laboratory performed the bleeding time assay comparing Grb2 KO, Gads KO and Grb2/Gads DKO animals.

2.2.3.3. Model of $FeCl_3$-induced thrombosis in the carotid artery

The right carotid artery of an anesthetized mouse was exteriorized through a midline incision in the neck. An ultrasonic flow probe (0.5PSB699, Transonic Systems) was placed around the vessel to measure the blood flow. Experimental thrombosis was induced in the vessel by topical application of a filter paper soaked with 6 % $FeCl_3$ for 100 s, just below the placed flow probe. Blood flow was measured and recorded until full occlusion of the vessel (cessation of blood flow for at least 3 min) or until the end of an observation period of 30 min.

2.2.3.4. Model of $FeCl_3$-induced thrombosis in the mesenteric arterioles

Mice between the ages of 3-4 weeks were used for these experiments. Mice were anaesthetized and 56F8-DyLight 488 was injected *i.v.* to label platelets (2 µg/mouse). The mesentery was carefully exteriorized through a midline abdominal incision. Arterioles with a diameter of ~35-60 µm, free from excess fat were selected and immobilized on a petri dish with the help of gauze saturated with saline. Injury was induced by topical application of a drop of 20% $FeCl_3$ solution, placed over the arteriole with the help of a triangular filter paper. The process of injury, platelet adhesion, aggregation and thrombus formation were visualized using an inverted fluorescence microscope (Axiovert 200 equipped with a 100W HBO fluorescence lamp and a CookSNAP-EZ camera, Visitron) and recorded using the MetaVue software. Images were acquired until full vessel occlusion (cessation of blood for more than 1 min), or for a maximum period of 40 min.

2.2.3.5. Model of mechanical injury-induced thrombosis in the aorta

The abdominal aorta and the inferior vena cava of an anaesthetized mouse were visualized through a midline incision to access the abdominal cavity. The wall of the aorta was carefully separated from that of the vena cava and an ultrasonic flow probe was placed around the aorta to measure blood flow. Experimental thrombosis was induced by mechanically injuring the vessel through tight compression with forceps for 15 s, just above the placed flow probe. Blood flow was measured and recorded until full occlusion of the vessel (cessation of blood flow for at least 3 min) or until the end of an observation period of 30 min.

2.2.3.6. Transient middle cerebral artery occlusion (tMCAO) model of ischemic stroke

Dr. Eva Geuß from the Department of Neurology, University Hospital of Würzburg performed these experiments as described previously.[117] Mice were anesthetized with 2 % isoflurane, and the carotid artery was exposed. A silicon rubber-coated nylon monofilament was advanced through the carotid artery to occlude the middle cerebral artery for 60 min, after which it was removed to allow reperfusion. Following 23 h of reperfusion, the mice were tested for global neurological defects by the Bederson score (0 - best functional outcome, 5 - worst deficit),[118] as well as for motor functional and coordination deficits by the grip test (5 -

best, 0 - worst).[119] The brains of the mice were also quantified for edema corrected infarct volumes with the aid of 2,3,5-triphenyltetrazolium chloride (TTC) staining on brain sections.

3. Results

3.1. TMEM16F-mediated platelet membrane phospholipid scrambling is critical for hemostasis and thrombosis but not thrombo-inflammation in mice

3.1.1. Generation of TMEM16F knockout mice

The targeting strategy used for the generation of TMEM16F constitutive, and megakaryocyte- and platelet-specific conditional KO mice, is depicted in Figure 12.

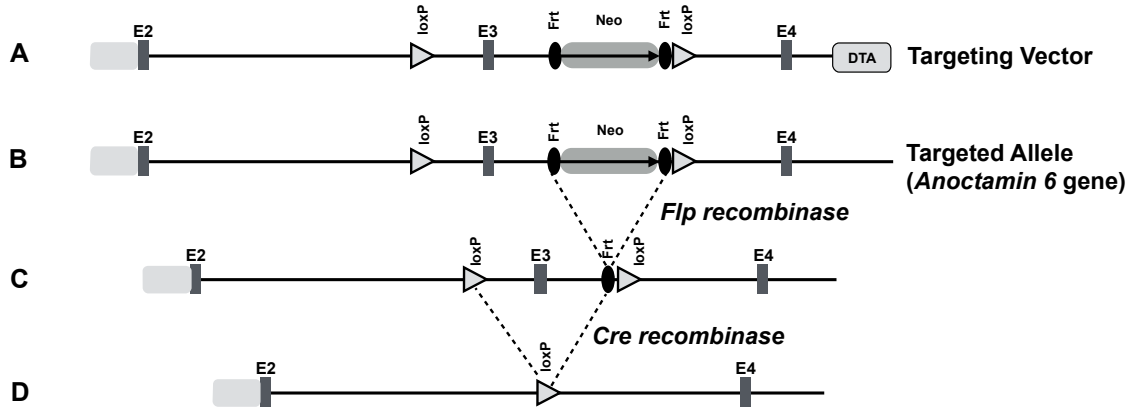

Figure 12. Targeting strategy for generation of TMEM16F constitutive (TMEM16F KO) and megakaryocyte- and platelet-specific KO mice (TMEM16F cKO). (A) Targeting vector – The gene encoding the protein TMEM16F, *Anoctamin 6* (*Ano6*) has 20 exons, spanning 184 kb on chromosome 15 in mice. For generation of cKO mice, the targeting strategy was designed to conditionally knock out exon 3 (E3) by *Cre-loxP* system. This was expected to result in frame shift for protein translation resulting in a 27 amino acid (aa) truncated protein (23 aa N-terminal sequence of Ano6 and 4 aa frame-shifted nonsense aa). Compared to the full-length protein of 911 aa, this truncated protein was expected to be non-functional. To achieve this, loxP fragments were inserted into the introns flanking exon 3. A neomycin resistance (neo) cassette flanked by Frt sites was used for selection of targeted alleles. (B) Mice bearing the targeted allele were intercrossed with mice expressing the *Flp* recombinase to eliminate the Neo selection cassette flanked by Frt sites to obtain floxed mice (C). (D) The floxed mice were intercrossed with mice expressing the *Cre*-recombinase under the control of megakaryocyte- and platelet-specific precursor platelet factor-4 (*Pf4*) to obtain megakaryocyte- and platelet-specific conditional KO mice. Constitutive KO mice were obtained using the knockout-first targeting strategy, taking advantage of the presence of the neomycin resistance selection cassette, which was expected to prevent gene translation and protein expression (B). (Baig *et al*., *ATVB* 2016)[120]

TMEM16F constitutive knockout mice (*Ano6*$^{-/-}$ - from here on referred to as TMEM16F KO mice) were generated using the 'knockout first' strategy, based on the presence of the

neomycin resistance cassette that is expected to prevent gene translation and thus protein expression.

A PCR-based genotyping approach confirmed the success of this targeting strategy (Figure 13A). Matings were set up to generate 25% WT, 25% constitutive KO and 50% heterozygous mice. However, genotyping results revealed that as reported previously,[46, 47] TMEM16F KO mice are embryonic lethal and hardly any KO animals survive until birth (Figure 13B).

To determine the developmental stage beyond which TMEM16F KO embryos are unable to survive, embryo analysis was carried out following timed matings. These studies revealed that while embryos with a constitutive deletion of *Ano6* gene expression are present in expected Mendelian ratios until embryonic day 12.5 (E12.5), this is not the case for E14.5 (Figure 13B). Embryo resorption was frequently observed at E14.5. These results indicate that most TMEM16F KO mice die between E12.5 and E14.5 stages of embryonic development. However, visual examination of the surviving KO embryos at E12.5 did not reveal any obvious pathology, such as major bleedings or exencephaly as reported previously (Figure 13C).[46]

A

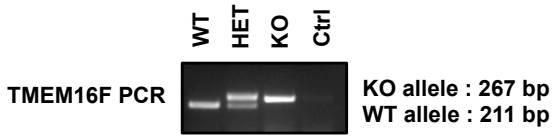

B

	EXPECTED	EMBRYONIC		POSTNATAL
		E 12.5	E 14.5	
+/+ (WT)	25%	13 (21%)	23 (40%)	41 (45%)
+/- (HET)	50%	32 (52%)	30 (51%)	42 (47%)
-/- (KO)	25%	17 (27%)	5 (9%)	7 (8%)
Total		62	58	90

C

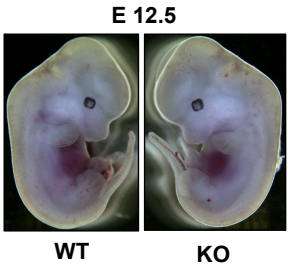

Figure 13. Constitutive deletion of *Ano6* gene expression results in embryonic lethality. (A) Genotyping strategy to distinguish between WT, heterozygous (HET) and TMEM16F KO mice. With the primers used, DNA from WT mice produced a band at 211 bp, DNA from KO mice produced a band at 267 bp, whereas DNA from HET mice produced both bands. (B) Genotypic distribution of progeny of HET x HET matings at embryonic day 12.5 (E12.5), E14.5, as well as postnatally. As per Mendelian distribution, this mating strategy was expected to produce 25% WT mice, 50% HET mice and 25% KO mice. Mice were present at an expected Mendelian ratio at E12.5, but the number of KO mice surviving until E14.5 was dramatically reduced, with only 8% KO mice surviving until birth. (C) The KO embryos surviving until E12.5 did not show any obvious pathology on visual examination.

To obtain conditional knockout mice (hereafter referred to as TMEM16F cKO mice), mice carrying the targeted allele were first intercrossed with mice expressing the *Flp* recombinase, in order to eliminate the neomycin resistance selection cassette flanked by the Frt sites (Figure 12B). The 'floxed' mice thus obtained (Figure 12C), expressing loxP fragments in the introns flanking exon 3 were further intercrossed with mice expressing the *Cre* recombinase under the control of the platelet factor 4 (*Pf4)* promoter to obtain megakaryocyte- and platelet-specific conditional knockout mice (cKO) (Figure 12D).

To confirm the success of the targeting strategy, RT-PCR analysis using mRNA obtained from WT and cKO platelets was performed which showed the complete absence of the region encoded by exon 3 at mRNA level (Figure 14A). Furthermore, when lysates from WT and cKO platelets were analyzed in a Western blot approach using a specific antibody against TMEM16F, the cKO platelets lacked TMEM16F at protein level - confirming the absence of the protein in platelets of cKO mice (Figure 14B). The cKO mice were born with an expected Mendelian distribution and were observed to be healthy (Figure 14C).

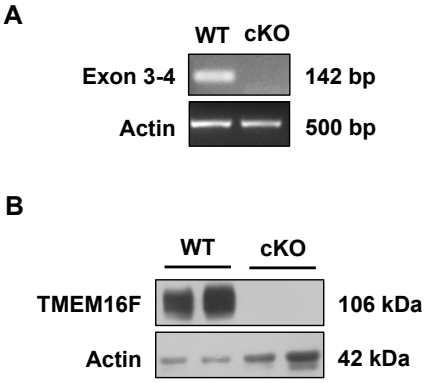

C

Number of litters	45
Average litter size	6
Total number of mice	267
WT mice	130 (49%)
cKO mice	137 (51%)

Figure 14. Generation of TMEM16F cKO mice. (A) RT-PCR of platelet cDNA samples from WT (*Ano6*$^{fl/fl}$) and cKO (*Ano6*$^{fl/fl\ Pf4\text{-}Cre+/-}$) mice showing absence of exon 3 encoded region of TMEM16F at mRNA level in cKO platelets. (B) Western blot of platelet lysates from WT and cKO animals using a specific antibody against TMEM16F showing its complete loss at protein level, confirming success of the targeting strategy. Actin was used as loading control. (C) Colony characteristics of TMEM16F cKO mouse line. Mating between *Ano6*$^{fl/fl}$ and *Ano6*$^{fl/fl\ Pf4\text{-}Cre+/-}$ mice yielded an average litter size of 6. WT and cKO animals were born with expected Mendelian distribution (~50% WT and ~50% cKO). (Baig *et al*., *ATVB* 2016)[120]

3.1.2. TMEM16F cKO animals display overall normal blood parameters

The intrinsic as well as extrinsic pathways of coagulation were intact in the cKO mice as determined by the global coagulation assays, prothrombin time (PT) and activated partial

thromboplastin time (aPTT). Additionally, whole blood parameters including platelet count and size were comparable between WT and cKO animals (Table 1, Figure 15A,B).

	WT	cKO	p
WBC x 10^3/µL	8.29 ± 2.31	9.29 ± 2.44	n.s.
RBC x 10^3/µL	6.50 ± 0.87	6.40 ± 0.68	n.s.
HGB (g/dL)	9.62 ± 1.75	9.76 ± 1.20	n.s.
HCT (%)	34.10 ± 4.67	33.65 ± 4.08	n.s.
PT (s)	9.3 ± 0.5	9.6 ± 0.2	n.s.
aPTT (s)	25.4 ± 1.1	27.3 ± 3.4	n.s.

Table 1. TMEM16F cKO mice have normal blood counts and global coagulation times. HGB, hemoglobin; HCT, hematocrit; PT, prothrombin time; aPTT, activated partial thromboplastin time. Data shown as mean ± SD (n = 15 mice per group. n.s = not significant; unpaired Student's *t* test. (Baig *et al*., *ATVB* 2016)[120]

The surface expression of major glycoproteins present on platelets was determined by a FACS assay employing specific FITC-labeled antibodies. There were no significant differences between platelets obtained from WT and cKO animals (Figure 15C).

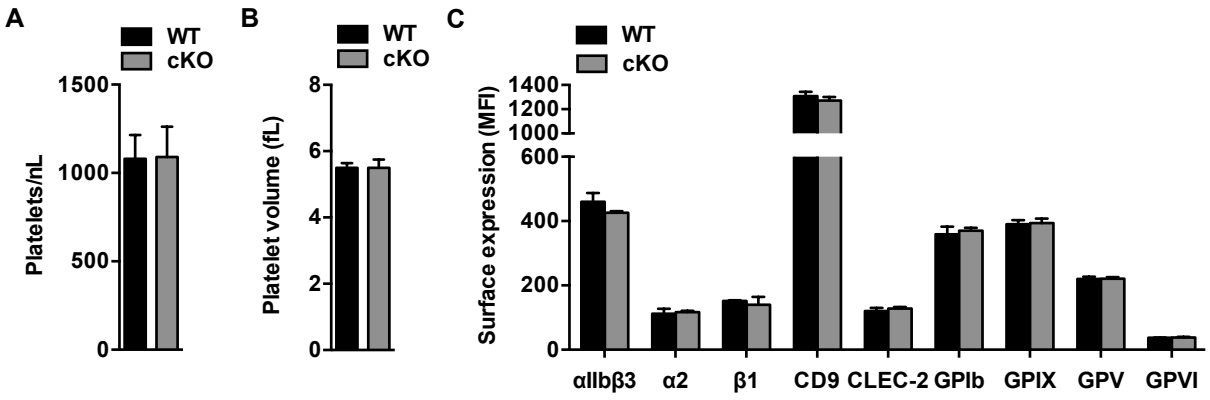

Figure 15. TMEM16F cKO animals display normal platelet count, size and platelet surface glycoprotein expression. (A) Absolute count of circulating platelets measured by a flow cytometric method (platelets/nL ± SD, n=15) (B) Platelet volume measured by a Sysmex hematology analyzer KX-21^{TM} (MPV, mean platelet volume in femtolitre (fL) ± SD, n=15). cKO animals were found to have a platelet count and volume similar to WT animals. (C) Surface expression levels of the major glycoproteins present on the platelet surface determined by flow cytometry using specific fluorophore-labeled antibodies. Results are expressed as MFI ± SD (n = 4 mice per group; representative data of 3 individual experiments). cKO platelets were found to have an unaltered expression of surface glycoproteins compared to WT platelets. (Baig *et al*., *ATVB* 2016)[120]

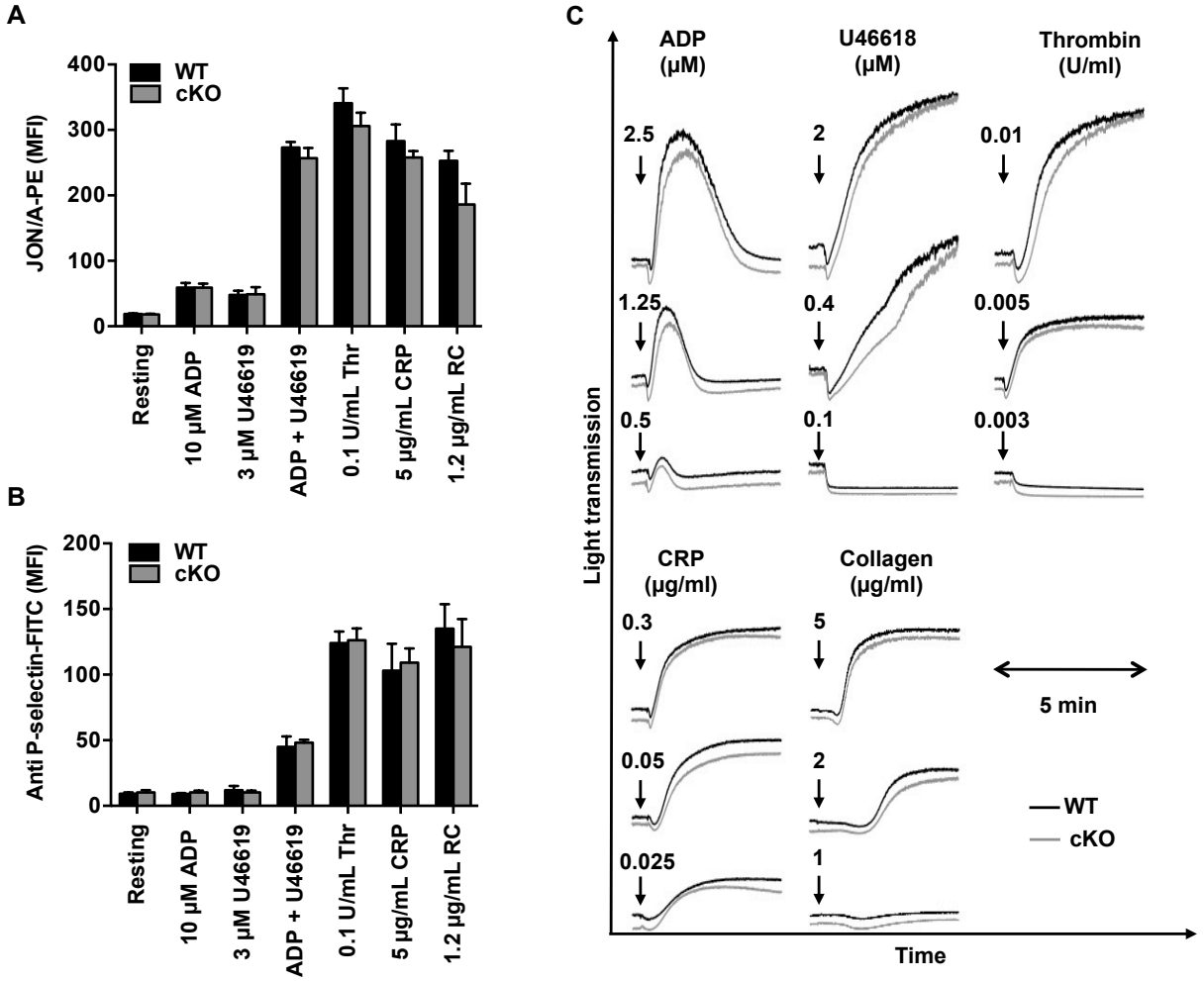

Figure 16**.** TMEM16F cKO platelets have unaltered activation and aggregation responses. (A) Measurement of integrin αIIbβ3 activation on stimulation with indicated agonists by flow cytometry using JON/A-PE antibody. (B) Flow cytometry-based measurement of α-granule release as indicated by P-selectin exposure. Both experiments were performed to evaluate degree of platelet activation and cKO platelets were found to have unaltered activation responses compared to WT platelets. Results are expressed as MFI ± SD (n = 4 mice per group; representative data of 3 individual experiments). (C) Aggregation traces from WT or cKO platelet suspensions recorded on a Fibrintimer 4 channel aggregometer. The platelet suspensions were stimulated with high, intermediate or low doses of agonists that activate the GPCR-signaling pathways (ADP, U46619, thrombin), or those that stimulate the ITAM signaling pathways (CRP, collagen). Representative traces from 3 individual experiments using 2 vs 2 mice. (Baig *et al*., *ATVB* 2016)[120]

Furthermore, the activation response of the mutant platelets in response to agonist stimulation was determined by assessing the transformation of integrin αIIbβ3 to an active conformation, and the exposure of P-selectin, stored in platelet α-granules in a FACS assay.

In both cases, cKO platelets responded to an extent comparable to WT platelets on stimulation with agonists that activate the major platelet signaling pathways (Figure 16A,B).

Following initial activation, platelet-platelet interactions through binding of integrin αIIbβ3 to fibrinogen lead to platelet aggregation. The aggregation abilities of WT and cKO platelets were tested using the method of aggregometry. No differences were observed in the aggregation responses of WT and cKO platelets at low, intermediate or high doses of agonists that stimulate the GPCR or the ITAM signaling pathways (Figure 16C).

These results demonstrated that cKO platelets undergo activation and aggregation without any defects *in vitro*.

3.1.3. TMEM16F cKO platelets display severely impaired but not abolished procoagulant characteristics

Strong platelet activation triggers a sustained increase in intracellular calcium concentrations leading to procoagulant transformation of the cells through exposure of negatively charged aminophospholipids at the outer leaflet of their plasma membrane. The ability of WT or cKO platelets to expose the major aminophospholipid - phosphatidylserine (PS) - to the outer leaflet of their plasma membrane was measured by specific binding of annexin A5 in a FACS analysis.

As shown in Figure 17A, under the conditions tested - co-stimulation with CRP/Thrombin to activate both ITAM and GPCR signaling pathways (to produce a sustained increase in intracellular calcium levels), or treatment with the calcium ionophores A23187 or ionomycin, caused robust PS exposure in WT platelets. However, a significantly lower percentage of cKO platelets exposed PS as compared to WT platelets under all three conditions.

Interestingly, the fraction of cKO platelets that exposed PS, did so to a significantly lower extent. To analyze this differential PS exposure in more detail, the platelet population was gated into three groups – annexin A5 high (platelet population with the greatest extent of PS exposure; 90% of events in the WT ionomycin-treated condition); annexin A5 negative (platelet population with no PS exposure; 99% of events in WT resting condition) and annexin A5 low (platelet population with a low degree of PS exposure; intermediate population between annexin A5 high and negative populations).

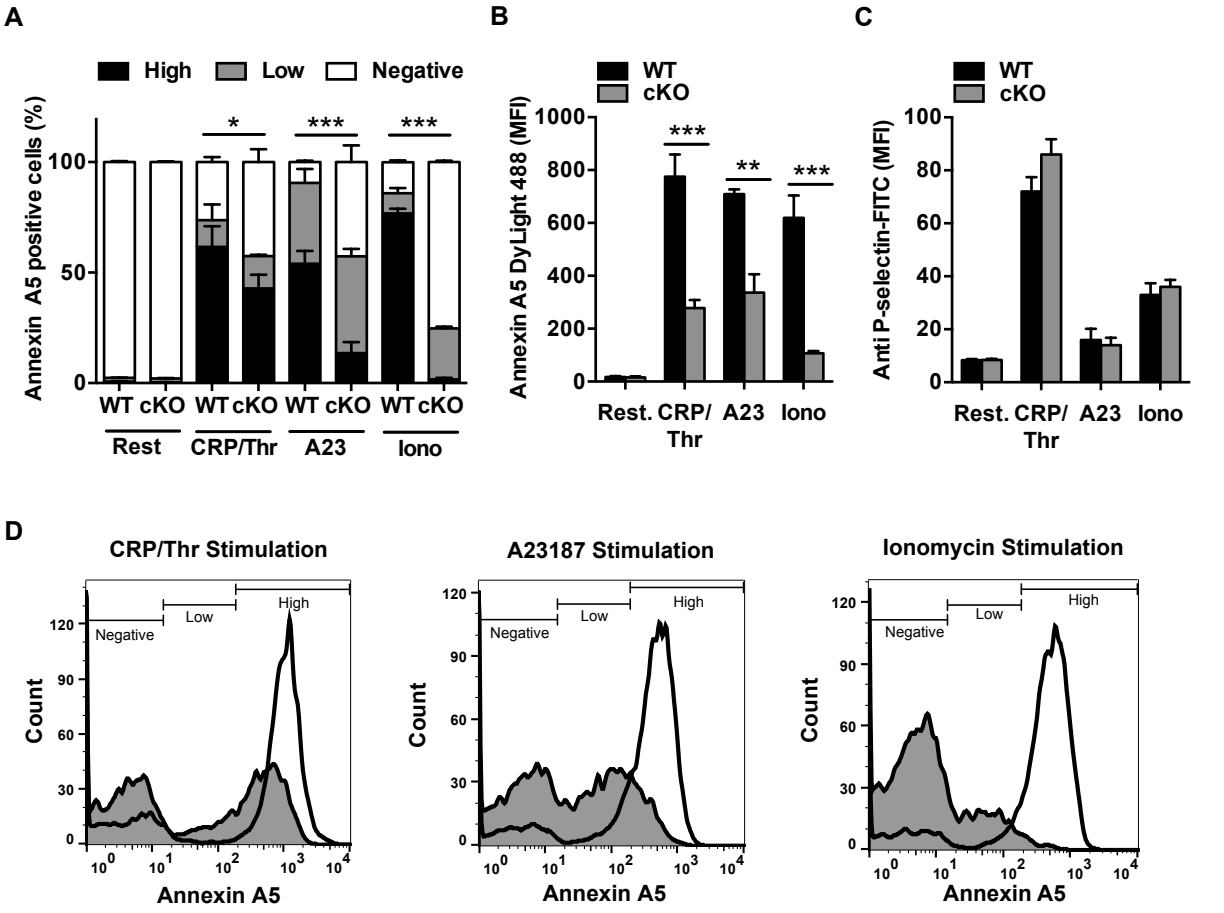

Figure 17. TMEM16F platelets display reduced procoagulant characteristics –significant reduction in PS exposure (A) Measurement of PS exposure by flow cytometry using specific binding of annexin A5 to platelet surface-exposed PS. The platelet population was divided into 3 groups - annexin A5 negative (white bars; 99% of events in WT resting condition), annexin A5 high (black bars; 90% of events in the WT ionomycin - treated condition), and an intermediate population, annexin A5 low (gray bars). There was a dramatic reduction in the percentage of platelets exposing PS, especially for the annexin A5 high population. Results shown as percentage positive cells ± SD, significance shown for annexin A5 high population. (B) Mean fluorescence intensity values ± SD for annexin A5 binding in the same experiment as A, also reflecting significantly reduced PS exposure in cKO platelets. (C) Measurement of α-granule release and extent of platelet activation by quantification of P-selectin exposure by flow cytometry. cKO platelets were activated to a similar extent as WT platelets under stimulation conditions at which a dramatic reduction in PS exposure was observed. (D) Representative histograms for annexin A5 binding analyses showing gating of annexin A5 high, low and negative populations (WT histogram non-filled, cKO histogram grey-filled). n = 4 mice per group; representative data of 3 individual experiments. *P<0.05, **P<0.01, ***P<0.001; unpaired Student's t test. (Baig *et al*., *ATVB* 2016)[120]

It was the 'high'-annexin A5 positive fraction (black bars, Figure 17A) that was significantly reduced in the cKO samples in all three conditions, and almost abolished on stimulation with A23 or ionomycin. The cKO platelet population positive for annexin A5 only had a very low degree of PS exposure (Figure 17A, grey bars).

This significantly reduced PS exposure was also apparent by the significantly lower mean fluorescence intensities of annexin A5 DyLight 488 binding to cKO platelets as compared to WT platelets (Figure 17B). The distribution of WT and cKO platelet populations between annexin A5 high, low or negative binding can be seen in representative FACS histograms in Figure 17D. Importantly, the differences in PS exposure between WT and cKO platelets could not be attributed to different extents of platelet activation, as conditions of stimulation tested for PS exposure, led to comparable P-selectin exposure levels in both groups (Figure 17C).

The ability of platelets to become procoagulant was further tested *ex vivo* under flow conditions in a flow chamber assay. Whole blood obtained from WT or cKO animals was allowed to perfuse over glass cover slides coated with micro-spots of collagen and tissue factor at arterial shear rates.

Platelets were found to adhere, aggregate and form three-dimensional thrombi at the collagen/tissue factor micro-spots. Analysis of the surface area covered by $DiOC_6$-labeled platelets revealed that both WT and cKO platelets adhered and formed aggregates to the same extent (Figure 18Ai), and were thus similarly activated.

Two characteristics of procoagulant platelets were assessed in this assay – firstly, the ability of platelets to expose PS on the outer leaflet of their plasma membrane, assessed by positive staining of AF568-annexin A5. cKO platelets were found to expose significantly lower PS as compared to WT platelets (Figure 18Aii), confirming the results of the FACS assay.

In addition, procoagulant platelets have been shown to acquire a 'ballooned morphology' through a regulated process to increase the surface over which PS is exposed and thus further augment the surface over which the coagulation factors can bind to form the tenase and the prothrombinase complexes.[44] This transformation following activation on coming into contact with collagen and tissue factor was clearly visible for the WT platelets. However, a strikingly low number of cKO platelets were found to acquire the ballooned morphology (Figure 18Aiii).

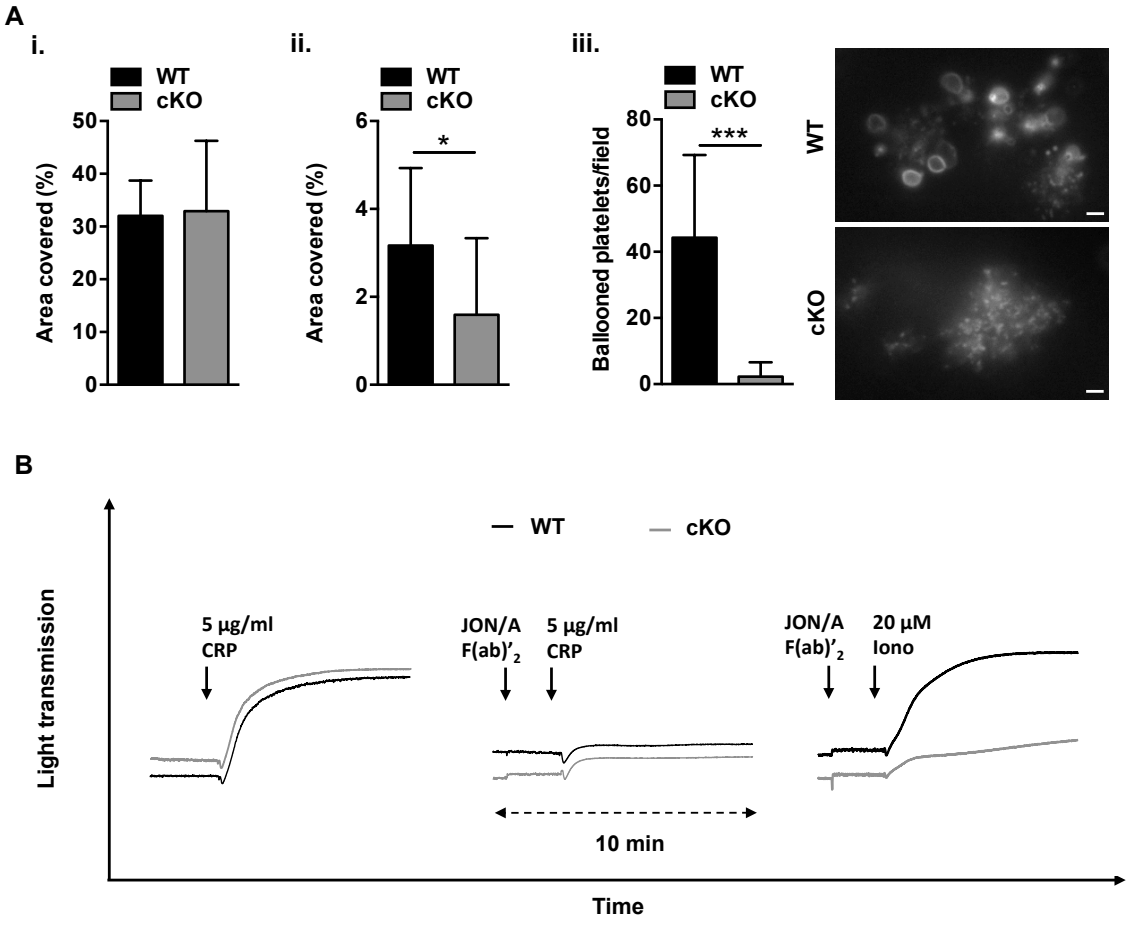

Figure 18. TMEM16F platelets display reduced procoagulant characteristics – severely impaired ability to undergo membrane ballooning. (A) Whole blood from WT or cKO mice was labeled with $DiOC_6$ to mark platelets and AF568-annexin A5 to mark platelet surface exposed PS. Labeled blood was perfused over a collagen/tissue factor micro spot on coverslips placed in a parallel flow chamber, at $1000s^{-1}$ for 4.5 min. Quantification of platelet surface coverage (i) and PS surface coverage (ii). Both were quantified using integrated fluorescent intensity of the acquired images using ImageJ software. (iii) Quantification of count of platelets with a ballooned membrane (number of ballooned platelets/image ± SD) and representative images showing impaired ability of adherent cKO platelets to acquire a ballooned morphology (scale bar, 2 µm). Data obtained from testing 9 WT vs 11 cKO mice. *P<0.05, ***P<0.001; unpaired Student's t test. (B) Traces obtained from recording changes in light transmission through a platelet suspension on a Fibrintimer 4 channel aggregometer, as a measure of extent of platelet ballooning in suspension. Both WT and cKO platelets undergo classical aggregation on stimulation with CRP manifested as an increase in light transmission through the platelet suspensions. Aggregation on stimulation with CRP is abolished on pre-treatment of the platelet suspension with JON/A F(ab)'$_2$ fragments that block αIIbβ3. Yet ionomycin stimulation of JON/A F(ab)'$_2$ fragments treated WT platelets causes an increase in light transmission. This indicates that this increase in light transmission correlates with transformation of platelets to a more rounded and translucent morphology (ballooned) and not classical aggregation. The ability of cKO platelets to transform to a ballooned morphology on simulation with ionomycin is severely impaired. Representative data of 3 individual experiments, n = 4 mice per group in each experiment. (Baig *et al*., *ATVB* 2016)[120]

Further, it was previously shown that platelets in suspension stimulated with the calcium ionophore ionomycin do not undergo classical aggregation, but remodel into the ballooned form. This allows higher light transmission through the suspension due to the translucent

nature of the ballooned structures.[113] Therefore, recording changes in light transmission through a suspension of resting/activated platelets using an aggregometer was employed as a second method to determine membrane ballooning potential of WT and cKO platelets.

As a positive control, WT or cKO platelet suspensions were stimulated with CRP and were found to aggregate to a similar extent. As expected, this ability to aggregate on CRP stimulation was completely blocked in platelets pre-treated with JON/A F(ab)'$_2$ fragments which block platelet integrin αIIbβ3 and thus prevent platelet aggregation (Figure 18B).

However, when WT platelets were treated with ionomycin after pre-treatment with JON/A F(ab)'$_2$ fragments, increase in light transmission was still observed, not due to platelet aggregation, but due to transformation to a ballooned morphology. On the other hand, only a residual increase in light transmission was observed in cKO platelets indicating a severely defective ability to undergo membrane ballooning, as was also seen in the flow chamber assay.

Taken together, these results showed that cKO platelets have dramatically reduced, yet not abolished procoagulant potential.

3.1.4. TMEM16F accelerates platelet-driven thrombin and fibrin formation

The role of procoagulant platelets is to provide a catalytic surface for the binding of the tenase and prothrombinase complexes of the coagulation cascade, to greatly amplify the production of thrombin. To assess the consequences of the defective procoagulant activity of TMEM16F cKO platelets on thrombin production, evaluation of thrombin generation kinetics was performed using thrombinoscope measurements. These measurements were conducted in unstimulated platelet-rich plasma (PRP), PRP co-stimulated with CRP and PAR-4 peptide (to simultaneously stimulate ITAM and GPCR-coupled signaling pathways), and PRP stimulated with the calcium ionophore A23187.

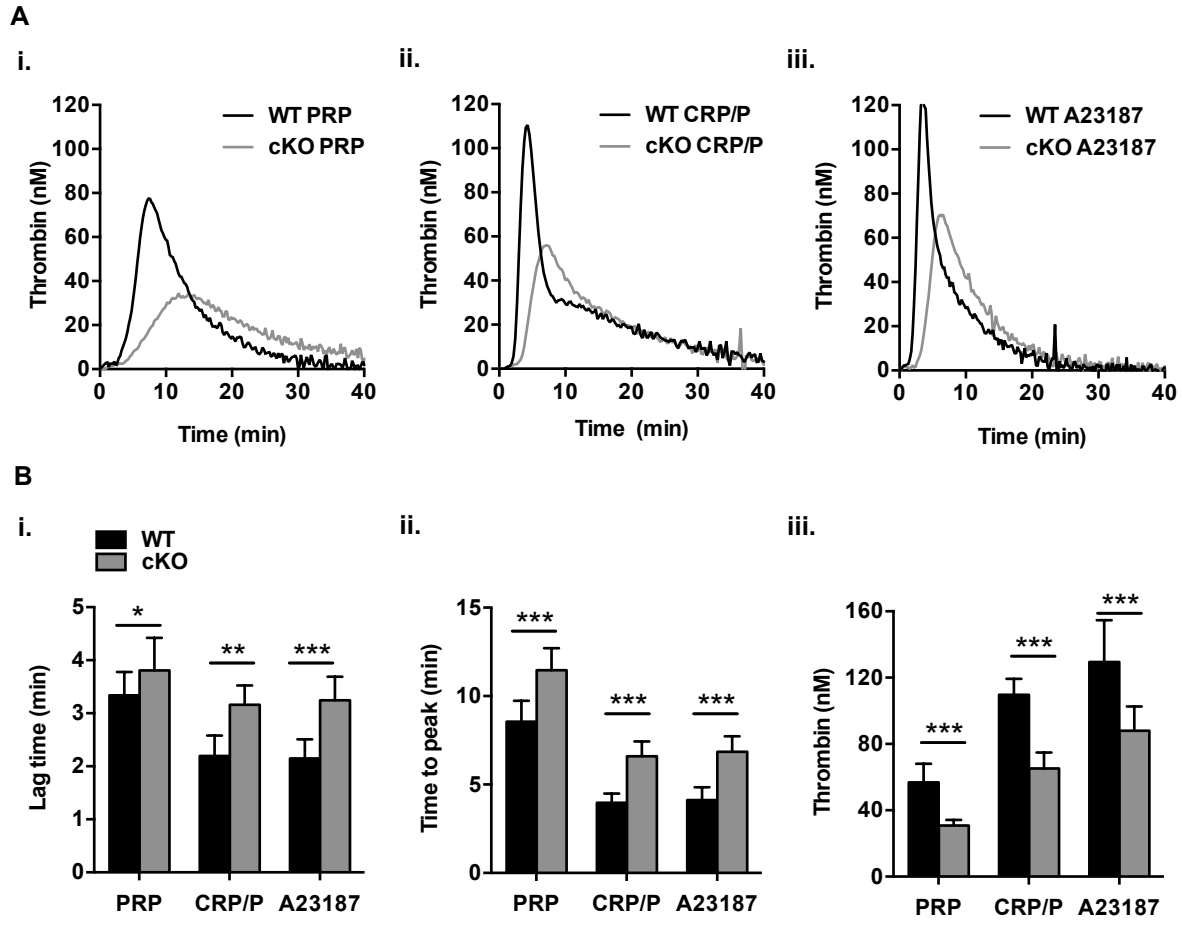

Figure 19. TMEM16F cKO platelets support decelerated thrombin generation. Tissue factor-initiated thrombin generation at 37 °C was measured in a thrombinoscope. (A) Representative calibrated automated thrombogram (CAT) curves of the three conditions tested in WT vs cKO samples (i) PRP – Platelet-rich plasma (ii) CRP/P – PRP co-stimulated with CRP (20 µg/mL) and PAR-4 peptide (5 mmol/L) (iii) A23187 – PRP stimulated with calcium ionophore A23187 (10 µM). The curves for the cKO samples are shifted to the right compared to WT samples, indicating decelerated onset of thrombin generation. (B) Quantification of thrombin generation kinetics. cKO platelets take significantly longer to initiate the production of thrombin (Lag time, left). In addition, the time taken to achieve peak concentration of thrombin during the measurement is also significantly delayed in the cKO samples compared to WT samples (Time to peak, middle). Finally, the peak concentration of thrombin produced in a measurement is significantly lower for the WT samples compared to the cKO samples (Thrombin, nM, right). Results shown as mean ± SD, data pooled from 3 independent experiments, n = 4 animals per group. **P*<0.05, ***P*<0.01, ****P*<0.001; unpaired Student's *t* test. (Baig *et al*., *ATVB* 2016)[120]

The thrombograms obtained from the thrombinoscope measurements allow for the interpretation of three kinetic parameters. The first is 'lag time', which is the time gap between starting the measurement by addition of tissue factor and the initiation of thrombin generation in the sample. The lag time was significantly longer in the cKO samples as compared to WT samples under the conditions tested (Figure 19Bi). The second kinetic parameter is 'time to peak' which is the time required until the peak amount of thrombin production takes place in

the sample. Under all three conditions tested, the time to reach peak thrombin levels was significantly delayed in the cKO samples as compared to WT samples (Figure 19Bii). The third parameter is the highest concentration of thrombin produced in the sample, and the cKO samples produced significantly lower peak thrombin levels as compared to WT samples (Figure 19Biii).

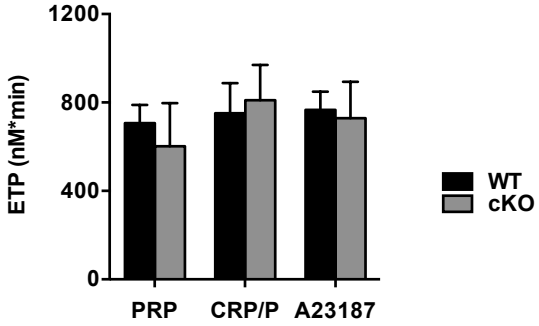

Figure 20. Total amount of thrombin production supported by TMEM16F cKO platelets is comparable to WT platelets. Tissue factor-initiated thrombin generation at 37 °C was measured in a thrombinoscope. Quantification of the integrated amount of thrombin produced over time - Endogenous Thrombin Potential (ETP), under the three conditions tested: PRP – Platelet-rich plasma; CRP/P – PRP co-stimulated with collagen related peptide (20 µg/mL) and PAR-4 peptide (5 mmol/L); A23187 – PRP stimulated with calcium ionophore A23187 (10 µM). cKO platelets support production of total amount of thrombin comparable to WT platelets. Results shown as mean ± SD, data pooled from 3 independent experiments. (Baig *et al*., *ATVB* 2016)[120]

Representative thrombograms illustrating thrombin production over time in WT vs cKO samples are shown in Figure 19A. Notably, the thrombin production supported by cKO platelets was only decelerated as compared to that supported by WT platelets and not reduced. At the end of the measurement, comparable total amounts of thrombin were generated in the WT and cKO samples, as shown by measurement of 'Endogenous Thrombin Potential' (ETP), which is the integrated amount of thrombin produced during the course of the measurement (Figure 20).

Thrombin produced in a growing thrombus is required to catalyze the conversion of soluble fibrinogen in plasma to insoluble fibrin to form a clot. The implications of the decelerated thrombin production in cKO samples for generation of fibrin were tested in the *ex vivo* flow chamber assay described in section 3.1.4.

Whole blood was pre-labeled with AF647-fibrinogen and perfused over glass cover slides coated with micro-spots of collagen and tissue factor. The time to appearance of the characteristic fibrous structure of insoluble fibrin was visually determined. Fibrin formation

took place in all the WT samples within the 8 min observation period. However, for the cKO samples, either fibrin formation did not take place within the 8 min period (in more than 50% of the samples), or it was significantly delayed as compared to the fibrin formation in the WT samples (Figure 21A).

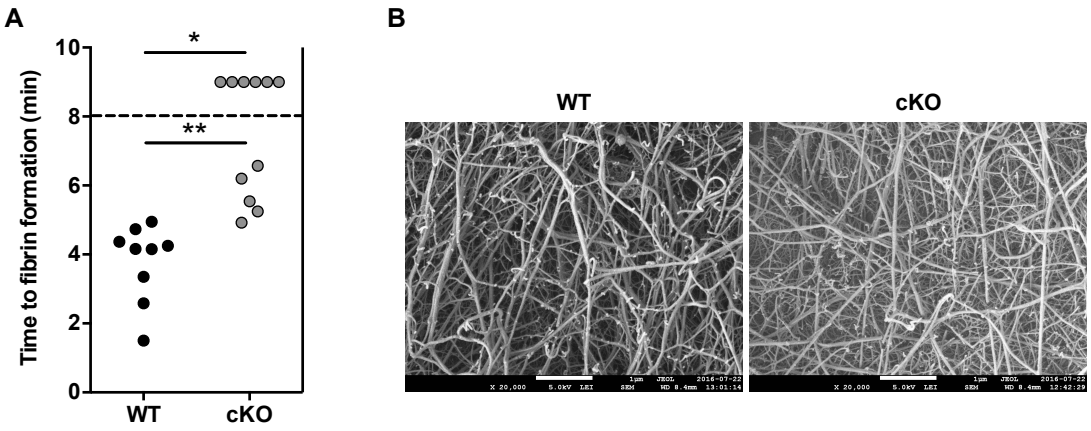

Figure 21. TMEM16F cKO platelets support delayed fibrin formation. Citrate anticoagulated whole blood from WT or cKO mice was labeled with AF647-fibrinogen to detect fibrin(nogen). This labeled blood was perfused over a collagen/tissue factor microspot on coverslips placed in a parallel flow chamber, at 1000s^{-1} until the characteristic thread-like formation of fibrin was observed (***P*<0.01; unpaired Student's *t* test) or until a maximum observation period of 8 min (**P*<0.05; Fischer exact test). (A) Comparison of the recorded times of fibrin formation. Each dot represents one run. (B) For samples in which fibrin formation took place, coverslips were washed and prepared for imaging by Scanning Electron Microscopy. Representative images of fibrin fibers observed in WT and cKO samples. Scale bar 1 µm. (Baig *et al*., *ATVB* 2016)[120]

The cKO samples in which delayed fibrin formation was observed were further analyzed by scanning electron microscopy to examine the ultrastructure of the fibrin fibers in comparison to those formed in the WT samples. Representative images are shown in Figure 21B. There were no obvious differences between the fibrin fibers in the WT and cKO samples.

These results show that the scramblase activity of TMEM16F is required to accelerate the thrombin production supported by platelets, which in turn is required to accelerate fibrin formation.

3.1.5. TMEM16F in platelets is important for hemostasis and arterial thrombosis

Scott Syndrome patients with a loss of function mutation in *Ano6* are known to suffer from uncontrolled provoked bleeding episodes.[6] In line with this, TMEM16F KO mice generated previously by another laboratory were reported to display prolonged bleeding times.[27] However, in both cases, not only the platelets, but also other cell types like red blood cells, white blood cells, as well as the endothelium lack procoagulant potential. Thus, the specific contribution of TMEM16F-mediated platelet procoagulant activity for the processes hemostasis and thrombosis had remained unclear.

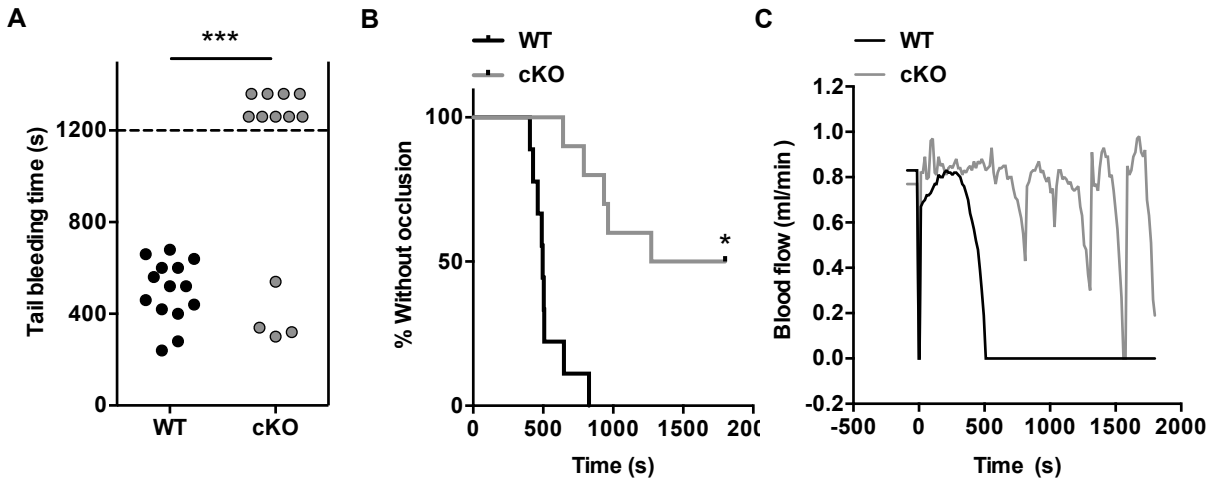

Figure 22. TMEM16F cKO mice display impaired hemostasis and are protected in an experimental model of arterial thrombosis. (A) Measurement of tail bleeding time using the filter paper method. Each dot represents time of cessation of bleeding of one mouse. TMEM16F cKO mice were found to display significantly prolonged bleeding times. ****P*<0.001; Fischer exact test. (B) TMEM16F cKO mice are protected in an experimental model of $FeCl_3$-induced arterial thrombosis in the carotid artery. The vessels in 50% of the mice tested did not occlude within the observation period of 30 min (**P*<0.05; Fischer exact test), and in the remaining 50% of the mice, vessel occlusion occurred significantly later than in WT mice (Mean time to occlusive thrombus formation, WT=8.8±2.2 min; cKO=15.3±3.9 min; **P*<0.05; unpaired Student's *t* test). 8 WT vs 10 cKO mice were tested in the model. (C) Representative chart comparing blood flow through the carotid artery of a WT (black line) and cKO (grey line) mouse before and after induction of thrombosis by application of $FeCl_3$. In case of the WT vessel, blood flow ceased completely within 10 min of injury due to stable occlusion of the vessel, whereas for the cKO vessel, frequent incidences of embolization were observed and stable vessel occlusion did not occur. (Baig *et al.*, *ATVB* 2016)[120]

To address this directly, WT and cKO mice were challenged in a tail bleeding time assay using the filter paper method. The majority of the cKO animals did not stop bleeding within the 20 min observation period during which all WT animals stopped bleeding (Figure 22A).

The cKO animals were also challenged in an experimental model of arterial thrombosis where thrombosis is induced by a chemical injury to the vessel wall with a filter paper soaked with $FeCl_3$. While all WT animals tested in the model were found to form an occlusive thrombus in the vessel within 30 min of observation time, 50% of the cKO animals tested were completely protected from occlusive thrombus formation. In the remaining 50% of the animals, time to occlusive thrombus formation was significantly prolonged as compared to the WT animals (Figure 22B). These results are in good agreement with the *ex vivo* fibrin formation observed in WT vs cKO samples (Figure 21A).

It is important to note that this impairment in occlusive thrombus formation did not arise from defects in initial platelets adhesion and aggregation, but was rather due to frequent embolization of the forming thrombi, which was observed in the majority of the cKO animals tested. Representative blood flow traces are shown in Figure 22C.

These results demonstrated that TMEM16F-mediated platelet procoagulant activity plays a vital role *in vivo* for the processes of hemostasis as well as arterial thrombosis.

3.1.6. Platelet TMEM16F activity does not contribute to cerebral thrombo-inflammation

Both platelets and coagulation have been shown to play a role in the progression of thrombo-inflammation post ischemic stroke.[121] However, it is not known whether the interface between the two through the transformation of platelets to a procoagulant state is important for the pathogenesis of reperfusion injury.

As TMEM16F-mediated procoagulant activity was observed to play a role in the progression of arterial thrombosis, mice were subjected to the tMCAO model of ischemic stroke to investigate the effects of loss of platelet TMEM16F on the progression of ischemic stroke.

In contrast to results obtained in the experimental model of arterial thrombosis, cKO animals developed infarct volumes similar to those observed in WT animals 24 h post tMCAO as revealed by TTC staining of brain sections (Figure 23A). In addition, the mice subjected to tMCAO were analyzed for the degree of functional dysfunction by measuring the Bederson score as readout of neurological deficit, and the grip test as a measure of motor deficits. The cKO animals had a functional outcome similar to WT mice - in terms of both motor and neurological function (Figure 23B,C).

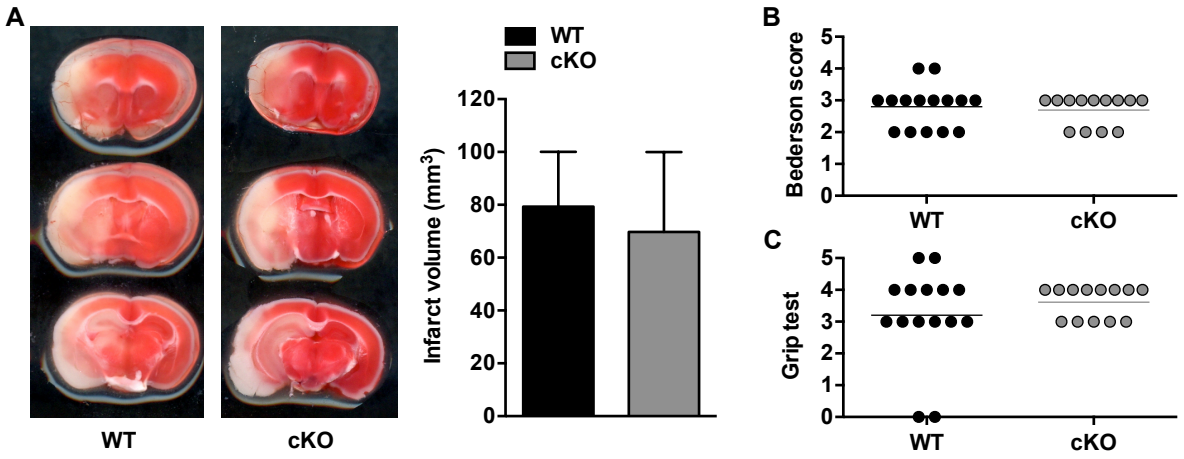

Figure 23. TMEM16F cKO mice display infarct volumes and functional outcomes similar to WT mice in a model of ischemic stroke. (A) Representative images of TTC stained sections of brains from WT and cKO animals post 60 min of ischemia followed by 23 h of reperfusion. The tissue stained pink by TTC is the viable brain tissue, whereas the white area is the infarcted region. (B) Edema corrected quantification of the infarct region in WT vs cKO brains. 15 WT vs 13 cKO animals, data shown as mean ± SD. *P*>0.05, unpaired Student's *t* test (C) Representation of outcomes in measurement of Bederson score (indication of global neurological defects; 0 normal, 5 worst deficit) and (D) Representation of analysis of motor function and coordination defects measured by Grip test (5 normal, 0 worst deficit). Each dot represents one animal. (Baig *et al*., *ATVB* 2016)[120]

These results show that while the scramblase TMEM16F is important for the processes of hemostasis and thrombosis, it does not significantly contribute towards the patho-physiology of postischemic cerebral thrombo-inflammation.

3.2. Generation of humanized coagulation factor XII (FXII) knockin mice as a model for testing novel anti-thrombotic agents

The targeting strategy designed to generate humanized FXII knockin mice (hFXII KI) that would express human FXII instead of endogenous mouse FXII is described in section 2.1.3. The hFXII KI mice were distinguished from WT mice using the genotyping protocols described in section 2.2.1.1.2.

To confirm the success of the targeting strategy, the plasma from heterozygous hFXII KI mice (hFXII KI/+) and homozygous hFXII KI mice were tested by Western blot analysis using a specific antibody that detects human FXII but not mouse FXII. Plasma from WT mice and human plasma were used as negative and positive controls respectively (Figure 24A). These studies confirmed the expression of 80 kDa human FXII in hFXII KI/+ and hFXII KI mice.

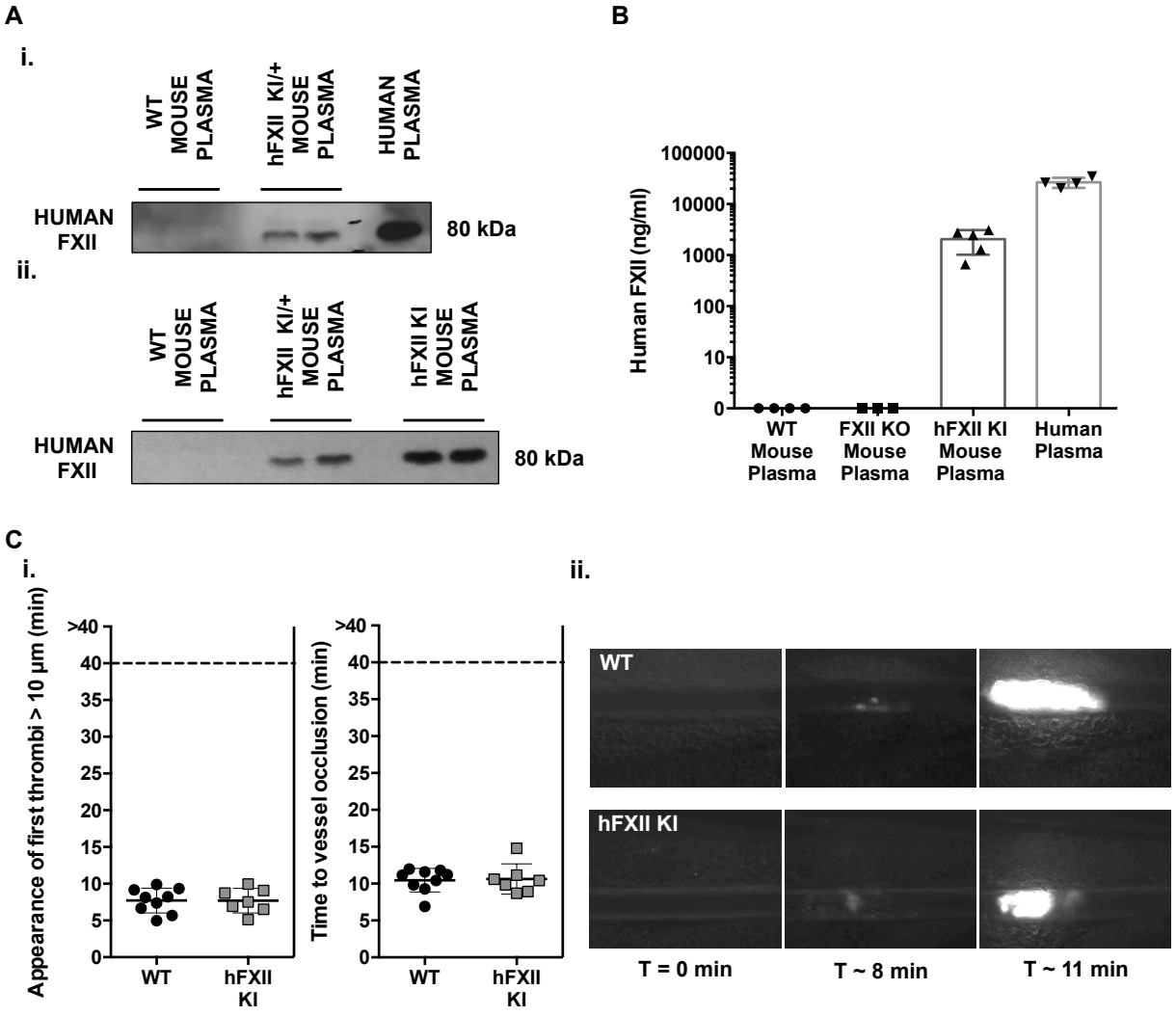

Figure 24. hFXII KI mice express human coagulation factor (FXII) and display normal occlusion times in an experimental model of arterial thrombosis. (A) i. Western blot of plasma from hFXII WT and heterozygous hFXII KI mice (hFXII KI/+) using a specific antibody against human FXII. Human plasma was used as a positive control. ii. Western blot of plasma from hFXII WT, hFXII KI/+ and hFXII KI mice using a specific antibody against human FXII. These Western blots confirmed the expression of human FXII in hFXII KI mice. (B) Quantitative ELISA for human FXII. The expression levels of human FXII in hFXII mouse plasma were determined using a specific quantitative ELISA. Human plasma was used as a positive control, and plasma from WT and FXII KO mice were used as negative controls. The concentration of human FXII in mutant mouse plasma was 2.4 ± 0.8 µg/mL, while the concentration in human plasma was 26.7 ± 6 µg/mL. (C) hFXII KI mice had occlusion times comparable to occlusion times in WT animals in an experimental model of $FeCl_3$-induced arterial thrombosis in the mesenteric arterioles. i. Quantification of appearance of first thrombi (>10 µm), and vessel occlusion. Each dot represents one vessel ii. Representative images showing development of occlusive thrombi in mesenteric arterioles of WT and hFXII KI mice following injury with a drop of 20% $FeCl_3$ solution.

Next, the concentration of human FXII expressed in hFXII KI mice was determined using a specific quantitative ELISA that detects human FXII but not mouse FXII. FXII was not detected in samples from WT mice, or from FXII knockout (FXII KO mice) demonstrating the

specificity of the ELISA for human FXII. The average concentration of human FXII in hFXII KI mice was 2.4 ± 0.8 µg/mL, whereas the concentration in human plasma was 26.7 ± 6 µg/mL (Figure 24B). The normal concentration of FXII in human plasma was reported in the literature to be at ~30 µg/mL, and thus corresponds to the values detected in this assay.[122, 123] However, the approximately 10 fold difference in the expression of human FXII in human plasma and hFXII KI mice could arise either due to species specific differences between humans and mice, or due to presence of residual mouse FXII in the hFXII KI mice. A Western blot using specific antibodies against mouse FXII and a quantitative ELISA to determine average concentrations of FXII in WT mouse plasma are required to test these hypotheses.

However, when challenged in an experimental model of $FeCl_3$-induced arterial thrombosis in the mesenteric arterioles, the time to appearance of first thrombi greater than 10 µm, as well as occlusion times in the hFXII KI mice were comparable to those observed in WT animals (time to appearance of thrombi greater than 10 µm: WT=7.7±1.7 min, hFXII Mut=7.7±1.7 min; time to vessel occlusion: WT=10.5±1.6 min, hFXII KI=10.6±2 min) (Figure 24C). Therefore, replacement of mouse FXII with human FXII does not impair the role of the coagulation factor in the patho-physiology of arterial thrombosis. These results demonstrated that human FXII is functional within the mouse physiology, as also suggested by results in previous reports where *i.v* injection of human FXII into FXII KO mice reversed the protection from infarct development in the KO mice lacking endogenous FXII in the tMCAO model of ischemic stroke.[38]

Thus, the hFXII KI mice can be used as a model to test novel antithrombotic agents developed against human FXII, in a convenient experimental animal model.

3.3. The adapter proteins Grb2 and Gads have partially redundant roles for activation and hemostatic function of mouse platelets

3.3.1. Generation of Grb2/Gads double knockout mice

Grb2 and Gads are the only members of the Grb2 family of adapter proteins that are expressed in platelets.[59, 102] Megakaryocyte- and platelet-specific conditional KO mice lacking Grb2 specifically in their megakaryocytes and platelets have been described previously.[92] Constitutive KO mice lacking the adapter protein Gads have also been described.[95]

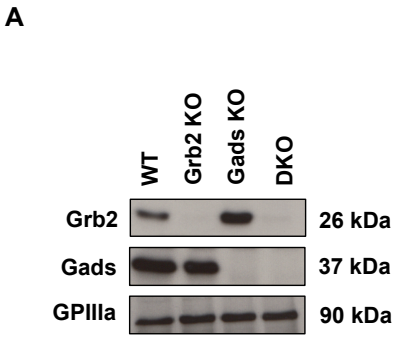

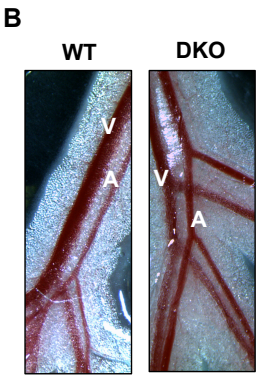

C

Mating 1:	*Grb2* $^{fl/fl\ Pf4\text{-}Cre\ -/-}$ x *Grb2* $^{fl/fl\ Pf4\text{-}Cre\ +/-}$	
	EXPECTED	**OBTAINED**
WT	50%	32 (50.8%)
Grb2 KO	50%	31 (49.2%)
Total		63

Mating 2:	*Gads* $^{-/-}$ */Grb2* $^{fl/fl\ Pf4\text{-}Cre\ -/-}$ x *Gads* $^{-/-}$*/Grb2* $^{fl/fl\ Pf4\text{-}Cre\ +/-}$	
	EXPECTED	**OBTAINED**
Gads KO	50%	48 (47.1%)
DKO	50%	54 (52.9%)
Total		102

Figure 25. Generation of Grb2/Gads double knockout mice (DKO). *Grb2*$^{fl/fl\ Pf4\text{-}Cre\ +/-}$ and *Grb2*$^{fl/fl}$ mice on a *Gads*$^{-/-}$ background were crossed to obtain mice double deficient for both adapter proteins. (A) Western blot of platelet lysates from WT, *Grb2* KO, *Gads* Gads KO or Grb2/Gads DKO mice using specific antibodies against Grb2 or Gads. Complete loss of both adapters at protein level was confirmed in DKO platelets. The GPIIIa subunit of platelet integrin GPIIb/IIIa was used as loading control. (B) Images of mesenteric circulation of WT and DKO mice showing arterioles (A), venules (V) and normal blood and lymphatic vessel separation as blood filled lymphatic vessels were not observed. (C) Mating strategy used for generation of WT, Grb2 KO, Gads KO and DKO mice. Mice of all four genotypes were born with an expected Mendelian distribution.

To generate double deficient mice lacking both adapter proteins in their megakaryocytes and platelets, the *Grb2*$^{fl/fl\ Pf4\text{-}Cre+/-}$ mice (Grb2 KO) were intercrossed with the *Gads*$^{-/-}$ (Gads KO) mice as described in section 2.1.3. Using the mating strategy described in section 2.1.3 and Figure 25C, mice of all 4 genotypes – wild-type (WT, *Grb2*$^{fl/fl}$ mice), Grb2 KO (*Grb2*$^{fl/fl\ Pf4\text{-}Cre+/-}$ mice), Gads KO (*Gads*$^{-/-}$/ *Grb2*$^{fl/fl}$ mice) & Grb2/Gads double knockout mice (DKO, *Gads*$^{-/-}$/ *Grb2*$^{fl/fl\ Pf4\text{-}Cre+/-}$ mice) were born conforming to expected Mendelian distribution (Figure 25C).

Western blot analysis confirmed lack of Grb2 in Grb2 KO platelets, of Gads in Gads KO platelets, and both Grb2 and Gads in DKO platelets at protein level, confirming the success of the mating strategy used for the generation of the double deficient mice (Figure 25A).

Several components of the hemITAM signaling pathway play an important role in the regulation of separation of blood and lymphatic vasculature - mice deficient in CLEC-2, Syk, SLP76 and PLCγ2 show bood/lymphatic mixing. To investigate whether the combined

deficiency of Grb2 and Gads has an influence on the separation of lymphatics from blood vasculature, the mesenteric circulation of the DKO mice was visualized and compared with that of the WT mice. Distinct arterioles and venules were observed in the mesenteric circulation network of the DKO mice comparable to WT mice, and there was no evidence of blood and lymphatic vessel mixing demonstrating that the adapters Grb2 and Gads do not play a role in this process (Figure 25B)

3.3.2. Grb2/Gads DKO animals display overall normal blood parameters

A hematology analyzer was used to determine whole blood parameters including white blood cell and red blood cell counts, hemoglobin, hematocrit and mean platelet volume. There were no significant differences between WT, Grb2 KO, Gads KO and DKO mice (Table 2 and Figure 26B). The absolute count of platelets in the peripheral circulation was specifically determined by a flow cytometry-based method employing beads of a known count and was comparable between all four groups of mice (Figure 26A).

	WT	Grb2 KO	Gads KO	DKO
WBC x 10^3/µL	6.25 ± 2.73	5.25 ± 1.98	5.25 ± 2.44	4.50 ± 0.87
RBC x 10^3/µL	6.30 ± 0.74	6.48 ± 0.54	6.18 ± 0.67	5.83 ± 1.58
HGB (g/dL)	7.75 ± 1.20	8.75 ± 0.97	8.25 ± 1.56	8.00 ± 2.00
HCT (%)	31.50 ± 3.97	33.00 ± 2.65	30.75 ± 2.82	29.25 ± 6.70

Table 2. Grb2 KO, Gads KO and Grb2/Gads DKO mice have normal blood counts. HGB, hemoglobin; HCT,hematocrit. Data shown as mean ± SD (n = 8 mice per group. Values obtained for the three groups of KO mice are not significantly different from values obtained for WT mice; unpaired Student's *t* test).

In addition, the average lifespan of platelets in WT and the three groups of KO mice was determined. Platelets form Grb2 KO, Gads KO and Grb2/Gads DKO mice had a lifespan comparable to platelets from WT mice with a similar reduction in the population of platelets labeled at day 0, over the observation period of four days (Figure 26C).

A FACS assay employing specific FITC-labeled antibodies was used to determine the expression of major signaling glycoproteins present on the surface of platelets. There were no significant differences between platelets obtained from WT, Grb2 KO, Gads KO or Grb2/Gads DKO animals (Figure 27).

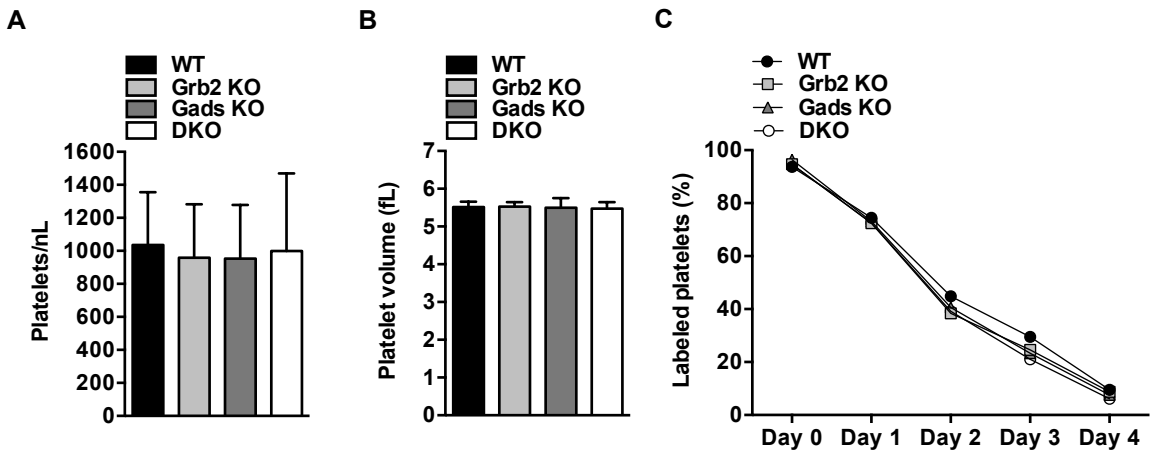

Figure 26. Grb2/Gads DKO animals have normal platelet count, size and lifespan. (A) Absolute count of circulating platelets measured by flow cytometry (platelets/nL ± SD, n=8, pooled values from two independent experiments). (B) Platelet volume as measured by a hematology analyzer, Sysmex KX-21TM (MPV, mean platelet volume in femtolitre (fL) ± SD, n=8, pooled values from two independent experiments). (C) Platelet lifespan analyzed by measurement of labeled platelets by flow cytometry over a period of 4 days (percentage of labeled platelets ± SD, n=6, pooled values from two independent experiments). Both single KO and DKO animals had a platelet count, size and lifespan comparable to WT animals (unpaired Student's *t* test).

Based on these results, the single KO animals (Grb2 KO and Gads KO) as well as the double deficient animals (Grb2/Gads DKO) were considered to have overall normal blood parameters, comparable to WT mice.

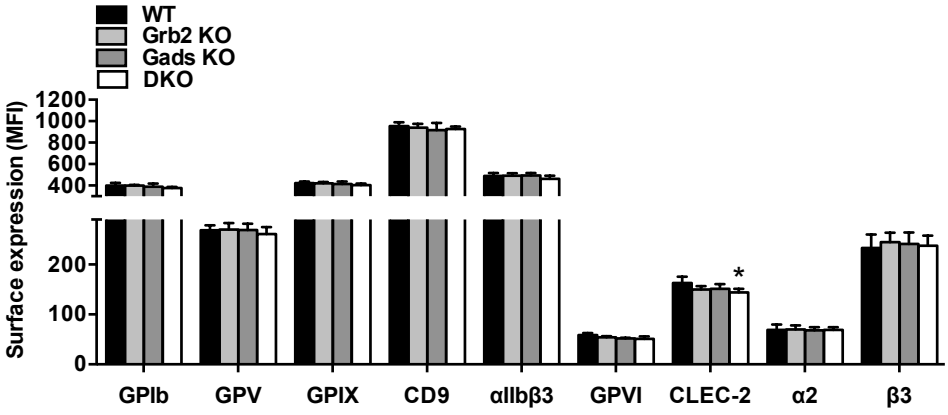

Figure 27. Platelets from Grb2/Gads DKO animals have normal surface expression of major signaling glycoproteins. Expression levels of glycoproteins present on the platelet surface were determined by flow cytometry using fluorophore-labeled antibodies. Results are expressed as MFI ± SD (n = 4 mice per group; representative data of 3 individual experiments). The Grb2 KO, Gads KO as well as Grb2/Gads DKO platelets were found to have grossly normal levels of surface glycoproteins compared to WT platelets. *P<0.05; unpaired Students *t* test

3.3.3. Grb2 KO, Gads KO and Grb2/Gads DKO animals display a specific platelet activation and aggregation defect following stimulation of the (hem)ITAM signaling pathways

The ability of platelets to be activated upon stimulation was determined by measurement of change of integrin αIIbβ3 to an active conformation, and the release of α-granules (determined by measurement of exposure of P-selectin) in a flow cytometry based assay.

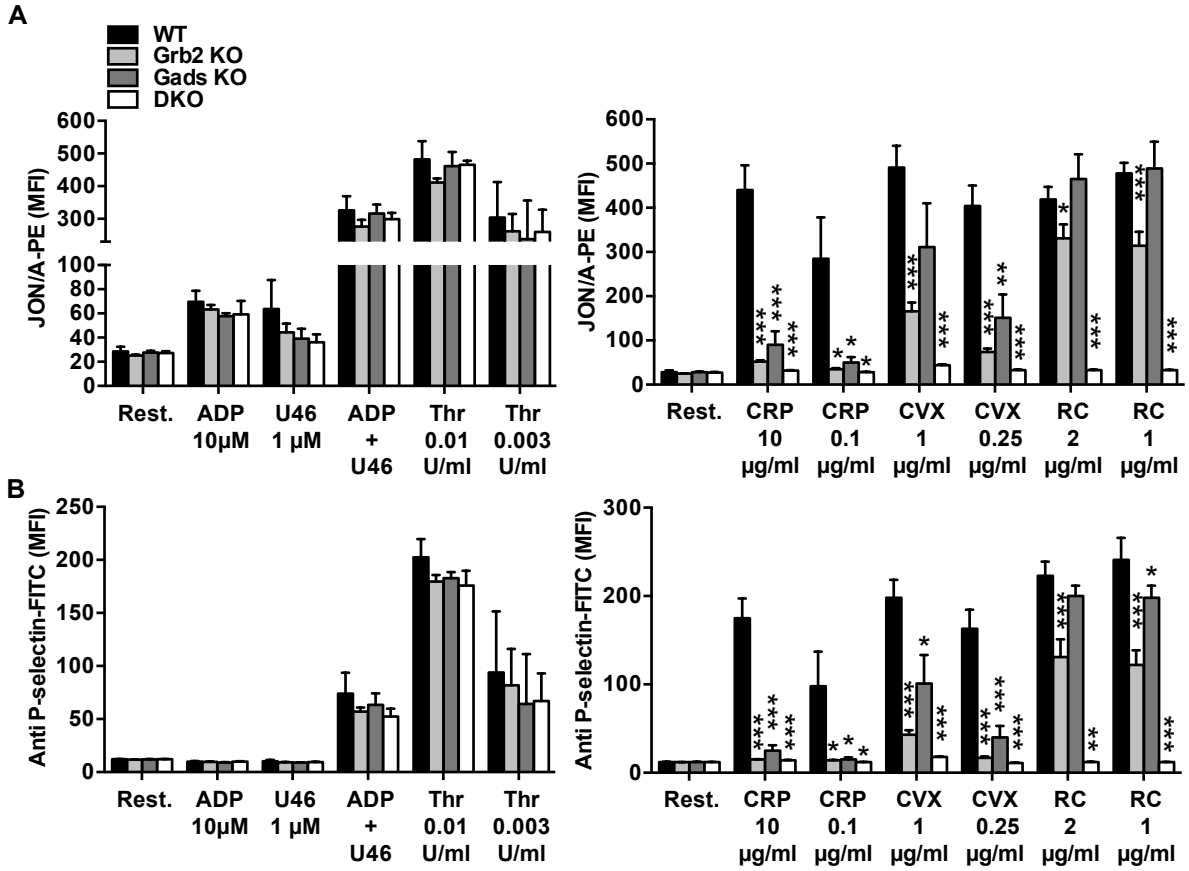

Figure 28. (hem)ITAM-specific activation is abolished in Grb2/Gads DKO platelets (**A**) Measurement of integrin αIIbβ3 activation on stimulation with the indicated agonists by flow cytometry using JON/A-PE antibody. (**B**) Measurement of α-granule release as indicated by P-selectin exposure. Both experiments were performed to evaluate degree of platelet activation. Results are expressed as MFI ± SD (n = 4 mice per group; representative data of 3 individual experiments). The single KO and DKO platelets are activated to a similar extent as WT platelets when stimulated with agonists that activate the GPCR-coupled signaling pathways (ADP, U46 - U46619 and Thr - thrombin), but have a severely defective activation response on stimulation with agonists that activate the (hem)ITAM signaling pathway (CRP – collagen-related peptide, Cvx - convulxin and RC - rhodocytin). **P*<0.05, ***P*<0.01, ****P*<0.001; unpaired Student *t* test.

When stimulated with GPCR agonists like ADP, TxA_2 analog U46619 or thrombin – the Grb2 KO, Gads KO as well as the Grb2/Gads DKO platelets were activated to an extent similar to

WT platelets. However, when stimulated with agonists that trigger the ITAM signaling pathway (CRP or convulxin), or the hem-ITAM signaling pathway (rhodocytin), platelets derived from all three groups of KO mice had a severely impaired activation response – seen for assessment of both integrin activation and degranulation. This impaired activation was most pronounced in platelets derived from Grb2/Gads DKO mice, followed by platelets derived from Grb2 KO animals. The least degree of impairment was observed for the platelets derived from Gads KO mice where the highest agonist concentrations activated the mutant platelets to an extent comparable to WT platelets (Figure 28).

Defective DKO platelet activation on stimulation with (hem)ITAM agonists was expected as the adapter proteins Grb2 and Gads are known components of the LAT-signalosome that lies downstream of (hem)ITAM signaling. Severely defective activation on stimulation with (hem)ITAM agonists in platelets derived from Grb2 KO mice has been reported previously. Notably, however, it is interesting that the deficiency of both adapters Grb2 and Gads reduces the MFI values to almost resting values under conditions at which partial platelet activation is observed in the platelet samples derived from the single KO animals pointing towards redundant functions of Grb2 and Gads for platelet activation.

Similarly, on assessing the aggregation response of the platelets from the four groups of mice, it was observed that the Grb2 KO, Gads KO, and the Grb2/Gads DKO platelets have an aggregation response comparable to WT platelets when stimulated with the GPCR agonist thrombin (Figure 29). However, when stimulated with the ITAM-specific agonists CRP or collagen, or with the hemITAM agonist rhodocytin, all three groups of KO mice show an impaired aggregation response. Like in the case of the assessment of platelet activation by flow cytometry, the degree of impairment of the aggregation response was most severe for the Grb2/Gads DKO platelets followed by Grb2 KO platelets.

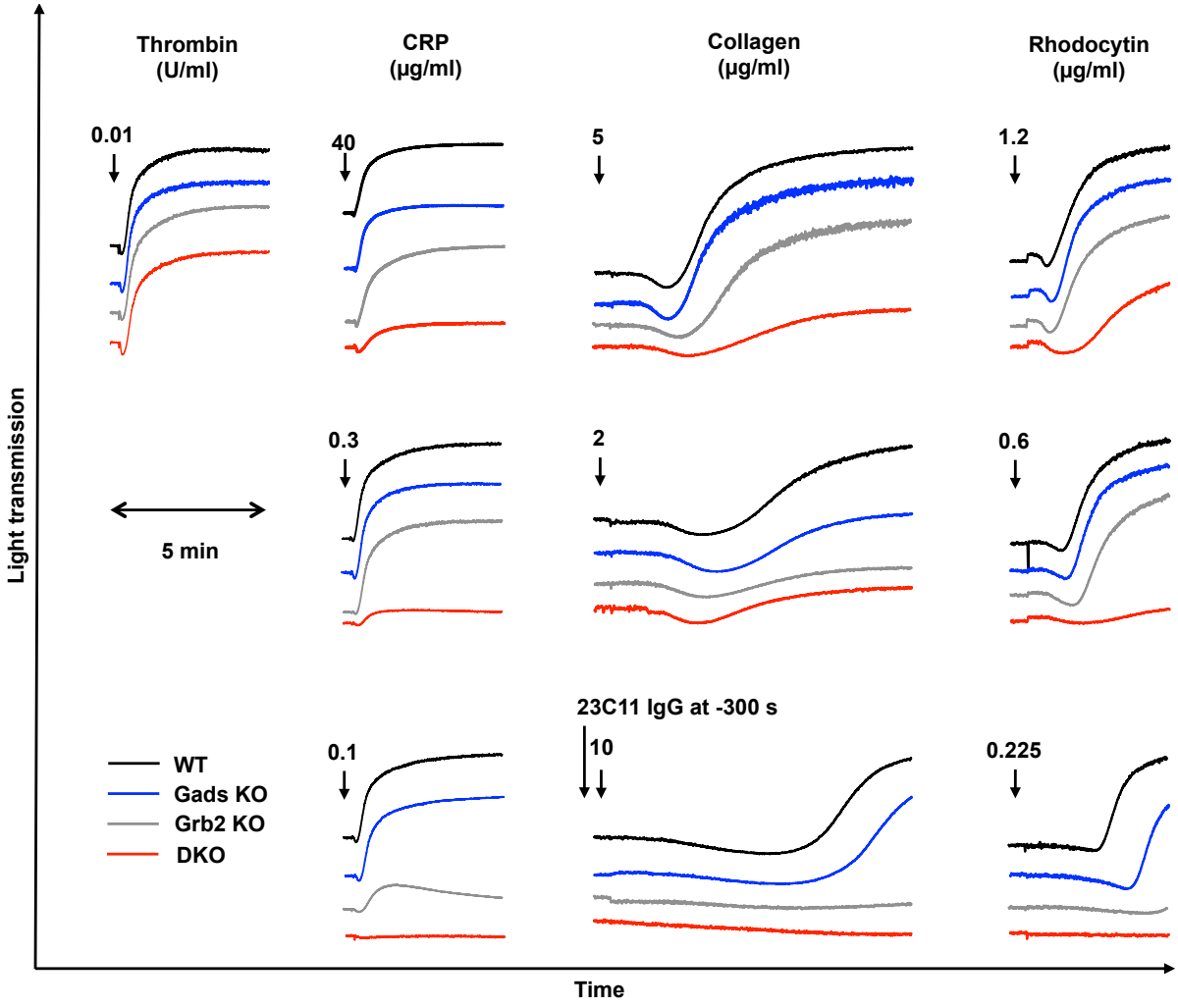

Figure 29. Grb2/Gads DKO platelets display severely impaired aggregation in response to (hem)ITAM-stimulation but not GPCR-stimulation. Aggregation traces from WT or cKO platelet suspensions recorded on a Fibrintimer 4 channel aggregometer. The platelet suspensions were stimulated with high, intermediate or low doses of agonists that activate the GPCR-signaling pathways (ADP, U46619, thrombin), or those that stimulate the ITAM signaling pathways (CRP, collagen). Representative traces from 3 individual experiments using 2 vs 2 mice.

Furthermore, a reduction in aggregation capacity was observed for the DKO platelet samples at agonist concentrations at which the Grb2 KO and the GADS KO platelet samples could aggregate to an extent comparable to WT samples. Even with a very strong stimulation with CRP using a concentration as high as 40 µg/mL, the severely impaired aggregation response in the DKO platelets persisted.

On stimulation with collagen, residual aggregation was observed in the DKO platelet samples. Since collagen stimulates both α2β1 and GPVI, the platelet samples were pre-treated with the antibody 23C11 to block the α2β1 receptors to delineate the effect of GPVI-mediated signaling alone on the aggregation response. Under these conditions, both the

Grb2 KO platelets, and the Grb2/Gads DKO platelets were unable to aggregate. The results of the aggregation studies thus also point towards functional redundancy between Grb2 and Gads.

3.3.4. Grb2 and Gads in mouse platelets have partially redundant function for platelet activation

Previous studies from our laboratory have shown that Grb2 KO mice exhibit severely defective platelet activation on stimulation with (hem)ITAM agonists in *in vitro* assays but that occlusion times are comparable to WT mice when challenged in *in vivo* experimental models of arterial thrombosis. It was speculated that one reason for this difference in the *in vitro* and *in vivo* results is functional compensation by the second member of the adapter protein family, Gads. In addition, TxA_2-induced GPCR signaling pathways were shown to partially compensate for defective (hem)ITAM signaling such that treatment of Grb2 KO animals with acetylsalicylic acid (blocks TxA_2 synthesis) predisposes the Grb2 KO animals to prolonged bleeding times as well as prolonged times for occlusive thrombus formation when tested in experimental models of hemostasis and thrombosis.[92] Gruner *et. al*. have also reported such compensatory mechanisms.[124]

In an effort to look at the differential impairment of platelet activation and aggregation in both single KO and Grb2/Gads DKO samples in more detail, and to dissect prevailing compensatory mechanisms, platelet activation of samples derived from mice of all four groups was tested following dual stimulation with a (hem)ITAM-specific agonist (CRP, convulxin or rhodocytin) in combination with a GPCR agonist (ADP or U46619).

Co-stimulation of WT platelet samples with (hem)ITAM agonists in combination with the TxA_2 analog U46619 produced an additive response for platelet activation. In the case of Grb2 and Gads single KO samples, co-stimulation substantially rescued the impaired activation responses obtained on stimulation with a single (hem)ITAM agonist. However, co-stimulation could not ameliorate the activation responses in the Grb2/Gads DKO samples in comparison to stimulation with a (hem)ITAM agonist alone (Figure 30). Similar results were obtained on dual-stimulation using a (hem)ITAM agonist in conjunction with the GRCR agonist ADP (Figure 30).

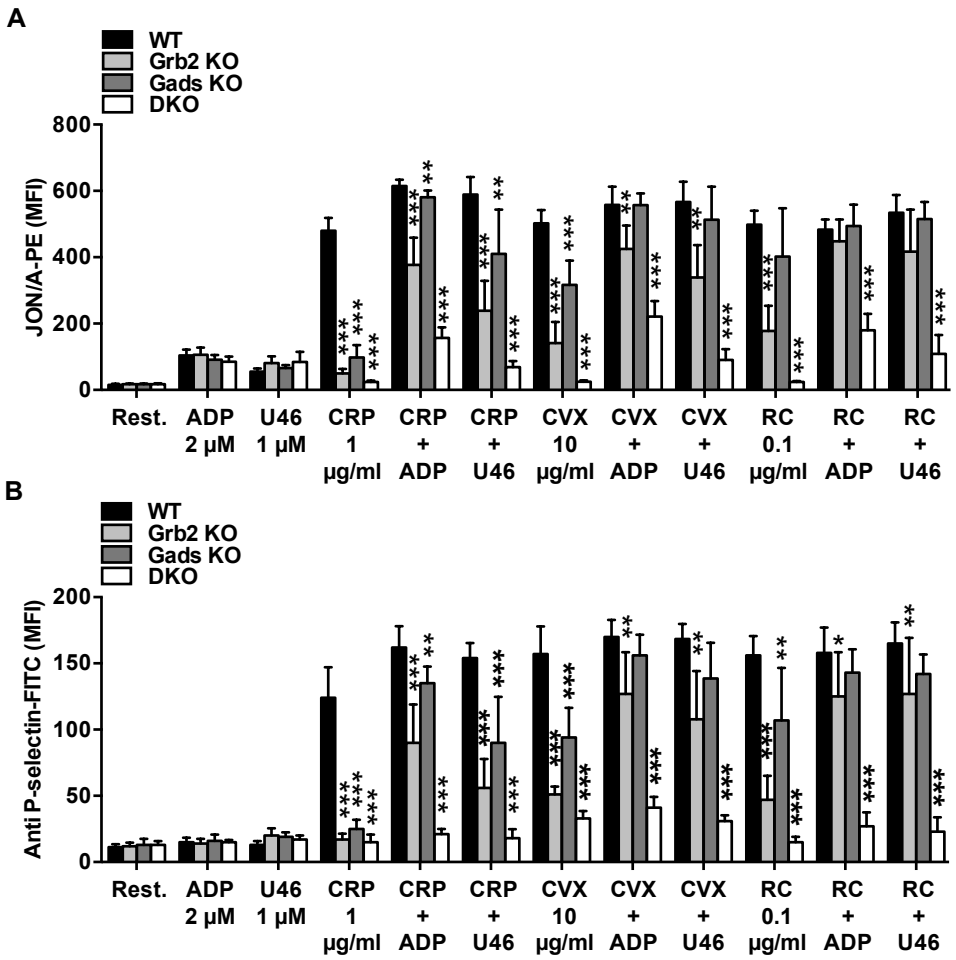

Figure 30. Grb2 and Gads have redundant function for mouse platelet activation. (**A**) Measurement of integrin αIIbβ3 activation by flow cytometry using the JON/A-PE antibody. (**B**) Measurement of α-granule release as indicated by P-selectin exposure by flow cytometry. Results are expressed as MFI ± SD (n = 4 mice per group; representative data of 3 individual experiments). Stimulation of platelet suspensions with a (hem)ITAM (CRP, Cvx or RC) agonist in conjunction with a GPCR-agonist (ADP or U46) had a synergistic effect on platelet activation responses seen in single KO platelets leading to a substantial rescue of the activation defect observed on stimulation with (hem)ITAM agonists alone. This was not the case for DKO platelets pointing towards functional redundancy between Grb2 and Gads. *P<0.05, **P<0.01, ***P<0.001; unpaired Student t test.

The persistent severely impaired platelet activation in samples from DKO mice confirmed partial functional redundancy between the adapter proteins Grb2 and Gads for platelet activation.

3.3.5. Defective phosphatidylserine (PS) exposure and (hem)ITAM signal transduction in Grb2/Gads DKO platelets

Platelet activation that initiates the (hem)ITAM signaling cascade culminates in an increase in intracellular calcium concentrations through release of calcium from intracellular stores, which in turn activates the platelet scramblases and causes the platelets to become procoagulant and expose phosphatidylserine (PS) on their surface.

The degree of calcium mobilization downstream of (hem)ITAM signaling was indirectly assessed through measurement of platelet PS exposure in samples from both single KO and Grb2/Gads DKO mice. Washed platelets were treated with different agonist and PS-exposure was measured through specific binding of DyLight-488-labeled annexin A5 to PS in a flow cytometry-based assay.

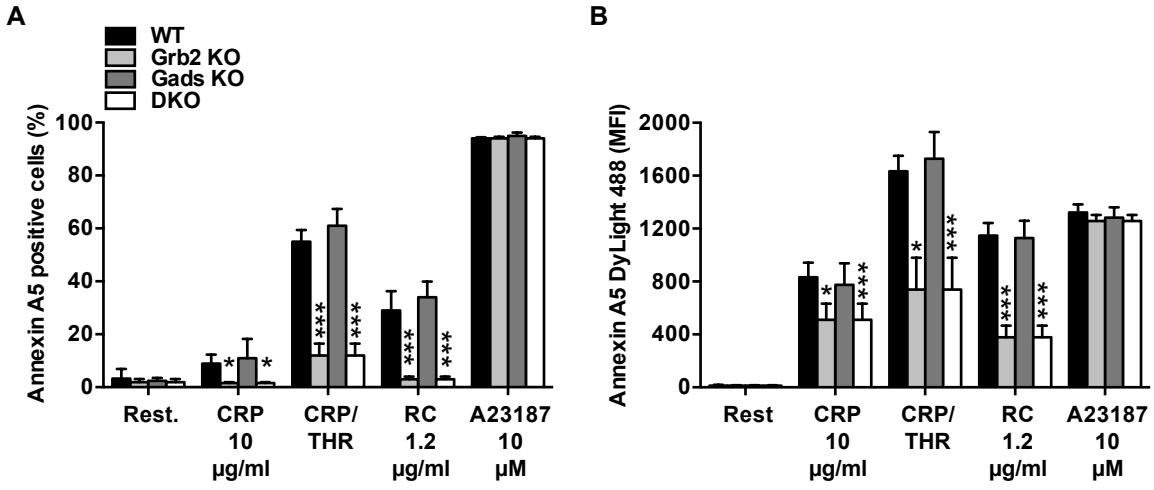

Figure 31. Defective PS-exposure in Grb2 KO and Grb2/Gads DKO platelets. Measurement of PS exposure by flow cytometry using specific binding of annexin A5 to platelet surface-exposed PS. (**A**) Quantification of the percentage of the platelet population with PS exposure. (**B**) Mean fluorescence intensity values for Annexin A5 binding in the same experiment as A. Grb2 KO and DKO platelets were found to have significantly reduced PS exposure following stimulation with agonists that effect increased intracellular calcium concentrations through stimulation of a signaling cascade. This impairment of PS exposure was not seen on stimulation with the calcium ionophore A23187 that effects increase in calcium concentration by directly acting on calcium stores. Results shown as mean ± SD, n=4 animals per group. *P<0.05, **P<0.01, ***P<0.001; unpaired Student t test.

When treated with agonists that initiate the (hem)ITAM signaling cascade (CRP; co-stimulation with CRP/thrombin; rhodocytin), the degree of PS exposure was comparable between WT and Gads KO platelet samples, whereas in both Grb2 KO as well as Grb2/Gads DKO platelet samples it was severely defective. However, when platelet samples were

treated with the calcium ionophore A23187 that bypasses any signaling and causes an increase in intracellular calcium by acting directly on the intracellular calcium stores, the degree of PS exposure, in the Gads KO, Grb2 KO and the DKO platelet samples was comparable to WT samples (Figure 31).

These results indicate that while the mechanisms that lead to PS exposure following calcium mobilization are intact, defective (hem)ITAM signal transduction in Grb2 and Grb2/Gads DKO platelets is responsible for impaired calcium mobilization and subsequently impaired PS exposure.

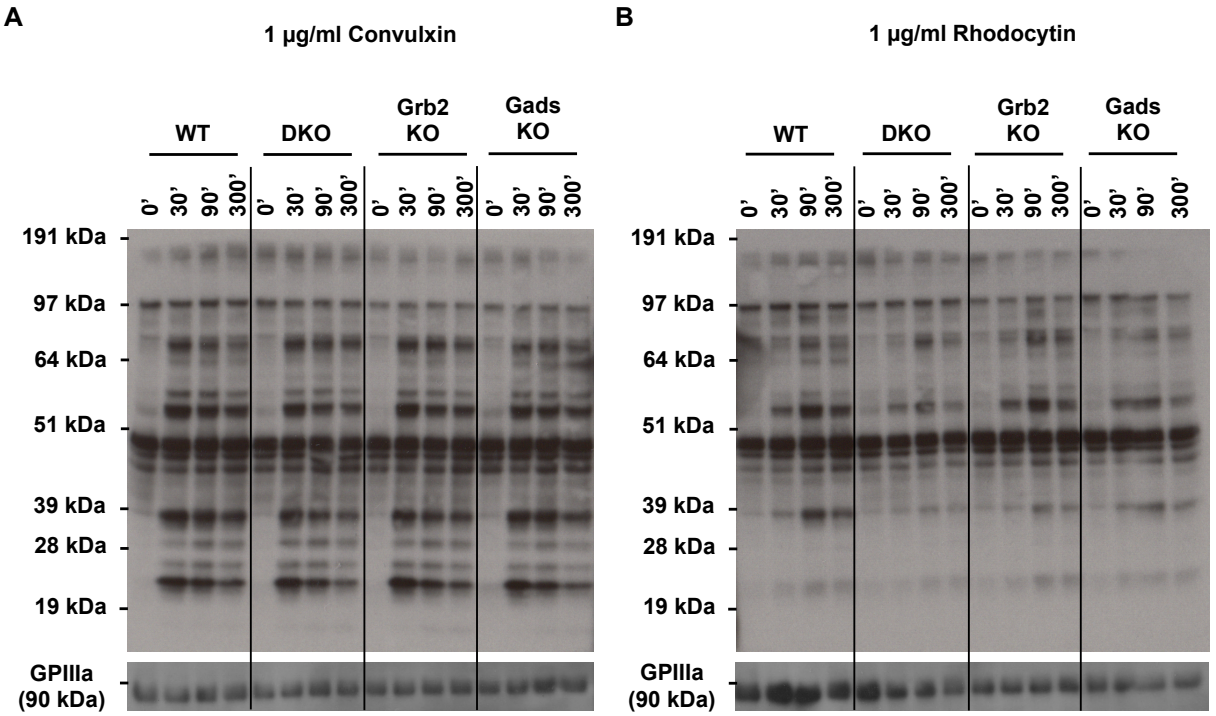

Figure 32. Assessment of the global tyrosine phosphorylation pattern in Grb2 KO, Gads KO and DKO platelet lysates in comparison to WT platelet lysates using the pan anti-phosphotyrosine antibody 4G10. (The black lines marking the lanes for samples from the four different genotypes are only for the purpose of clarity; samples from all four genotypes were run on the same gel).

To further evaluate downstream signal transduction following (hem)ITAM stimulation in the three groups of KO mice, the general pattern of protein tyrosine phosphorylation was assessed using the pan-tyrosine phosphorylation detection antibody, 4G10. Lysates were prepared from platelet samples stimulated with either the GPVI specific agonist convulxin, or the CLEC-2-specific agonist rhodocytin under stirring conditions to stimulate the (hem)ITAM signaling cascades. The pattern of tyrosine phosphorylation was comparable between WT

samples and the samples from the three groups of KO mice – Grb2 KO, Gads KO and Grb2/Gads DKO (Figure 32).

To dissect if specific signaling proteins are impaired in the absence of Grb2, Gads or both, the degree of tyrosine phosphorylation of individual proteins was assessed following stimulation of platelet suspensions. Convulxin stimulation leads to the phosphorylation of the ITAM motif associated with the GPVI-FcRγ-chain complex that initiates a downstream signaling cascade involving Src family kinase-dependent phosphorylation of tyrosine residues of the Syk kinase, assembly of the LAT signalosome and phosphorylation of tyrosine residues of the effector enzyme PLCγ2.

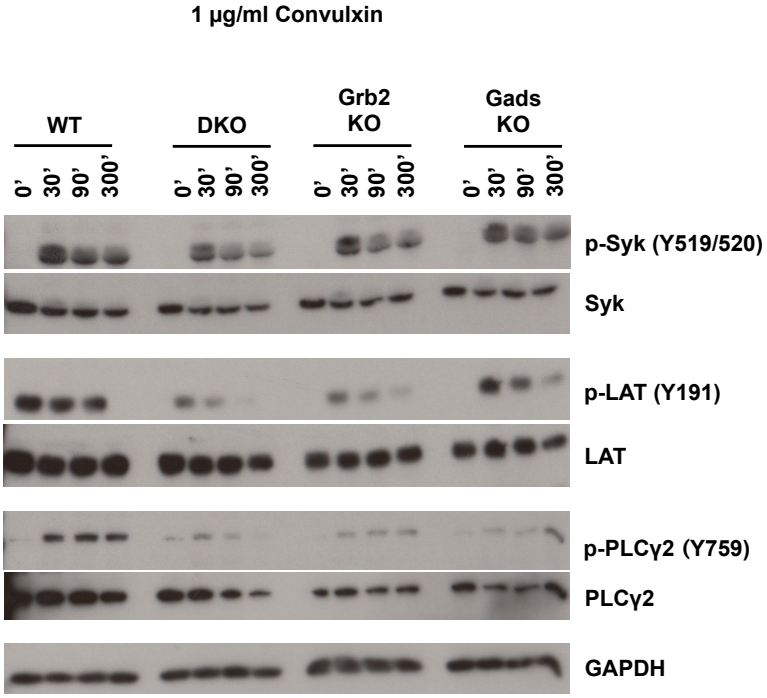

Figure 33. Impaired ITAM-induced signal transduction in Grb2 KO, Gads KO and DKO platelets in comparison to WT platelets. Tyrosine phosphorylation of Syk, LAT and PLCγ2, components of the signaling cascade downstream of GPVI activation. Washed platelets from all four groups were stimulated with 1 µg/mL convulxin under stirring conditions at 37 °C. Aliquots were taken at the indicated time points and lysed in ice cold lysis buffer. Reduced proteins were separated on 10% SDS-PAGE gels. Phospho-specific antibodies were used to probe for tyrosine phosphorylation of indicated proteins. Respective total protein amounts and GAPDH served as loading controls. Results shown are representative blots of 3 individual experiments.

On stimulation of platelet suspensions with convulxin, as reported previously,[92, 95] the phosphorylation of LAT at Y191 was reduced for platelets samples obtained from Grb2 KO

mice and Gads KO mice at 30 s, 90 s and 300 s post stimulation - the reduction being more prominent in the case of Grb2 KO samples. This was even further reduced for the Grb2/Gads DKO samples, with barely any signal detectable at 300 s post stimulation. Similarly, phosphorylation of PLCγ2 was reduced in samples from all three groups of KO mice in comparison to the WT samples, but interestingly residual phosphorylation was observed even in the absence of both adapters Grb2 and Gads (Figure 33).

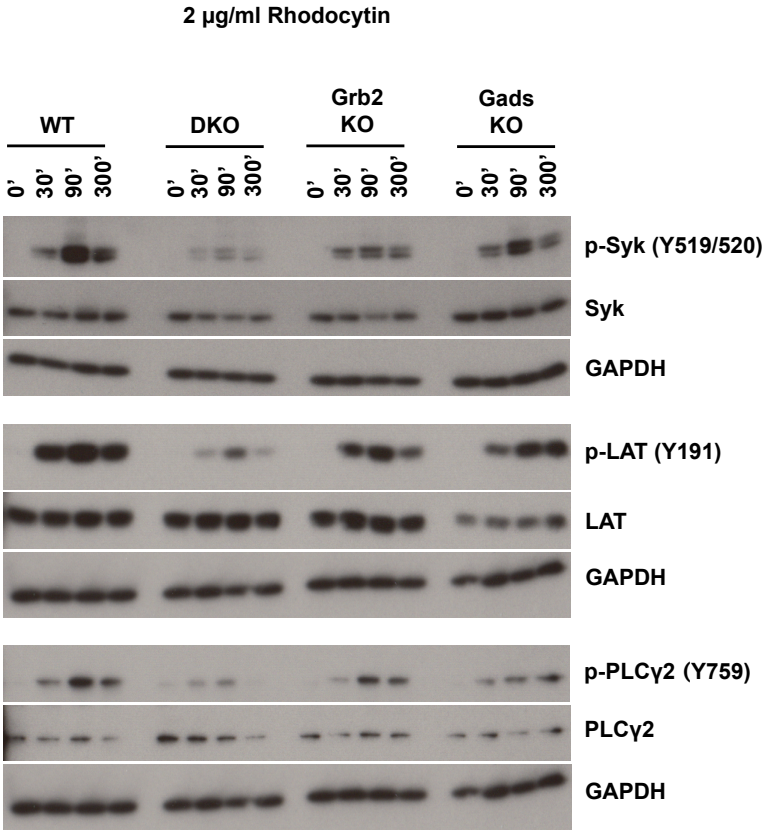

Figure 34**.** Impaired (hem)ITAM-induced signal transduction in Grb2 KO, Gads KO and DKO platelets in comparison to WT platelets. Tyrosine phosphorylation of Syk, LAT and PLCγ2, components of the signaling cascade downstream of CLEC-2 activation. Washed platelets from all four groups were stimulated with 1 µg/mL convulxin under stirring conditions at 37 °C. Aliquots were taken at the indicated time points and lysed in ice cold lysis buffer. Reduced proteins were separated on 10% SDS-PAGE gels. Phospho-specific antibodies were used to probe for tyrosine phosphorylation of indicated proteins. Respective total protein amounts and GAPDH served as loading controls. Results shown are representative blots of 3 individual experiments.

Surprisingly, a small decrease in phosphorylation of Syk (an event which occurs upstream of the assembly of the LAT signalosome of which Grb2 and Gads form a part) was also observed (Figure 33). Such observations have been previously reported for samples obtained from Gads KO mice on stimulation with CRP where the authors hypothesized this

phenomenon to arise from either the increased accessibility of tyrosine residues in Syk to protein tyrosine phosphatases in the absence of Gads, or due to defects in the feedback role for Syk in mediating its own phosphorylation.[95]

Similarly, the degree of tyrosine phosphorylation of individual proteins was also assessed following stimulation of platelet suspensions with rhodocytin. As in the case of convulxin stimulation, phosphorylation of LAT at Y191 was markedly reduced for Gads KO, Grb2 KO and Grb2/Gads DKO samples – the decrease being most pronounced in the Grb2/Gads DKO platelet samples. This differential degree of reduction in tyrosine phosphorylation of LAT was mirrored for phosphorylation of PLCγ2 at Y759 (Figure 34).

Additionally, a significant reduction in phosphorylation of Syk at Y519/520 was also observed on rhodocytin stimulation, most prominently for samples obtained from Grb2/Gads DKO mice, followed by those obtained from Grb2 KO mice. A minor reduction in Syk phosphorylation was also seen for samples obtained from Gads KO mice (Figure 34).

Taken together, these results reveal defective (hem)ITAM signal transduction in the Grb2/Gads DKO animals which is markedly more pronounced than the defects observed in the Grb2 KO or Gads KO samples under the same experimental conditions.

3.3.6. *In vivo* consequences of Grb2/Gads double deficiency

In order to determine the *in vivo* consequences of the functional compensation observed between Grb2 and Gads in *in vitro* studies, Grb2/Gads DKO mice were challenged in *in vivo* experimental models of hemostasis and arterial thrombosis and were compared to WT mice and Grb2 and Gads single KO mice.

In the experimental model of hemostasis (measurement of tail bleeding times by the filter paper method) the Grb2/Gads DKO mice bled significantly longer than WT mice (Figure 35A). This defective in hemostasis was more severe that that previously reported in the Grb2 KO mice (Figure 10).[92]

In the mechanical-injury induced experimental model of arterial thrombosis, in contrast to the Grb2 and Gads single KO mice, Grb2/Gads DKO animals exhibited significantly prolonged times to occlusive thrombus formation in comparison to WT mice. Furthermore, in approximately 30% of the DKO animals, stable occlusive thrombi did not form in the vessels in the 30 min observation period (Figure 35).

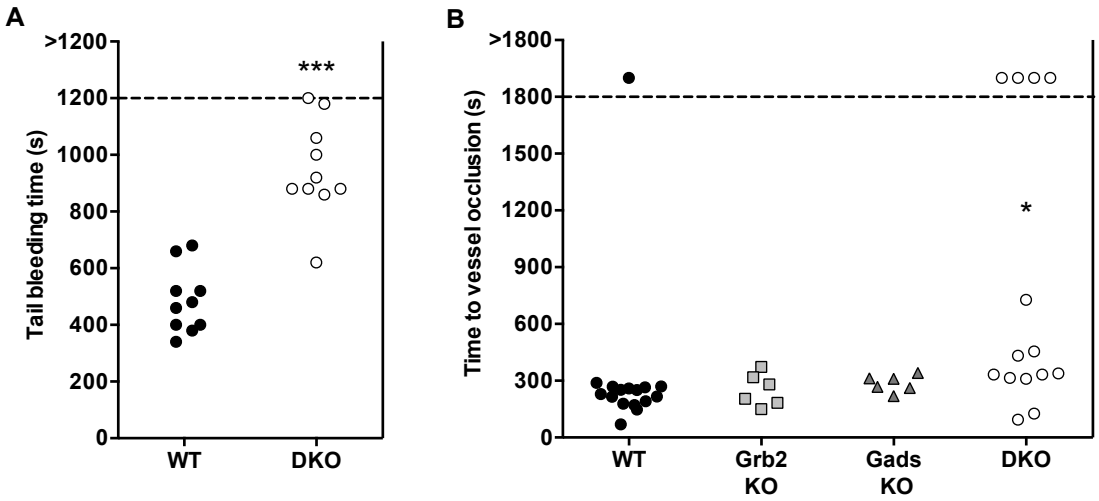

Figure 35. Grb2/Gads DKO mice display impaired hemostasis and partially defective arterial thrombosis. (A) Measurement of bleeding time by filter paper method. Each dot represents time of cessation of bleeding of one mouse. DKO mice were found to have significantly prolonged bleeding times as compared to WT mice (***P<0.001; unpaired Student t test). (B) Experimental model of mechanical injury-induced arterial thrombosis in the abdominal aorta. Each dot represents time to occlusive thrombus in the vessel of one mouse. DKO mice were partially protected in this model (*P<0.05; unpaired Student t test).

These results showed that the adapters Grb2 and Gads have partially redundant functions in platelet-mediated hemostasis and deficiency of both adapter proteins results in impaired hemostasis and partially defective arterial thrombosis in mice.

4. Discussion

4.1. TMEM16F-mediated platelet membrane phospholipid scrambling is critical for hemostasis and thrombosis but not thrombo-inflammation in mice

Two key defects in platelet procoagulant activity have been recognized in patients of Scott Syndrome, impaired surface exposure of phosphatidylserine (PS) and abolished platelet membrane ballooning. The data presented in this thesis demonstrated that TMEM16F cKO mice that lack the protein specifically in megakaryocytes and platelets phenocopy these established defects in Scott Syndrome platelets and can serve as a useful animal model for the disease.

TMEM16F plays an important role during embryonic development as constitutive KO mice generated using several different approaches show embryonic or perinatal lethality. Of note, the abnormalities in the KO mice that result in this lethality are inconsistently reported between laboratories. While skeletal deformities have been identified in one investigation, defects as diverse as abdominal and intracranial bleeding as well as exencephaly have been reported in another. However, no obvious visible defects were observed in E12.5 embryos in the KO mouse line characterized in this thesis. Embryonic lethality could be one reason why so far only 4 Scott Syndrome patients have been identified. Alternatively, or in addition, this phenomenon could arise from the fact that the routinely used clinical tests cannot identify this syndrome because Scott Syndrome platelets show unaltered activation responses and the global coagulation parameters PT and aPTT are also normal in these patients.

From the results obtained in this work, it is noteworthy that in the absence of platelet TMEM16F, PS exposure is not completely abolished and different degrees of procoagulant activity persist in the cKO platelets under various conditions of agonist stimulation tested. Such observations have also been documented previously, both in the case of Scott Syndrome patients[55, 125] and in dogs with Canine Scott Syndrome,[35] though not always adequately discussed or emphasized upon.

The mechanisms underlying the disparate impairment of PS exposure in cKO platelets following stimulation with different agonists – a more profound impairment following ionophore (ionomycin or A23187) stimulation compared to CRP/thrombin dual stimulation, and even dissimilarities between the degree of impairment between A23187 and ionomycin stimulation, are currently incompletely understood. However, as the activation of scramblases

is dependent on intracellular calcium concentrations, distinct calcium mobilization patterns following stimulation with varied agonists could account for these differences.

Only Fujii *et al.* have reported abolished platelet PS-exposure in megakaryocyte- and platelet-specific TMEM16F KO mice upon co-stimulation with CRP and thrombin,[28] but the experimental conditions used by the authors in this particular investigation are very different from the experimental conditions described in this thesis. They determined *ex vivo* platelet PS exposure in a FACS assay using platelets incubated at 20 °C, much below the physiological temperature of 37 °C. Therefore the results cannot be employed to correlate with platelet function *in vivo*. In addition, the gating strategy used for the analysis of the flow cytometry histograms is different from the gating strategy used in the current thesis in that it does not take into account the 'annexin A5 low' platelet population that forms the bulk of the residual PS exposing population observed in our studies. Although these differences in the experimental setup can account for the inconsistent observations in the two studies, it is important to note that reanalysis of the FACS data presented in this thesis using the gating strategy employed by Fujii *et al.,* or repeating experiments at 20 °C, and additionally testing varied agonist combinations and concentrations, could not reproduce this previously reported finding in our mouse model. Under all conditions, pronouncedly reduced, but residual PS exposure was consistently seen when stimulating cKO platelets with physiological agonist combinations.

Therefore, while TMEM16F is currently the only identified scramblase in platelets, these results point towards the existence of alternative mechanisms that mediate activation-induced platelet PS exposure. The identification of these TMEM16F-independent pathways is required to further understand the differential impact of its absence on different agonist stimulations.

The remodeling of activated platelets into a ballooned morphology, which is the second characteristic that determines platelet procoagulant response was also severely impaired in cKO platelets in comparison to WT platelets. In cells adherent on a collagen-coated surface, this response was almost completely abolished with negligible occurrence of ballooned platelets in cKO samples under conditions in which WT samples show numerous ballooned structures. However, in suspension, a minor residual ballooning was observed in cKO platelet samples as compared to WT platelet suspensions - this further argues that TMEM16F is not the sole mediator of platelet procoagulant response.

The dramatically reduced cKO platelet procoagulant potential had a definitive impact on the role of these cells in supporting thrombin generation and fibrin formation. Tissue factor-initiated thrombin generation was measured in unstimulated PRP and PRP stimulated with either CRP/PAR-4 peptide (to mimic as closely as possible the CRP/thrombin stimulation in the flow cytometry assay to determine platelet PS exposure), or with A23187. Unfortunately, thrombin generation studies could not be performed in PRP stimulated with ionomycin, the agonist that shows the greatest reduction in the PS exposure in cKO platelets in the flow cytometry assay, as ionomycin is quenched by the albumin present in PRP.[126] Unlike previous reports,[27, 28] we observed that the lack of TMEM16F influences the kinetics of thrombin generation rather than the overall amounts of thrombin finally produced. This was apparent by the rightward-shift in the thrombograms of cKO samples in comparison to the WT samples. The decelerated thrombin generation translated into a delay in fibrin formation in blood samples from cKO mice in comparison to WT samples as evidenced by the *ex vivo* fibrin formation assay carried out by allowing blood to perfuse over a collagen/tissue factor microspot at arterial shear rates.

The delayed thrombin and fibrin formation had important consequences for hemostasis and thrombosis *in vivo* that were both impaired in cKO mice in comparison to WT mice. Prolonged bleeding times were also reported for two TMEM16F constitutive KO mouse models, determined by either the filter paper or the saline method.[27, 46] In contrast a recent investigation on TMEM16F megakaryocyte- and platelet-specific KO mice reported comparable bleeding times between the conditional KO mice and WT mice.[28] While the bleeding time experiment in the current study was performed by the filter paper method, Fujii *et al.* tested bleeding times in WT and TMEM16F conditional KO mice by the saline method. Mechanisms underlying hemostasis are known to partially differ between these two experimental models.[127] However, the bleeding time results in the current study correlate well with those from *ex vivo* (fibrin generation) and *in vivo* (arterial thrombosis) experiments performed and also reflect the provoked bleeding episodes that are the major clinical manifestation of Scott Syndrome.

A previous investigation has reported TMEM16F constitutive KO mice to be protected in an experimental model of arterial thrombosis.[27] In another TMEM16F megakaryocyte- and platelet-specific KO mouse line, unstable, fragile thrombi developed in veins of conditional KO mice in an experimental model of photochemical injury-induced venous thrombosis.[28] The here presented work is the first report showing that TMEM16F cKO mice exhibited impaired thrombosis in an experimental model of $FeCl_3$ injury-induced thrombus formation in the

carotid artery, underscoring the importance of TMEM16F-regulated platelet procoagulant activity for the progression of arterial thrombosis in addition to venous thrombosis. Furthermore, the frequent embolization of growing thrombi that was observed in the current study indicates an important role for TMEM16F-scramblase activity in stabilizing developing thrombi in pathological thrombosis.

Both, platelets and the coagulation system are known contributors to ischemia-reperfusion injury,[37] but interestingly the here presented results strongly suggest that TMEM16F-mediated platelet procoagulant activity does not play a role in the pathology of this process. Infarct volumes and neurological and motor function outcome were similar in WT and TMEM16F cKO mice in the tMCAO model of ischemic stroke. In addition, neither increased mortality nor incidences of intracranial hemorrhage were observed in cKO mice tested in this experimental model. These results are noteworthy because, as briefly described in the introduction section, several investigations have reported a prominent role for thrombin and its receptors (protease-activated receptors, PARs) in ischemic brain injury. Thrombin receptors PARs-1,3 and 4 are abundantly expressed in the brain.[41] The expression of PAR-1 in rat hippocampal slice cultures is upregulated following exposure to ischemic conditions.[128] PAR-1 and PAR-4 KO mice are protected in experimental models of focal cerebral ischemia.[129, 130] In addition, thrombin levels by themselves are elevated after transient global ischemia in the rat brain and aggravate infarct progression following ischemic injury as inhibition of thrombin by the inhibitor hirudin has been shown to ameliorate the outcome in the tMCAO model.[42] However, several factors can account for unaltered stroke progression under conditions of decelerated platelet-driven thrombin generation in the cKO mice. A recent report has shown a prominent role for procoagulant endothelium in supporting hemostasis/thrombosis in an experimental model of laser-induced vascular injury, highlighting the function of procoagulant cells other than platelets in supporting thrombin generation.[131] Therefore, as ischemic stroke progresses over a longer time scale than arterial thrombosis in our experimental models, thrombin generation promoted by procoagulant cells other than platelets including activated endothelial cells, red blood cells, lymphocytes and neurons could potentially compensate for the impaired TMEM16F cKO platelet-driven thrombin generation. Definite conclusions in this regard can only be achieved through further studies such as generation of endothelial-specific TMEM16F conditional KO mice and testing them in experimental models of arterial thrombosis and ischemic stroke side by side to megakaryocyte- and platelet-specific TMEM16F conditional KO mice.

To summarize, three broad conclusions can be drawn from our studies on megakaryocyte- and platelet-specific TMEM16F conditional KO mice (Figure 36). Firstly, TMEM16F is not the sole mediator of platelet procoagulant activity. Second, the scramblase TMEM16F regulates kinetics of the thrombin generation supported by procoagulant platelets. And finally, the modulation of thrombin generation kinetics by platelet TMEM16F is important for hemostasis and arterial thrombosis but not for thrombo-inflammation post focal cerebral ischemia.

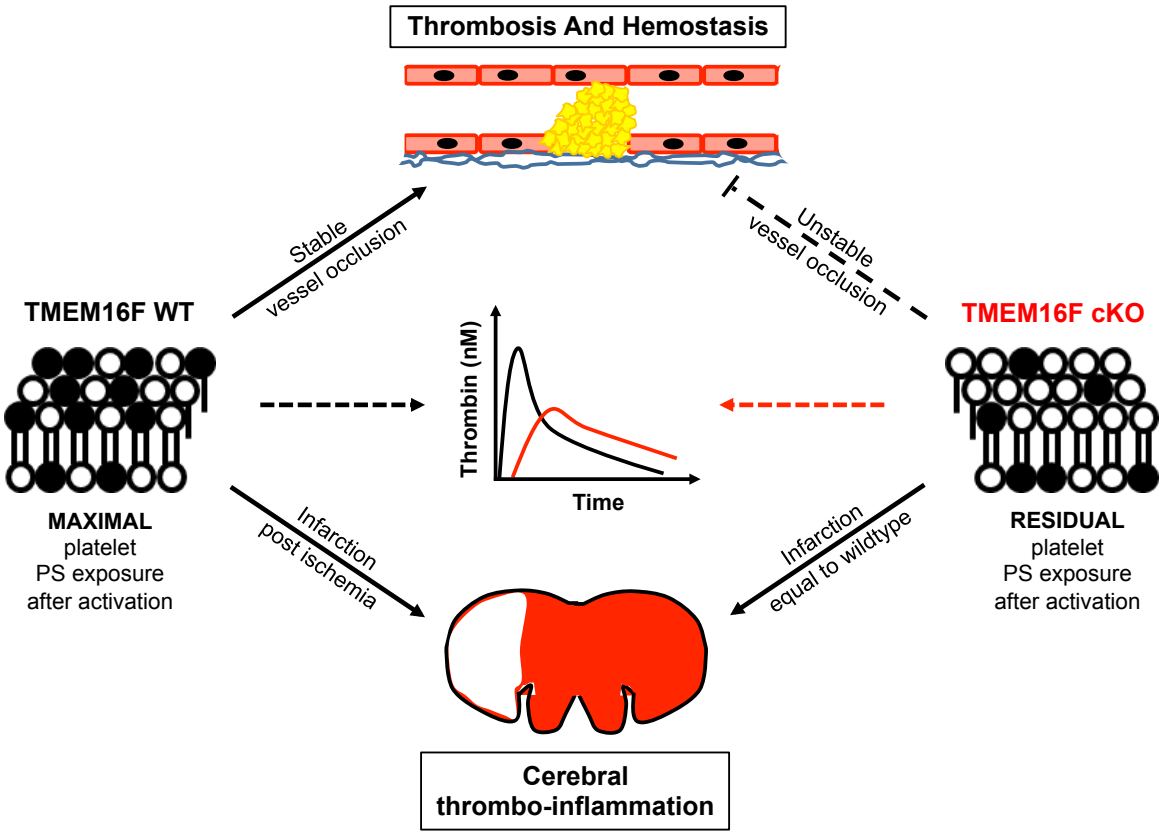

Figure 36. An illustration of the key findings from experiments conducted on megakaryocyte- and platelet-specific TMEM16F conditional KO mice. TMEM16F-independent pathways lead to residual activation-induced PS exposure in cKO platelets that decelerates procoagulant platelet-driven thrombin generation. The platelet membrane phospholipid scrambling regulated by TMEM16F is vital for maintaining hemostasis as well as for the progression of arterial thrombosis. However, this process is dispensable for cerebral thrombo-inflammation in mice.[120]

4.2. Generation of humanized coagulation factor XII (FXII) knockin mice as a model for testing novel anti-thrombotic agents

The data presented in this thesis constitutes the initial characterization of a novel humanized FXII KI mouse strain. In recent years, FXII has emerged as an attractive target for

antithrombotic therapy giving impetus to research directed towards development of anti-FXII pharmacological agents.[64] Previous reports in the literature provided indications that human FXII was functional within the murine physiology,[38, 60] and studies presented herein support this hypothesis. However, it is necessary to investigate additional aspects of this mouse strain prior to utilizing them as models for testing novel anti-thrombotic agents. These experiments form the aim of future work in our laboratory. Global coagulation parameters PT and especially aPTT will be determined using plasma from hFXII KI mice, along with measurement of expression and activity of the other coagulation factors of the coagulation cascade to ensure unaltered levels. Furthermore, the basis for the inconsistent concentration of human FXII in plasma obtained from human controls versus mutant mice – whether this is a species-specific difference or is related to the targeting strategy - will be determined with the help of quantitative ELISAs that specifically measure murine FXII. Differences in concentrations of coagulation factors between mice and humans have been reported.[5] Reduced protein expression in humanized mutant mice has also been reported in the literature, for e.g. cDNA knockin of human *Cdg1* (gene that encodes the guanine nucleotide exchange factor CalDAG-GEFI) into the murine *Cdg1* locus resulted in approximately 90% reduction in expression of the CalDAG-GEFI protein in mutant murine platelets.[132] Experiments are also planned to determine whether human FXII expressed by the mutant mice can also compensate for murine FXII under thrombo-inflammatory conditions such as ischemic stroke by subjecting the mutant mice to the experimental tMCAO model. Once the mouse-strain is thoroughly characterized, the efficacy of two new human-FXIIa inhibitors under conditions of arterial thrombosis and ischemic stroke will be determined in comparison to the previously reported FXIIa-inhibitor rHA-infestin-4 and the humanized anti-FXIIa antibody 3F7.[39, 67]

4.3. The adapter proteins Grb2 and Gads have partially redundant functions for activation and hemostatic activity of mouse platelets

Studies investigating the role of Grb2 or Gads in platelet function have suggested that one adapter protein may functionally compensate for the lack of the other in platelet activation.[92, 95] The existence of functional compensation between closely related proteins downstream of (hem)ITAM signaling in platelets is well documented. Redundancy has been observed between positive regulators of (hem)ITAM signaling (Vav1 and Vav3; Btk and Tec)[75, 78], as well as negative regulators (SLAP and SLAP2).[76] The data presented in this thesis provide experimental evidence for redundant function between Grb2 and Gads - the two members of

the Grb2 family of adapter proteins expressed in platelets - through studies on platelet activity conducted in Grb2/Gads double knockout mice. The direct comparison of platelets from Grb2 KO, Gads KO and Grb2/Gads DKO mice in *in vitro* and *in vivo* studies reveals that Grb2 is the dominant adapter protein that can markedly compensate for Gads deficiency, and plays a key role in signal transduction downstream of GPVI or CLEC-2 stimulation. By contrast, Gads plays a supportive role in this signaling pathway, especially evident in experimental models of hemostasis and thrombosis *in vivo* as opposed to *in vitro* studies on platelet function.

In investigations performed by Dütting *et al.*, the residual platelet activation and aggregation in the Grb2 deficient platelets was reported to be functionally relevant as significant defects in hemostasis and thrombosis were only observed when simultaneously blocking TxA_2-induced GPCR signaling. Defective (hem)ITAM signaling was hypothesized to be compensated by GPCR-signaling in addition to putative functional compensation by Gads.[92] Moreover, synergistic action on co-stimulation with the (hem)ITAM-agonist CRP and the GPCR-agonist ADP has been previously reported through studies conducted in platelets double deficient for the kinases Btk and Tec that also lie downstream of (hem)ITAM signaling. Btk/Tec double deficient platelets display dramatically impaired spreading on collagen. However, this defect can be rescued by co-stimulation with ADP.[78] We investigated these compensatory pathways by determining platelet activation in Grb2 KO, Gads KO and Grb2/Gads KO platelets simultaneously by flow cytometry following stimulation with a (hem)ITAM agonist (CRP, convulxin or rhodocytin) in conjunction with a GPCR-agonist (ADP or the thromboxane-analog U46619). For Grb2 KO and Gads KO platelets, we indeed observed a synergistic effect of co-stimulation with either ADP or U46618, with a substantial rescue of the platelet activation defect that was seen on stimulation with a (hem)ITAM agonist alone. However, even co-stimulation failed to elicit activation from double deficient platelets. This further extends the observation that Grb2 and Gads have redundant roles for platelet activation.

Interestingly, although the combined deficiency of the two adapter proteins impacts both, ITAM and hemITAM signaling, it has a greater influence on GPVI- than CLEC-2-induced platelet activation and aggregation, demonstrating a more prominent role of the adapter proteins in the former signaling pathway than the latter. This observation might explain in part why even the loss of both adapter proteins did not lead to alterations in separation of blood-lymphatic vasculature in Grb2/Gads DKO mice. These findings are noteworthy since the podoplanin-CLEC-2-axis has been shown to be essential to regulate proper separation between the blood and lymphatic vasculature with a severe blood-lymph mixing defect reported in mice deficient in either podoplanin or CLEC-2.[133, 134] In addition, mutant mice that

lack some other components of the signaling cascade that lie downstream of CLEC-2 activation have also been reported to present with the blood-lymph mixing defect. This includes mice deficient in Syk, SLP-76 and PLCγ2 – all proteins that are common to ITAM and hemITAM signaling.

Signal transduction in Grb2 KO, Gads KO and Grb2/Gads DKO platelets was studied in more detail by directly comparing phosphorylation of tyrosine residues of key individual signaling proteins in platelets from all groups of knockout mice in comparison to WT platelets following stimulation with either convulxin or rhodocytin. Defects in tyrosine phosphorylation of LAT and PLCγ2 have been reported for Grb2 KO and Gads KO platelets and were confirmed in the current study. Notably, DKO platelets exhibit a greater reduction in LAT and PLCγ2 phosphorylation than seen in the absence of either Gads or Grb2, in agreement with the results of the flow cytometry-based platelet activation studies.

Surprisingly, we also observed a consistent decrease in phosphorylation of the kinase Syk at Y519/520 in all three groups of KO mice. This decrease was most prominent for Grb2/Gads DKO samples followed by Grb2 and Gads KO platelet samples respectively. Additionally, the defective Syk phosphorylation was more striking following rhodocytin stimulation in comparison to convulxin stimulation. This is despite the fact that Syk lies upstream of the assembly of the LAT signalosome in the sequence of events in the (hem)ITAM signaling cascade. One possible explanation for this observation is defective feedback activation of (hem)ITAM signaling in platelets from the three groups of KO mice. A previous report has described a feedback role for Syk in further augmenting its own phosphorylation in rhodocytin-stimulated platelets.[95] Additionally a recent report has shown further enhancement of GPVI activation and signaling through clustering of the receptor following initial activation-triggered increased dimerization.[135] With respect to the current study, investigating tyrosine phosphorylation of the ITAM motifs of FcRγ-chain will potentially help to test this hypothesis. If the reduced tyrosine phosphorylation of Syk was due to impaired feedback activation, a reduced tyrosine phosphorylation of FcRγ-chain should also be observed. This hypothesis would also explain the differential impairment in tyrosine phosphorylation of Syk on rhodocytin stimulation compared to convulxin stimulation. This is because convulxin is a very powerful agonist for GPVI stimulation. One molecule of the snake venom toxin is capable of clustering four GPVI receptors, thereby potentially partially masking the impaired feedback activation of GPVI through clustering in the KO platelet samples. In addition, Hughes *et al.* who also previously documented a small reduction in the phosphorylation of tyrosine residues of Syk in Gads KO platelet samples on stimulation with (hem)ITAM agonists, speculated that

this may occur due to increased accessibility of tyrosine residues of Syk to protein tyrosine phosphatases in the absence of Gads. This hypothesis could also partially account for the reduced phosphorylation of tyrosine residues of Syk in Grb2 KO, Gads KO and Grb2/Gads DKO platelet samples in the current study.

Another aspect of the results of the tyrosine phosphorylation studies is that albeit being dramatically reduced, tyrosine phosphorylation of LAT and PLCγ2 are not completely abolished. This demonstrates the existence of Grb2/Gads-independent pathways that mediate PLCγ2 activation on stimulation with (hem)ITAM agonists in the absence of both adapter proteins. This is in line with previously reported phosphorylation of PLCγ2 that was also impaired but not abolished in LAT KO platelets on stimulation with high concentrations of (hem)ITAM agonists.[136] Moreover, residual activation of PLCγ2 is also reported on stimulation of SLP-76 KO platelets with collagen and CRP.[137]

To dissect the functional relevance of redundant function between Grb2 and Gads for the processes of hemostasis and thrombosis *in vivo*, Grb2/Gads DKO animals were tested in experimental models of hemostasis and arterial thrombosis. DKO mice showed significantly prolonged bleeding times in comparison to WT mice. This impairment of hemostatic function was more severe than that previously reported in Grb2 KO mice,[92] underscoring important redundant functions between the adapters Grb2 and Gads in maintaining hemostasis. Furthermore, occlusive thrombus formation was moderately impaired in DKO animals under conditions where vessel occlusion times in the Grb2 KO and Gads KO mice were comparable to those recorded for WT mice. These results are interesting as most proteins in the (hem)ITAM signaling pathway including GPVI, CLEC-2, Syk and LAT, are well known to play a more prominent function in the pathological process of thrombosis in comparison to their limited role for hemostasis. These results further extend the observation in Grb2 KO mice that display moderately impaired hemostasis but normal thrombosis.[92] Taken together, these data shed new light on the divergent role of signaling molecules downstream of (hem)ITAM signaling for the processes of hemostasis and thrombosis.

4.4. Concluding remarks

The study on TMEM16F cKO mice elucidates key differences in the role of procoagulant platelets in the pathology of arterial thrombosis and ischemic stroke. However, it also opens several new lines for investigation. Further studies will be required to adequately address the cause of residual platelet procoagulant activity in cKO mice. It will also be interesting to

identify the cell types that predominantly contribute to increased thrombin levels in the brain following cerebral ischemia through studies using tissue/cell-type-specific conditional KO mice. Given that a genome-wide association mapping study has identified the *Ano6* gene among the top three candidates to play a role in nanoparticle-induced acute lung injury,[53] a strong possibility arises that whilst platelet-TMEM16F activity is dispensable for cerebral thrombo-inflammation, it may contribute significantly to thrombo-inflammatory processes in other organs and pathological conditions, and forms an interesting avenue to investigate in future studies. An organ-specific role for platelets has been previously described under conditions of inflammatory bleeding.[138, 139]

Analysis of platelet function in Grb2/Gads DKO mice has revealed partially overlapping roles of the proteins Grb2 and Gads for platelet activity. One adapter can incompletely compensate for the lack of the other for activation and hemostatic function of murine platelets. Additionally, the specific role of these adapters downstream of (hem)ITAM signaling is dispensable for the regulation of blood-lymphatic vessel separation. The basis of the divergence in the function of the constituents of (hem)ITAM signaling cascade with respect to regulating separation of blood-lymphatic vasculature, hemostasis and thrombosis remains to be elucidated within further studies.

The hFXII KI mice described in this thesis offer all the advantages of a rodent model – cost effectiveness, convenient handling and maintenance in the laboratory, and a well-characterized genetic background that would allow reproducible studies. Most importantly, the hFXII KI mice have the added advantage that novel pharmacological agents can be directly tested against human factor XII in an *in vivo* system within preclinical studies to facilitate the process of delineating candidates for more intensive clinical studies. Therefore, the planned further in-depth characterization of this mouse line will allow for their utilization as a model for testing novel antithrombotic agents.

5. References

1. Stegner D, Nieswandt B. Platelet receptor signaling in thrombus formation. *Journal of molecular medicine (Berlin, Germany)*. 2011;89:109-121

2. Varga-Szabo D, Pleines I, Nieswandt B. Cell adhesion mechanisms in platelets. *Arterioscler Thromb Vasc Biol*. 2008;28:403-412

3. Versteeg HH, Heemskerk JW, Levi M, Reitsma PH. New fundamentals in hemostasis. *Physiol. Rev.* 2013;93:327-358

4. Schmitt A, Guichard J, Masse JM, Debili N, Cramer EM. Of mice and men: Comparison of the ultrastructure of megakaryocytes and platelets. *Experimental hematology*. 2001;29:1295-1302

5. Tsakiris DA, Scudder L, Hodivala-Dilke K, Hynes RO, Coller BS. Hemostasis in the mouse (mus musculus): A review. *Thromb Haemost*. 1999;81:177-188

6. Zwaal RF, Comfurius P, Bevers EM. Scott syndrome, a bleeding disorder caused by defective scrambling of membrane phospholipids. *Biochim. Biophys. Acta*. 2004;1636:119-128

7. Balasubramanian K, Schroit AJ. Aminophospholipid asymmetry: A matter of life and death. *Annu. Rev. Physiol.* 2003;65:701-734

8. Nagata S, Suzuki J, Segawa K, Fujii T. Exposure of phosphatidylserine on the cell surface. *Cell Death Differ.* 2016;23:952-961

9. Lhermusier T, Chap H, Payrastre B. Platelet membrane phospholipid asymmetry: From the characterization of a scramblase activity to the identification of an essential protein mutated in scott syndrome. *J Thromb Haemost*. 2011;9:1883-1891

10. Segawa K, Kurata S, Yanagihashi Y, Brummelkamp TR, Matsuda F, Nagata S. Caspase-mediated cleavage of phospholipid flippase for apoptotic phosphatidylserine exposure. *Science (New York, N.Y.)*. 2014;344:1164-1168

11. Basse F, Stout JG, Sims PJ, Wiedmer T. Isolation of an erythrocyte membrane protein that mediates Ca^{2+}-dependent transbilayer movement of phospholipid. *J. Biol. Chem.* 1996;271:17205-17210

12. Bevers EM, Williamson PL. Phospholipid scramblase: An update. *FEBS Lett.* 2010;584:2724-2730

13. Suzuki J, Umeda M, Sims PJ, Nagata S. Calcium-dependent phospholipid scrambling by tmem16f. *Nature*. 2010;468:834-838

14. Duran C, Hartzell HC. Physiological roles and diseases of tmem16/anoctamin proteins: Are they all chloride channels? *Acta pharmacologica Sinica*. 2011;32:685-692

15. Brunner JD, Lim NK, Schenck S, Duerst A, Dutzler R. X-ray structure of a calcium-activated tmem16 lipid scramblase. *Nature*. 2014;516:207-212

16. Suzuki J, Fujii T, Imao T, Ishihara K, Kuba H, Nagata S. Calcium-dependent phospholipid scramblase activity of tmem16 protein family members. *J. Biol. Chem.* 2013;288:13305-13316

17. Gyobu S, Ishihara K, Suzuki J, Segawa K, Nagata S. Characterization of the scrambling domain of the tmem16 family. *Proc Natl Acad Sci U S A*. 2017;114:6274-6279

18. Pedemonte N, Galietta LJ. Structure and function of tmem16 proteins (anoctamins). *Physiol. Rev.* 2014;94:419-459

19. Malvezzi M, Chalat M, Janjusevic R, Picollo A, Terashima H, Menon AK, Accardi A. Ca2+-dependent phospholipid scrambling by a reconstituted tmem16 ion channel. *Nature communications*. 2013;4:2367

20. Scudieri P, Caci E, Venturini A, Sondo E, Pianigiani G, Marchetti C, Ravazzolo R, Pagani F, Galietta LJ. Ion channel and lipid scramblase activity associated with expression of tmem16f/ano6 isoforms. *J Physiol*. 2015;593:3829-3848

21. Yu K, Whitlock JM, Lee K, Ortlund EA, Cui YY, Hartzell HC. Identification of a lipid scrambling domain in ano6/tmem16f. *eLife*. 2015;4:e06901

22. Picollo A, Malvezzi M, Accardi A. Tmem16 proteins: Unknown structure and confusing functions. *J. Mol. Biol.* 2015;427:94-105

23. Martins JR, Faria D, Kongsuphol P, Reisch B, Schreiber R, Kunzelmann K. Anoctamin 6 is an essential component of the outwardly rectifying chloride channel. *Proc Natl Acad Sci U S A*. 2011;108:18168-18172

24. Szteyn K, Schmid E, Nurbaeva MK, Yang W, Munzer P, Kunzelmann K, Lang F, Shumilina E. Expression and functional significance of the Ca(2+)-activated Cl(-) channel ano6 in dendritic cells. *Cell Physiol Biochem*. 2012;30:1319-1332

25. Grubb S, Poulsen KA, Juul CA, Kyed T, Klausen TK, Larsen EH, Hoffmann EK. Tmem16f (anoctamin 6), an anion channel of delayed Ca(2+) activation. *J. Gen. Physiol.* 2013;141:585-600

26. Shimizu T, Iehara T, Sato K, Fujii T, Sakai H, Okada Y. Tmem16f is a component of a ca2+-activated cl- channel but not a volume-sensitive outwardly rectifying Cl^- channel. *Am. J. Physiol. Cell Physiol.* 2013;304:C748-759

27. Yang H, Kim A, David T, Palmer D, Jin T, Tien J, Huang F, Cheng T, Coughlin SR, Jan YN, Jan LY. Tmem16f forms a Ca^{2+}-activated cation channel required for lipid scrambling in platelets during blood coagulation. *Cell*. 2012;151:111-122

28. Fujii T, Sakata A, Nishimura S, Eto K, Nagata S. Tmem16f is required for phosphatidylserine exposure and microparticle release in activated mouse platelets. *Proc Natl Acad Sci U S A*. 2015;112:12800-12805

29. Weiss HJ, Vicic WJ, Lages BA, Rogers J. Isolated deficiency of platelet procoagulant activity. *Am. J. Med.* 1979;67:206-213

30. Toti F, Satta N, Fressinaud E, Meyer D, Freyssinet JM. Scott syndrome, characterized by impaired transmembrane migration of procoagulant phosphatidylserine and hemorrhagic complications, is an inherited disorder. *Blood*. 1996;87:1409-1415

31. Weiss HJ, Lages B. Family studies in scott syndrome. *Blood*. 1997;90:475-476

32. Castoldi E, Collins PW, Williamson PL, Bevers EM. Compound heterozygosity for 2 novel tmem16f mutations in a patient with scott syndrome. *Blood*. 2011;117:4399-4400

33. Kunzelmann K, Nilius B, Owsianik G, Schreiber R, Ousingsawat J, Sirianant L, Wanitchakool P, Bevers EM, Heemskerk JW. Molecular functions of anoctamin 6 (tmem16f): A chloride channel, cation channel, or phospholipid scramblase? *Pflugers Arch*. 2014;466:407-414

34. Flores-Nascimento MC, Orsi FL, Yokoyama AP, Pereira FG, Lorand-Metze I, De Paula EV, Castro V, Annichino-Bizzacchi JM. Diagnosis of scott syndrome in patient with bleeding disorder of unknown cause. *Blood coagulation & fibrinolysis : an international journal in haemostasis and thrombosis*. 2012;23:75-77

35. Brooks MB, Catalfamo JL, Brown HA, Ivanova P, Lovaglio J. A hereditary bleeding disorder of dogs caused by a lack of platelet procoagulant activity. *Blood*. 2002;99:2434-2441

36. Brooks MB, Catalfamo JL, MacNguyen R, Tim D, Fancher S, McCardle JA. A tmem16f point mutation causes an absence of canine platelet tmem16f and ineffective activation and death-induced phospholipid scrambling. *J Thromb Haemost*. 2015;13:2240-2252

37. Stoll G, Kleinschnitz C, Nieswandt B. Molecular mechanisms of thrombus formation in ischemic stroke: Novel insights and targets for treatment. *Blood*. 2008;112:3555-3562

38. Kleinschnitz C, Stoll G, Bendszus M, Schuh K, Pauer HU, Burfeind P, Renne C, Gailani D, Nieswandt B, Renne T. Targeting coagulation factor xii provides protection from pathological thrombosis in cerebral ischemia without interfering with hemostasis. *J. Exp. Med.* 2006;203:513-518

39. Hagedorn I, Schmidbauer S, Pleines I, Kleinschnitz C, Kronthaler U, Stoll G, Dickneite G, Nieswandt B. Factor XIIa inhibitor recombinant human albumin infestin-4 abolishes occlusive arterial thrombus formation without affecting bleeding. *Circulation*. 2010;121:1510-1517

40. Krupka J, May F, Weimer T, Pragst I, Kleinschnitz C, Stoll G, Panousis C, Dickneite G, Nolte MW. The coagulation factor xiia inhibitor rha-infestin-4 improves outcome after cerebral ischemia/reperfusion injury in rats. *PloS one*. 2016;11:e0146783

41. Sokolova E, Reiser G. Prothrombin/thrombin and the thrombin receptors PAR-1 and PAR-4 in the brain: Localization, expression and participation in neurodegenerative diseases. *Thromb Haemost*. 2008;100:576-581

42. Karabiyikoglu M, Hua Y, Keep RF, Ennis SR, Xi G. Intracerebral hirudin injection attenuates ischemic damage and neurologic deficits without altering local cerebral blood flow. *J Cereb Blood Flow Metab*. 2004;24:159-166

43. Cuomo O, Pignataro G, Gala R, Scorziello A, Gravino E, Piazza O, Tufano R, Di Renzo G, Annunziato L. Antithrombin reduces ischemic volume, ameliorates neurologic deficits, and prolongs animal survival in both transient and permanent focal ischemia. *Stroke*. 2007;38:3272-3279

44. Agbani EO, van den Bosch MT, Brown E, Williams CM, Mattheij NJ, Cosemans JM, Collins PW, Heemskerk JW, Hers I, Poole AW. Coordinated membrane ballooning and procoagulant spreading in human platelets. *Circulation*. 2015;132:1414-1424

45. Heemskerk JW, Vuist WM, Feijge MA, Reutelingsperger CP, Lindhout T. Collagen but not fibrinogen surfaces induce bleb formation, exposure of phosphatidylserine, and procoagulant activity of adherent platelets: Evidence for regulation by protein tyrosine kinase-dependent ca2+ responses. *Blood*. 1997;90:2615-2625

46. Mattheij NJ, Braun A, van Kruchten R, Castoldi E, Pircher J, Baaten CC, Wulling M, Kuijpers MJ, Kohler R, Poole AW, Schreiber R, Vortkamp A, Collins PW, Nieswandt B, Kunzelmann K, Cosemans JM, Heemskerk JW. Survival protein anoctamin-6 controls multiple platelet responses including phospholipid scrambling, swelling, and protein cleavage. *FASEB J.* 2016;30:727-737

47. Ehlen HW, Chinenkova M, Moser M, Munter HM, Krause Y, Gross S, Brachvogel B, Wuelling M, Kornak U, Vortkamp A. Inactivation of anoctamin-6/tmem16f, a regulator of phosphatidylserine scrambling in osteoblasts, leads to decreased mineral deposition in skeletal tissues. *J. Bone Miner. Res.* 2013;28:246-259

48. Headland SE, Jones HR, Norling LV, Kim A, Souza PR, Corsiero E, Gil CD, Nerviani A, Dell'Accio F, Pitzalis C, Oliani SM, Jan LY, Perretti M. Neutrophil-derived microvesicles enter cartilage and protect the joint in inflammatory arthritis. *Science translational medicine*. 2015;7:315ra190

49. Ousingsawat J, Wanitchakool P, Kmit A, Romao AM, Jantarajit W, Schreiber R, Kunzelmann K. Anoctamin 6 mediates effects essential for innate immunity downstream of p2x7 receptors in macrophages. *Nature communications*. 2015;6:6245

50. Aoun J, Hayashi M, Sheikh IA, Sarkar P, Saha T, Ghosh P, Bhowmick R, Ghosh D, Chatterjee T, Chakrabarti P, Chakrabarti MK, Hoque KM. Anoctamin 6 contributes to Cl^- secretion in accessory cholera enterotoxin (ace)-stimulated diarrhea: An essential role for phosphatidylinositol 4,5-bisphosphate (PIP2) signaling in cholera. *J. Biol. Chem.* 2016;291:26816-26836

51. Batti L, Sundukova M, Murana E, Pimpinella S, De Castro Reis F, Pagani F, Wang H, Pellegrino E, Perlas E, Di Angelantonio S, Ragozzino D, Heppenstall PA. Tmem16f regulates spinal microglial function in neuropathic pain states. *Cell reports*. 2016;15:2608-2615

52. Hu Y, Kim JH, He K, Wan Q, Kim J, Flach M, Kirchhausen T, Vortkamp A, Winau F. Scramblase tmem16f terminates t cell receptor signaling to restrict t cell exhaustion. *J. Exp. Med.* 2016;213:2759-2772

53. Scoville DK, Botta D, Galdanes K, Schmuck SC, White CC, Stapleton PL, Bammler TK, MacDonald JW, Altemeier WA, Hernandez M, Kleeberger SR, Chen LC, Gordon T, Kavanagh TJ. Genetic determinants of susceptibility to silver nanoparticle-induced acute lung inflammation in mice. *FASEB J.* 2017;31:4600-4611

54. Zaitseva E, Zaitsev E, Melikov K, Arakelyan A, Marin M, Villasmil R, Margolis LB, Melikyan GB, Chernomordik LV. Fusion stage of hiv-1 entry depends on virus-induced cell surface exposure of phosphatidylserine. *Cell host & microbe*. 2017;22:99-110.e117

55. van Kruchten R, Mattheij NJ, Saunders C, Feijge MA, Swieringa F, Wolfs JL, Collins PW, Heemskerk JW, Bevers EM. Both tmem16f-dependent and tmem16f-independent pathways contribute to phosphatidylserine exposure in platelet apoptosis and platelet activation. *Blood*. 2013;121:1850-1857

56. Suzuki J, Denning DP, Imanishi E, Horvitz HR, Nagata S. Xk-related protein 8 and ced-8 promote phosphatidylserine exposure in apoptotic cells. *Science (New York, N.Y.)*. 2013;341:403-406

57. Suzuki J, Imanishi E, Nagata S. Exposure of phosphatidylserine by xk-related protein family members during apoptosis. *J. Biol. Chem.* 2014;289:30257-30267

58. Williamson P. Phospholipid scramblases. *Lipid insights*. 2015;8:41-44

59. Boyanova D, Nilla S, Birschmann I, Dandekar T, Dittrich M. Plateletweb: A systems biologic analysis of signaling networks in human platelets. *Blood*. 2012;119:e22-34

60. Renne T, Pozgajova M, Gruner S, Schuh K, Pauer HU, Burfeind P, Gailani D, Nieswandt B. Defective thrombus formation in mice lacking coagulation factor xii. *J. Exp. Med.* 2005;202:271-281

61. Fredenburgh JC, Gross PL, Weitz JI. Emerging anticoagulant strategies. *Blood*. 2017;129:147-154

62. Weidmann H, Heikaus L, Long AT, Naudin C, Schluter H, Renne T. The plasma contact system, a protease cascade at the nexus of inflammation, coagulation and immunity. *Biochim. Biophys. Acta*. 2017;1864:2118-2127

63. Naudin C, Burillo E, Blankenberg S, Butler L, Renne T. Factor xii contact activation. *Seminars in thrombosis and hemostasis*. 2017;43:814-826

64. Kenne E, Renne T. Factor xii: A drug target for safe interference with thrombosis and inflammation. *Drug Discov. Today*. 2014;19:1459-1464

65. Xu Y, Cai TQ, Castriota G, Zhou Y, Hoos L, Jochnowitz N, Loewrigkeit C, Cook JA, Wickham A, Metzger JM, Ogletree ML, Seiffert DA, Chen Z. Factor xiia inhibition by infestin-4: In vitro mode of action and in vivo antithrombotic benefit. *Thromb Haemost*. 2014;111:694-704

66. Chen JW, Figueiredo J-L, Wojtkiewicz GR, Siegel C, Iwamoto Y, Kim D-E, Nolte MW, Dickneite G, Weissleder R, Nahrendorf M. Selective factor xiia inhibition attenuates

silent brain ischemia: Application of molecular imaging targeting coagulation pathway. *JACC: Cardiovascular Imaging*. 2012;5:1127-1138

67. Larsson M, Rayzman V, Nolte MW, Nickel KF, Bjorkqvist J, Jamsa A, Hardy MP, Fries M, Schmidbauer S, Hedenqvist P, Broome M, Pragst I, Dickneite G, Wilson MJ, Nash AD, Panousis C, Renne T. A factor xiia inhibitory antibody provides thromboprotection in extracorporeal circulation without increasing bleeding risk. *Science translational medicine*. 2014;6:222ra217

68. Matafonov A, Leung PY, Gailani AE, Grach SL, Puy C, Cheng Q, Sun MF, McCarty OJ, Tucker EI, Kataoka H, Renne T, Morrissey JH, Gruber A, Gailani D. Factor xii inhibition reduces thrombus formation in a primate thrombosis model. *Blood*. 2014;123:1739-1746

69. Nieswandt B, Bergmeier W, Schulte V, Rackebrandt K, Gessner JE, Zirngibl H. Expression and function of the mouse collagen receptor glycoprotein vi is strictly dependent on its association with the fcrgamma chain. *J. Biol. Chem.* 2000;275:23998-24002

70. Watson SP, Herbert JM, Pollitt AY. Gpvi and clec-2 in hemostasis and vascular integrity. *J Thromb Haemost*. 2010;8:1456-1467

71. Stegner D, Haining EJ, Nieswandt B. Targeting glycoprotein vi and the immunoreceptor tyrosine-based activation motif signaling pathway. *Arterioscler Thromb Vasc Biol*. 2014;34:1615-1620

72. Bergmeier W, Stefanini L. Platelet itam signaling. *Current opinion in hematology*. 2013;20:445-450

73. Severin S, Pollitt AY, Navarro-Nunez L, Nash CA, Mourao-Sa D, Eble JA, Senis YA, Watson SP. Syk-dependent phosphorylation of clec-2: A novel mechanism of hem-immunoreceptor tyrosine-based activation motif signaling. *J. Biol. Chem.* 2011;286:4107-4116

74. Hughes CE, Pollitt AY, Mori J, Eble JA, Tomlinson MG, Hartwig JH, O'Callaghan CA, Futterer K, Watson SP. Clec-2 activates syk through dimerization. *Blood*. 2010;115:2947-2955

75. Pearce AC, Senis YA, Billadeau DD, Turner M, Watson SP, Vigorito E. Vav1 and vav3 have critical but redundant roles in mediating platelet activation by collagen. *J. Biol. Chem.* 2004;279:53955-53962

76. Cherpokova D, Bender M, Morowski M, Kraft P, Schuhmann MK, Akbar SM, Sultan CS, Hughes CE, Kleinschnitz C, Stoll G, Dragone LL, Watson SP, Tomlinson MG, Nieswandt B. Slap/slap2 prevent excessive platelet (hem)itam signaling in thrombosis and ischemic stroke in mice. *Blood*. 2015;125:185-194

77. Suzuki-Inoue K, Inoue O, Frampton J, Watson SP. Murine gpvi stimulates weak integrin activation in plcgamma2-/- platelets: Involvement of plcgamma1 and pi3-kinase. *Blood*. 2003;102:1367-1373

78. Atkinson BT, Ellmeier W, Watson SP. Tec regulates platelet activation by gpvi in the absence of btk. *Blood*. 2003;102:3592-3599

79. Watson SP, Auger JM, McCarty OJ, Pearce AC. Gpvi and integrin alphaiib beta3 signaling in platelets. *J Thromb Haemost*. 2005;3:1752-1762

80. Mammadova-Bach E, Ollivier V, Loyau S, Schaff M, Dumont B, Favier R, Freyburger G, Latger-Cannard V, Nieswandt B, Gachet C, Mangin PH, Jandrot-Perrus M. Platelet glycoprotein vi binds to polymerized fibrin and promotes thrombin generation. *Blood*. 2015;126:683-691

81. Alshehri OM, Hughes CE, Montague S, Watson SK, Frampton J, Bender M, Watson SP. Fibrin activates gpvi in human and mouse platelets. *Blood*. 2015;126:1601-1608

82. Moog S, Mangin P, Lenain N, Strassel C, Ravanat C, Schuhler S, Freund M, Santer M, Kahn M, Nieswandt B, Gachet C, Cazenave JP, Lanza F. Platelet glycoprotein v binds to collagen and participates in platelet adhesion and aggregation. *Blood*. 2001;98:1038-1046

83. Francischetti IM, Saliou B, Leduc M, Carlini CR, Hatmi M, Randon J, Faili A, Bon C. Convulxin, a potent platelet-aggregating protein from crotalus durissus terrificus venom, specifically binds to platelets. *Toxicon*. 1997;35:1217-1228

84. Suzuki-Inoue K, Fuller GL, Garcia A, Eble JA, Pohlmann S, Inoue O, Gartner TK, Hughan SC, Pearce AC, Laing GD, Theakston RD, Schweighoffer E, Zitzmann N, Morita T, Tybulewicz VL, Ozaki Y, Watson SP. A novel syk-dependent mechanism of platelet activation by the c-type lectin receptor clec-2. *Blood*. 2006;107:542-549

85. Hagedorn I, Vogtle T, Nieswandt B. Arterial thrombus formation. Novel mechanisms and targets. *Hamostaseologie*. 2010;30:127-135

86. Dutting S, Bender M, Nieswandt B. Platelet gpvi: A target for antithrombotic therapy?! *Trends Pharmacol. Sci.* 2012;33:583-590

87. Lee RH, Bergmeier W. Platelet immunoreceptor tyrosine-based activation motif (itam) and hemitam signaling and vascular integrity in inflammation and development. *J Thromb Haemost*. 2016;14:645-654

88. May F, Hagedorn I, Pleines I, Bender M, Vogtle T, Eble J, Elvers M, Nieswandt B. Clec-2 is an essential platelet-activating receptor in hemostasis and thrombosis. *Blood*. 2009;114:3464-3472

89. van Eeuwijk JM, Stegner D, Lamb DJ, Kraft P, Beck S, Thielmann I, Kiefer F, Walzog B, Stoll G, Nieswandt B. The novel oral syk inhibitor, bl1002494, protects mice from arterial thrombosis and thromboinflammatory brain infarction. *Arterioscler Thromb Vasc Biol*. 2016;36:1247-1253

90. Andre P, Morooka T, Sim D, Abe K, Lowell C, Nanda N, Delaney S, Siu G, Yan Y, Hollenbach S, Pandey A, Gao H, Wang Y, Nakajima K, Parikh SA, Shi C, Phillips D, Owen W, Sinha U, Simon DI. Critical role for syk in responses to vascular injury. *Blood*. 2011;118:5000-5010

91. Kleinschnitz C, Pozgajova M, Pham M, Bendszus M, Nieswandt B, Stoll G. Targeting platelets in acute experimental stroke: Impact of glycoprotein ib, vi, and iib/iiia blockade on infarct size, functional outcome, and intracranial bleeding. *Circulation*. 2007;115:2323-2330

92. Dutting S, Vogtle T, Morowski M, Schiessl S, Schafer CM, Watson SK, Hughes CE, Ackermann JA, Radtke D, Hermanns HM, Watson SP, Nitschke L, Nieswandt B. Growth factor receptor-bound protein 2 contributes to (hem)immunoreceptor tyrosine-based activation motif-mediated signaling in platelets. *Circ Res*. 2014;114:444-453

93. Boulaftali Y, Hess PR, Getz TM, Cholka A, Stolla M, Mackman N, Owens AP, 3rd, Ware J, Kahn ML, Bergmeier W. Platelet itam signaling is critical for vascular integrity in inflammation. *J. Clin. Invest.* 2013;123:908-916

94. Leo A, Schraven B. Networks in signal transduction: The role of adaptor proteins in platelet activation. *Platelets*. 2000;11:429-445

95. Hughes CE, Auger JM, McGlade J, Eble JA, Pearce AC, Watson SP. Differential roles for the adapters gads and lat in platelet activation by gpvi and clec-2. *J Thromb Haemost*. 2008;6:2152-2159

96. Kalia N, Auger JM, Atkinson B, Watson SP. Critical role of fcr gamma-chain, lat, plcgamma2 and thrombin in arteriolar thrombus formation upon mild, laser-induced endothelial injury in vivo. *Microcirculation*. 2008;15:325-335

97. Judd BA, Koretzky GA. The role of the adapter molecule slp-76 in platelet function. *Oncogene*. 2001;20:6291-6299

98. Clements JL, Lee JR, Gross B, Yang B, Olson JD, Sandra A, Watson SP, Lentz SR, Koretzky GA. Fetal hemorrhage and platelet dysfunction in slp-76-deficient mice. *J. Clin. Invest.* 1999;103:19-25

99. Abtahian F, Guerriero A, Sebzda E, Lu MM, Zhou R, Mocsai A, Myers EE, Huang B, Jackson DG, Ferrari VA, Tybulewicz V, Lowell CA, Lepore JJ, Koretzky GA, Kahn ML. Regulation of blood and lymphatic vascular separation by signaling proteins slp-76 and syk. *Science (New York, N.Y.)*. 2003;299:247-251

100. Bezman NA, Lian L, Abrams CS, Brass LF, Kahn ML, Jordan MS, Koretzky GA. Requirements of slp76 tyrosines in itam and integrin receptor signaling and in platelet function in vivo. *J. Exp. Med.* 2008;205:1775-1788

101. Liu SK, Berry DM, McGlade CJ. The role of gads in hematopoietic cell signalling. *Oncogene*. 2001;20:6284-6290

102. Garcia A, Senis YA, Antrobus R, Hughes CE, Dwek RA, Watson SP, Zitzmann N. A global proteomics approach identifies novel phosphorylated signaling proteins in gpvi-activated platelets: Involvement of g6f, a novel platelet grb2-binding membrane adapter. *Proteomics*. 2006;6:5332-5343

103. Cheng AM, Saxton TM, Sakai R, Kulkarni S, Mbamalu G, Vogel W, Tortorice CG, Cardiff RD, Cross JC, Muller WJ, Pawson T. Mammalian grb2 regulates multiple steps in embryonic development and malignant transformation. *Cell*. 1998;95:793-803

104. Knight CG, Morton LF, Onley DJ, Peachey AR, Ichinohe T, Okuma M, Farndale RW, Barnes MJ. Collagen-platelet interaction: Gly-pro-hyp is uniquely specific for platelet gp vi and mediates platelet activation by collagen. *Cardiovasc Res*. 1999;41:450-457

105. Bergmeier W, Bouvard D, Eble JA, Mokhtari-Nejad R, Schulte V, Zirngibl H, Brakebusch C, Fassler R, Nieswandt B. Rhodocytin (aggretin) activates platelets lacking alpha(2)beta(1) integrin, glycoprotein vi, and the ligand-binding domain of glycoprotein ibalpha. *J. Biol. Chem.* 2001;276:25121-25126

106. Bergmeier W, Rackebrandt K, Schroder W, Zirngibl H, Nieswandt B. Structural and functional characterization of the mouse von willebrand factor receptor gpib-ix with novel monoclonal antibodies. *Blood*. 2000;95:886-893

107. Nieswandt B, Bergmeier W, Rackebrandt K, Gessner JE, Zirngibl H. Identification of critical antigen-specific mechanisms in the development of immune thrombocytopenic purpura in mice. *Blood*. 2000;96:2520-2527

108. Bergmeier W, Schulte V, Brockhoff G, Bier U, Zirngibl H, Nieswandt B. Flow cytometric detection of activated mouse integrin alphaiibbeta3 with a novel monoclonal antibody. *Cytometry*. 2002;48:80-86

109. Nieswandt B, Echtenacher B, Wachs FP, Schroder J, Gessner JE, Schmidt RE, Grau GE, Mannel DN. Acute systemic reaction and lung alterations induced by an antiplatelet integrin gpiib/iiia antibody in mice. *Blood*. 1999;94:684-693

110. Schulte V, Rabie T, Prostredna M, Aktas B, Gruner S, Nieswandt B. Targeting of the collagen-binding site on glycoprotein vi is not essential for in vivo depletion of the receptor. *Blood*. 2003;101:3948-3952

111. Shida Y, Rydz N, Stegner D, Brown C, Mewburn J, Sponagle K, Danisment O, Crawford B, Vidal B, Hegadorn CA, Pruss CM, Nieswandt B, Lillicrap D. Analysis of the role of von willebrand factor, platelet glycoprotein vi-, and alpha2beta1-mediated collagen binding in thrombus formation. *Blood*. 2014;124:1799-1807

112. Morowski M, Vogtle T, Kraft P, Kleinschnitz C, Stoll G, Nieswandt B. Only severe thrombocytopenia results in bleeding and defective thrombus formation in mice. *Blood*. 2013;121:4938-4947

113. Mattheij NJ, Gilio K, van Kruchten R, Jobe SM, Wieschhaus AJ, Chishti AH, Collins P, Heemskerk JW, Cosemans JM. Dual mechanism of integrin alphaiibbeta3 closure in procoagulant platelets. *J. Biol. Chem.* 2013;288:13325-13336

114. Tchaikovski SN, BJ VANV, Rosing J, Tans G. Development of a calibrated automated thrombography based thrombin generation test in mouse plasma. *J Thromb Haemost*. 2007;5:2079-2086

115. Gilio K, van Kruchten R, Braun A, Berna-Erro A, Feijge MA, Stegner D, van der Meijden PE, Kuijpers MJ, Varga-Szabo D, Heemskerk JW, Nieswandt B. Roles of platelet stim1 and orai1 in glycoprotein vi- and thrombin-dependent procoagulant activity and thrombus formation. *J. Biol. Chem.* 2010;285:23629-23638

116. Swieringa F, Baaten CC, Verdoold R, Mastenbroek TG, Rijnveld N, van der Laan KO, Breel EJ, Collins PW, Lance MD, Henskens YM, Cosemans JM, Heemskerk JW, van der Meijden PE. Platelet control of fibrin distribution and microelasticity in thrombus formation under flow. *Arterioscler Thromb Vasc Biol*. 2016;36:692-699

117. Gob E, Reymann S, Langhauser F, Schuhmann MK, Kraft P, Thielmann I, Gobel K, Brede M, Homola G, Solymosi L, Stoll G, Geis C, Meuth SG, Nieswandt B, Kleinschnitz C. Blocking of plasma kallikrein ameliorates stroke by reducing thromboinflammation. *Ann. Neurol.* 2015;77:784-803

118. Bederson JB, Pitts LH, Tsuji M, Nishimura MC, Davis RL, Bartkowski H. Rat middle cerebral artery occlusion: Evaluation of the model and development of a neurologic examination. *Stroke*. 1986;17:472-476

119. Moran PM, Higgins LS, Cordell B, Moser PC. Age-related learning deficits in transgenic mice expressing the 751-amino acid isoform of human beta-amyloid precursor protein. *Proc. Natl. Acad. Sci. USA*. 1995;92:5341-5345

120. Baig AA, Haining EJ, Geuss E, Beck S, Swieringa F, Wanitchakool P, Schuhmann MK, Stegner D, Kunzelmann K, Kleinschnitz C, Heemskerk JW, Braun A, Nieswandt B. Tmem16f-mediated platelet membrane phospholipid scrambling is critical for hemostasis and thrombosis but not thromboinflammation in mice-brief report. *Arterioscler Thromb Vasc Biol*. 2016;36:2152-2157

121. Nieswandt B, Kleinschnitz C, Stoll G. Ischaemic stroke: A thrombo-inflammatory disease? *J Physiol*. 2011;589:4115-4123

122. Hoffman R, Benz EJ, Shattil SJ, Furie B, Cohen HJ, Silberstein LE, McGlave P. *Hematology basic principles and practice*. 2000.

123. Bjorkqvist J, Nickel KF, Stavrou E, Renne T. In vivo activation and functions of the protease factor xii. *Thromb Haemost*. 2014;112:868-875

124. Gruner S, Prostredna M, Aktas B, Moers A, Schulte V, Krieg T, Offermanns S, Eckes B, Nieswandt B. Anti-glycoprotein vi treatment severely compromises hemostasis in mice with reduced alpha2beta1 levels or concomitant aspirin therapy. *Circulation*. 2004;110:2946-2951

125. Sims PJ, Wiedmer T, Esmon CT, Weiss HJ, Shattil SJ. Assembly of the platelet prothrombinase complex is linked to vesiculation of the platelet plasma membrane. Studies in scott syndrome: An isolated defect in platelet procoagulant activity. *J. Biol. Chem.* 1989;264:17049-17057

126. Hoffman T, Lizzio EF. Albumin in monocyte function assays. Differential stimulation of superoxide or arachidonate release by calcium ionophores. *J. Immunol. Methods*. 1988;112:9-14

127. Bender M, May F, Lorenz V, Thielmann I, Hagedorn I, Finney BA, Vogtle T, Remer K, Braun A, Bosl M, Watson SP, Nieswandt B. Combined in vivo depletion of glycoprotein vi and c-type lectin-like receptor 2 severely compromises hemostasis and abrogates arterial thrombosis in mice. *Arterioscler Thromb Vasc Biol*. 2013;33:926-934

128. Striggow F, Riek-Burchardt M, Kiesel A, Schmidt W, Henrich-Noack P, Breder J, Krug M, Reymann KG, Reiser G. Four different types of protease-activated receptors are widely expressed in the brain and are up-regulated in hippocampus by severe ischemia. *Eur. J. Neurosci.* 2001;14:595-608

129. Mao Y, Zhang M, Tuma RF, Kunapuli SP. Deficiency of par4 attenuates cerebral ischemia/reperfusion injury in mice. *J Cereb Blood Flow Metab*. 2010;30:1044-1052

130. Olson EE, Lyuboslavsky P, Traynelis SF, McKeon RJ. Par-1 deficiency protects against neuronal damage and neurologic deficits after unilateral cerebral hypoxia/ischemia. *J Cereb Blood Flow Metab*. 2004;24:964-971

131. Ivanciu L, Krishnaswamy S, Camire RM. New insights into the spatiotemporal localization of prothrombinase in vivo. *Blood*. 2014;124:1705-1714

132. Piatt R, Paul DS, Lee RH, McKenzie SE, Parise LV, Cowley DO, Cooley BC, Bergmeier W. Mice expressing low levels of caldag-gefi exhibit markedly impaired platelet activation with minor impact on hemostasis. *Arterioscler Thromb Vasc Biol*. 2016;36:1838-1846

133. Suzuki-Inoue K, Inoue O, Ding G, Nishimura S, Hokamura K, Eto K, Kashiwagi H, Tomiyama Y, Yatomi Y, Umemura K, Shin Y, Hirashima M, Ozaki Y. Essential in vivo roles of the c-type lectin receptor clec-2: Embryonic/neonatal lethality of clec-2-deficient mice by blood/lymphatic misconnections and impaired thrombus formation of clec-2-deficient platelets. *J. Biol. Chem.* 2010;285:24494-24507

134. Uhrin P, Zaujec J, Breuss JM, Olcaydu D, Chrenek P, Stockinger H, Fuertbauer E, Moser M, Haiko P, Fassler R, Alitalo K, Binder BR, Kerjaschki D. Novel function for blood platelets and podoplanin in developmental separation of blood and lymphatic circulation. *Blood*. 2010;115:3997-4005

135. Poulter NS, Pollitt AY, Owen DM, Gardiner EE, Andrews RK, Shimizu H, Ishikawa D, Bihan D, Farndale RW, Moroi M, Watson SP, Jung SM. Clustering of glycoprotein vi (gpvi) dimers upon adhesion to collagen as a mechanism to regulate gpvi signaling in platelets. *J Thromb Haemost*. 2017;15:549-564

136. Pasquet JM, Gross B, Quek L, Asazuma N, Zhang W, Sommers CL, Schweighoffer E, Tybulewicz V, Judd B, Lee JR, Koretzky G, Love PE, Samelson LE, Watson SP. Lat is required for tyrosine phosphorylation of phospholipase cgamma2 and platelet activation by the collagen receptor gpvi. *Mol. Cell. Biol.* 1999;19:8326-8334

137. Judd BA, Myung PS, Obergfell A, Myers EE, Cheng AM, Watson SP, Pear WS, Allman D, Shattil SJ, Koretzky GA. Differential requirement for lat and slp-76 in gpvi versus t cell receptor signaling. *J. Exp. Med.* 2002;195:705-717

138. Deppermann C, Kraft P, Volz J, Schuhmann MK, Beck S, Wolf K, Stegner D, Stoll G, Nieswandt B. Platelet secretion is crucial to prevent bleeding in the ischemic brain but not in the inflamed skin or lung in mice. *Blood*. 2017;129:1702-1706

139. Rayes J, Jadoui S, Lax S, Gros A, Wichaiyo S, Ollivier V, Denis CV, Ware J, Nieswandt B, Jandrot-Perrus M, Watson SP, Ho-Tin-Noe B. The contribution of

platelet glycoprotein receptors to inflammatory bleeding prevention is stimulus and organ dependent. *Haematologica*. 2018

6. Appendix

6.1. Abbreviations

ADP	adenosine diphosphate
AF	Alexa-fluor
ATP	adenosine triphosphate
AU	arbitrary units
aPTT	activated partial thromboplastin time
BCR	B cell receptor
BM	bone marrow
BSA	bovine serum albumin
BW	body weight
CAT	calibrated automated thrombogram
cKO	conditional knockout
CLEC-2	C-type lectin-like receptor 2
CRP	collagen-related peptide
ctrl	control
d	day
DAG	diacyl glycerol
DAPI	4',6-diamidino-2-phenylindole
DIC	differential interference contrast
DKO	double knockout
DNA	deoxyribonucleic acid
ECL	enhanced chemi-luminescence
ECM	extracellular matrix
EDTA	ethylenediaminetetraacetate
EGTA	ethylene glycol tetraacetate
ELISA	enzyme-linked immunosorbent assay
FcR	Fc receptors
FITC	fluorescein isothiocyanate
g	gravity
Grb2	growth factor receptor bound protein 2
Gads	Grb2 related adapter protein downstream of Shc
Grap	Grb2 related adapter protein
GP	glycoprotein
GPCR	G protein-coupled receptor
h	hour
HCT	hematocrit
HGB	hemoglobin
HRP	horseradish peroxidase
HSC	hematopoietic stem cells
i.p.	intraperitoneal(ly)
i.v.	intravenous(ly)

Ig	immunoglobulin
Iono	ionomycin
A23	A23187 (calcium ionophore)
IP	immunoprecipitation
IP_3	inositol-3,4,5-trisphosphate
ITAM	immunoreceptor tyrosine-based activation motif
kDa	kilodalton
KO	knockout
LAT	linker for activation of T cells
MCA	middle cerebral artery
MFI	mean fluorescence intensity
min	minute
MK	megakaryocyte(s)
MOPS	3-(*N*-morpholino)propanesulfonic
MPV	mean platelet volume
n.s.	not significant
NA	numerical aperture
o/n	overnight
PAR	protease activated receptor
PBS	phosphate-buffered saline
PCR	polymerase chain reaction
PE	phycoerythrin
PF4	platelet factor 4
PFA	paraformaldehyde
PGI_2	prostaglandin I_2, prostacyclin
PIP_2	phosphatidylinositol-4,5-bisphosphate
PKC	protein kinase C
PLC	phospholipase C
PRP	platelet-rich plasma
PPP	platelet poor plasma
PS	phosphatidylserine
PE	phosphatidylethanolamine
PC	phoaphatidylcholine
SM	sphingomyelins
PVDF	polyvinylidene difluoride
PT	prothrombin time
RBC	red blood cells
rpm	rotations per minute
RT	room temperature
s	seconds
SEM	scanning electron microscopy
SDS	sodium dodecyl sulfate
SDS-PAGE	sodium dodecyl sulfate polyacrylamide gel electrophoresis
SFKs	Src family kinases

SH	Src homology
SLAP	Src-like adapter protein
SLP-76	SH2-containing leukocyte protein 76
Syk	spleen tyrosine kinase
TBS	Tris-buffered saline
TCR	T cell receptor
TF	tissue factor
TxA_2	thromboxane
TMB	3,3,5,5-tetramethyl-benzidine
tMCAO	transient middle cerebral artery occlusion
TTC	2,3,5-triphenyltetrazolium chloride
U46	U46188 (thromboxane A2 analog)
VWF	von Willebrand factor
WB	Western blot
WBC	white blood cells
WT	wild-type
Xkr	Xk-related

6.2. Acknowledgements

First and foremost, I would like to express my heartfelt gratitude to my primary supervisor, Prof. Dr. Bernhard Nieswandt for giving me the opportunity to carry out research in his laboratory, as well as for his excellent guidance, support and constant encouragement.

I am particularly grateful to Prof. Johan Heemskerk for being ever available to troubleshoot experimental roadblocks, especially on the TMEM16F project. I have greatly benefited from his constructive comments and warm encouragement.

I would also like to thank Prof. Guido Stoll for agreeing to be part of my thesis committee, and for his valuable comments and suggestions at progress reports.

This journey was made easier with a great support system. I would like to thank Dr. David Stegner and Dr. Katharina Remer who always steered me in the right direction in our monthly group meetings.

I am deeply grateful to Dr. Elizabeth Haining for a great collaboration on projects. I would also like to thank Sarah Beck for performing thrombinoscope measurements for the TMEM16F project.

It would not have been possible to produce this document without the constant encouragement and feedback of friend and colleague, Dr. Deya Cherpokova. I am thankful to her and to Dr. Irina Pleines for proofreading this thesis.

I would also like to express my gratitude to Elke Hauck, Dr. Christine Mais and all our lab technicians - Birgit Midloch, Sylvia Hengst, Juliana Goldmann, Ewa Stepien-Bötsch and Stefanie Hartmann – for ensuring that that the laboratory runs ever so smoothly.

I am grateful to the Graduate School of Life Sciences at the University of Würzburg for the financial support and would like to express my deepest appreciation for the GSLS team for making life of an international student so comfortable by helping us out in every way possible.

Special thanks to all the past and current members of the Nieswandt lab for the great working atmosphere, as well as for making Würzburg feel like home.

Finally, I owe my deepest gratitude to my family - my late father Masroor, for passing on a penchant for science to me; my mother Anjum, for her unwavering belief in my abilities; my husband Yasir, who made my dreams his own and who always has my back; my sisters - Aali, Afeefa and Samia, and second set of parents - Fauzia and Zafar, for their love and affection.

6.3. Publications

6.3.1. Research articles

Baig AA,* Haining EJ,* Geuss E, Beck S, Swieringa F, Wanitchakool P, Schuhmann MK, Stegner D, Kunzelmann K, Kleinschnitz C, Heemskerk JW, Braun A, Nieswandt B. TMEM16F-mediated platelet membrane phospholipid scrambling is critical for hemostasis and thrombosis but not thromboinflammation in mice-brief report. *Arterioscler Thromb Vasc Biol*. 2016;36:2152-2157

Dutting S, Gaits-Iacovoni F, Stegner D, Popp M, Antkowiak A, van Eeuwijk JMM, Nurden P, Stritt S, Heib T, Aurbach K, Angay O, Cherpokova D, Heinz N, **Baig AA**, Gorelashvili MG, Gerner F, Heinze KG, Ware J, Krohne G, Ruggeri ZM, Nurden AT, Schulze H, Modlich U, Pleines I, Brakebusch C, Nieswandt B. A Cdc42/RhoA regulatory circuit downstream of glycoprotein Ib guides transendothelial platelet biogenesis. *Nature communications*. 2017;8:15838

6.3.2. Posters

TMEM16F-mediated platelet pro-coagulant activity does not contribute to infarct progression after ischemic stroke. 1st European Congress on Thrombosis and Haemostasis (ECTH), 2016, The Hague (Netherlands).

TMEM16F-mediated platelet pro-coagulant activity does not contribute to infarct progression after ischemic stroke. 62nd Annual meeting of the International Society on Thrombosis and Haemostasis (ISTH), Scientific and Standardization Committee (SSC), 2016, Montpellier (France).

TMEM16F-mediated platelet pro-coagulant activity is critical for hemostasis and thrombosis but not for infarct progression after ischemic stroke. 11th International Symposium of the Graduate School of Life Sciences (EUREKA!), 2016, Würzburg (Germany).

The thrombo-inflammatory role of platelets in ischemic stroke is independent of their procoagulant function. 10th International Symposium of the Graduate School of Life Sciences (EUREKA!), 2015, Würzburg (Germany).

6.4. Curriculum vitae

6.5. Affidavit

I hereby declare that my thesis entitled, “Studies on platelet interactions with the coagulation system and on modulators of platelet (hem)ITAM singling in genetically modified mice”, is the result of my own work. I did not receive any help or support from commercial consultants. All sources and/or materials applied are listed and specified in the thesis.

Furthermore, I confirm that this thesis has not yet been submitted as part of another examination process neither in identical nor in similar form.

Würzburg, May 2018 _____

Ayesha Anjum Baig

6.6. Eidesstattliche Erklärung

Hiermit erkläre ich an Eides statt, die Dissertation „Interaktion mit der Gerinnungskaskade und Modulation von hem(ITAM) Signalwegen in Thrombozyten - Untersuchungen an genetisch veränderten Mäusen“ eigenständig, d.h. insbesondere selbstständig und ohne Hilfe eines kommerziellen Promotionsberaters, angefertigt und keine anderen als die von mir angegebenen Quellen und Hilfsmittel verwendet zu haben.

Ich erkläre außerdem, dass die Dissertation weder in gleicher noch in ähnlicher Form bereits in einem anderen Prüfungsverfahren vorgelegen hat.

Würzburg, May 2018 _____

Ayesha Anjum Baig